VILNIAUS UNIVERSITETAS
CHEMIJOS IR GEOMOKSLŲ FAKULTETAS
GEOMOKSLŲ INSTITUTAS
GEOLOGIJOS IR MINERALOGIJOS KATEDRA

Dovydas Aranauskas

Geologija

Magistro baigiamasis darbas

MĖNULIO METEORITO NWA 15352 SUDĖTIS IR ASOCIACIJOS SU SMŪGINIU ĮVYKIU

Darbo vadovas (-ė)

doc. dr. Gražina Skridlaitė

Mokslinė patarėja

doc. dr. Victoria Pease

Vilnius 2025

VILNIUS UNIVERSITY
FACULTY OF CHEMISTRY AND GEOSCIENCES
INSTITUTE OF GEOSCIENCES
DEPARTMENT OF GEOLOGY AND MINERALOGY

Dovydas Aranauskas
Geology
Master thesis

COMPOSITION OF THE MOON METEORITE NWA 15352 AND ASSOCIATION WITH THE IMPACT EVENT

Scientific supervisor
prof. dr. Grazina Skridlaite
Scientific advisor
prof. dr. Victoria Pease

Vilnius 2025

CONTENT

SANTRAUKA

VILNIAUS UNIVERSITETAS
CHEMIJOS IR GEOMOKSLŲ FAKULTETAS

DOVYDAS ARANAUSKAS

Mėnulio meteorito NWA 15352 sudėtis ir asociacijos su smūginiu įvykiu

Šiame darbe tiriama NWA 15352 Mėnulio feldšpatinė brekčija. Atlikti detalūs petrologiniai ir mikrostruktūriniai tyrimai kartu su Pb-Pb isotopų analize atskleidė sudėtingą meteorito istoriją. NWA 15352 yra sudarytas iš įvairių mineralų ir uolienų fragmentų, įterptų į lydalo matricą (užpildą). Tarp mineralų dominuojantys yra Ca praturtintas plagioklazas, olivinas, piroksenas ir ilmenitas, o mažesniąją dalį sudaro špinelė, FeNi metalai, sulfatai ir vėlyvos fazės mineralai: cirkonas, fosfatai ir K praturtinas stiklas. Matricoje (užpilde) identifikuoti trys uolienų fragmentų tipai: anortozitų fragmentai, brekčijų fragmentai, ir lydalo fragmentai. Įtrūkimai esantys ant mineralų paviršiaus, netaisyklingi aštrius kampus turintys mineralai ir dalinai išsilydžiusios nuolaužos nurodo, kad uoliena galėjo patirti ne vieną smūginį įvykį ir jį lydintį šoko metamorfizmą. Šie smūginiai įvykiai uolieną trupino, išsklaidė, perlydė bei sumaišė skirtingos litologijos (sudėties/kilmės) uolienas, aptinkamas NWA 15352 brekčijoje. Didelis An (>90) kiekis randamas plagioklaze atskleidė, kad kai kurios uolienų nuolaužos greičiausiai yra kilusios iš Mėnulio aukštumų (Lunar highlands). Mg praturtinti špinelės fragmentai gali rodyti, kad kai kurie uolienų fragmentai yra kilę iš Mėnulio mantijos ir buvo iškelti į paviršių didelių kosminių smūgių metu. Tyrimo duomenys rodo, kad brekčijoje aptiktos skirtingų litologijų uolienų nuolaužos yra kilusios iš Mėnulio aukštumų (Lunar highlands) ir jūrų (Lunar maria), o tikėtiniausias NWA 15352 kilmės šaltinis yra riba tarp šių dviejų geologinių vienetų. Naudojant Pb-Pb izotopinę analizę nustatyta, kad Mėnulio bazalto nuolaužos amžius siekia 3.85 mlrd. ir asocijuojasi su „Imbrium" periodu. Tuo tarpu kraterių datavimas atskleidė, kad Mėnulio bazalto nuolaužos amžius persidengia su jūrų (Lunar maria) bazaltais, esančiais šiose Mėnulio dalyse: Mare Serenitatis, Mare Marginis, Mare Australe ir Fra Mauro Formation vienetu esančiu šalia Apollo 14 nusileidimo vietos.

SUMMARY

VILNIUS UNIVERSITY
FACULTY OF CHEMISTRY AND GEOSCIENCES

DOVYDAS ARANAUSKAS

Composition of the Moon meteorite NWA 15352 and association with the impact event

The lunar felspathic breccia NWA 15352 has been studied in this work. Detailed petrological and microstructure investigation performed together with a Pb-Pb isotope analysis revealed the complexity of its composition and history. NWA 15352 is composed of various mineral fragments and different types of clasts embedded in a melt matrix where dominant minerals are Ca-rich plagioclases, olivines pyroxenes and ilmenite with a minor spinel, FeNi metals, sulfates and late phases such as zircon, phosphates and K-rich glass. Three types of clasts were identified: anorthosite clasts, breccia clasts and melt clasts. Fractures on the mineral surfaces, angular shape of minerals and partially melted clasts may evidence multiple, the impact event related, shock events that crushed, scattered, remelted and mixed different lithologies of lunar material present in the NWA 15352. The high An (>90) content in plagioclase reveals that some clasts were likely to originate from the lunar highlands while presence of Mg-rich spinel fragments may indicate that the material was excavated from the lunar upper mantle through the large impact events. The mixture of clasts linked both to the lunar highlands and mare basalts, points toward the most likely source region for the NWA 15352 to be some place at the mare-highland boundary. The Pb-Pb isotope analysis reveals a 3846 ± 44 Ma crystallization age of the lunar basalt clast associated with an Imbrium period while the crater counting ages of mare basalts overlap with the regions on the lunar near side: Mare Serenitatis, Mare Marginis, Mare Australe, and Fra Mauro Formation Unit near the Apollo 14 landing site.

INTRODUCTION

Lunar exploration began when lunar rock samples were obtained from the Apollo and Luna missions that brought 382 kg of rock samples. These samples allowed for the direct study of the Moon's geology and provided new insights into how the Moon was formed. In the 1980s the first lunar meteorites were recognized in Antarctica (e.g. ALHA81005 1982; Takeda et al., 1986; Grossman, 1994). Since then, over 741 lunar meteorites have been recovered (last check of Meteorite Bulletin May 21, 2025. Most of them were found in the Sahara Desert, a dry area where weathering processes are slow and preservation is more likely to occur (Zhou, 2017).

A lunar meteorite is a rock that was ejected from the Moon by the impact of a meteoroid and was subsequently captured by the Earth’s gravitational field (Korotev, 2005). Investigation of lunar meteorites is important because they represent semi-random samples of the lunar surface compared to manned and unmanned missions which sampled specific locations; while mission samples represent specific collection sites, lunar meteorites provide a much wider view of lunar geology.

Lunar meteorites provide insights into processes of early Solar System formation. On Earth, due to geological processes like subduction and constantly recycled surfaces, rocks older than a few billion years old are rare. Meanwhile, the Moon has a preserved record dating from its formation 4.5 billion years ago (Hiesinger and Head, 2006). By studying these precious rock samples, we can better understand planetary processes, as well as the formation of the early Earth.

In this work, the Moon meteorite NWA 15352 was investigated. The sample was found in Algeria in 2020 and classified as a lunar feldspathic breccia (Gattacceca et al., 2023). No detailed investigations have been carried out on this meteorite.

Thesis aims:

The objectives of this work are to examine the Moon meteorite NWA 15352, perform a petrological and textural investigation of the sample, conduct Pb-Pb isotope analysis, date the sample, and associate it as close as possible with impact event/s and source region.

1 GEOLOGICAL CONTEXT

Information about Lunar geology comes from several sources: indirect, such as telescope observations, remote sensing data, and direct, such as rock samples brought by manned and unmanned missions, and lunar meteorites found on the Earth. Only by combining these different information sources can the best results about Lunar geology be achieved.

1.1 Lunar terranes

Based on remote sensing data mainly collected from the Lunar Prospector (Binder, 1998) and the Clementine missions (Nozette et al., 1994), the Lunar crust can be subdivided into three main terranes: Feldspathic Highlands Terrane (FHT), Procellarum (Potassium, Rare Earth Elements, Phosphorus) Terrane (PKT) and South-Polen Aitken Terrane (SPAT) (Jolliff et al., 2000). Terranes are characterized by Th and Fe contents (Fig. 1). The FHT forms the bright areas of the Lunar surface called highlands, the oldest crust part heavily cratered and mainly composed of anorthosite. It is believed that anorthosite is a product of colling lunar magma ocean where the Ca-plagioclase as a light mineral floating on top of a magma ocean, while heavier minerals such as olivine and pyroxene sank (Wood et al., 1970). PKT regions are enriched in KREEP elements (referring to the presence of Potassium, Rare Earth Elements, and Phosphorus). These KREEP-rich rocks are the products of residual melt enriched in incompatible elements during fractional crystallization of the magma ocean (Warren and Wasson, 1979). SPAT situated in the Lunar south pole is a ~2600 km diameter impact basin with a low topography (down to 12 km from the surrounding highlands) (Jolliff et al., 2000).

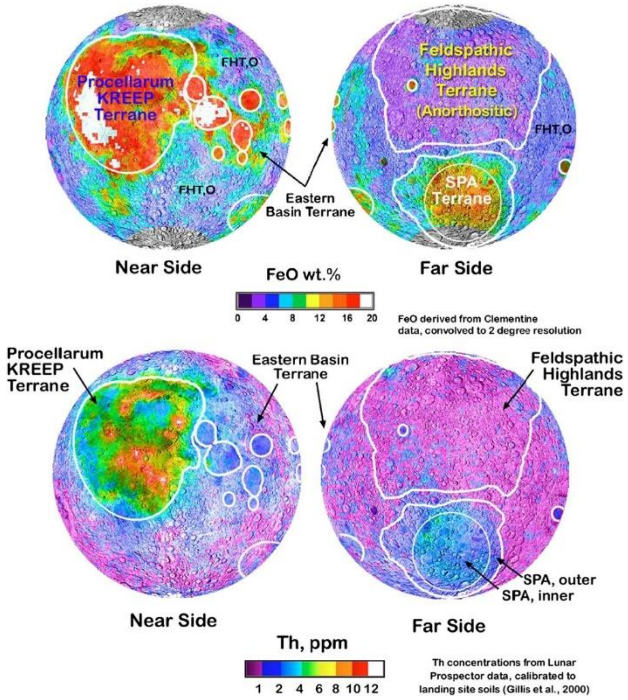

Fig. 1. Definition of major lunar surface terranes on the basis of FeO and Th abundances (from Jolliff et al., 2000).

1.2 Lunar rocks and lunar meteorites

Lunar rocks can be divided into four different groups: pristine highland rocks, pristine basaltic volcanic rocks, impact breccias, and regolith (Taylor et al., 1991). Most lunar rocks are impact breccias and consist of the all mentioned rock types (Fig. 2). Pristine highland rocks consist of ferroan anorthosites, Mg-suite rocks, and KREEP rocks found in the FHT (Lucey et al., 2006). Basaltic volcanic rocks are highly concentrated on the lunar nearside and fill impact basins (called maria, e.g. Imbrium basin). Lunar regolith covers the entire Lunar surface and is heavily reworked by continuous impact cratering processes. These rocks consist of breccia fragments, mineral fragments, glasses and agglutinates (McKay et al., 1991).

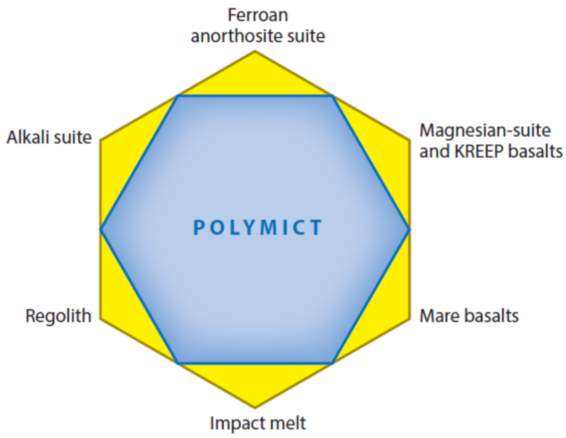

Fig. 2. Building block of the lunar breccia (from Spray, 2016)

Some scientists argue that most lunar meteorites left the Moon recently, in geological time (in the past 20 Ma), and were derived from craters of a few km in diameter. Among lunar meteorites, polymictic breccias are the most common (Korotev, 2005). These rocks are made up of different kinds of older rocks that have been lithified by heat and shock because of meteoroid impacts on the lunar surface (Korotev, 2005). Compared to the lunar rock classification, the classification of lunar meteorites is less consistent and less detailed; lunar meteorites are classified into six groups: basaltic, plutonic, granulitic breccia, impact-melt breccia, fragmental breccia and regolith breccia (Zeigler et al., 2023).

2 SAMPLE DESCRIPTION

The NWA 15352 sample was found in Algeria in 2020, with the total mass of samples of 4.13 kg. The samples are of quasi-ovoid shapes, have a black surface without fusion crust and are moderately weathered. It is a melt breccia made of rock and mineral fragments, set in a melted rock matrix (Fig. 3). Major minerals are pyroxene, feldspar, olivine and ilmenite. Accessory minerals are spinel, silica, zircon, and FeNi metal. Anorthosite and basalt clasts were found (Gattacceca et al., 2023).

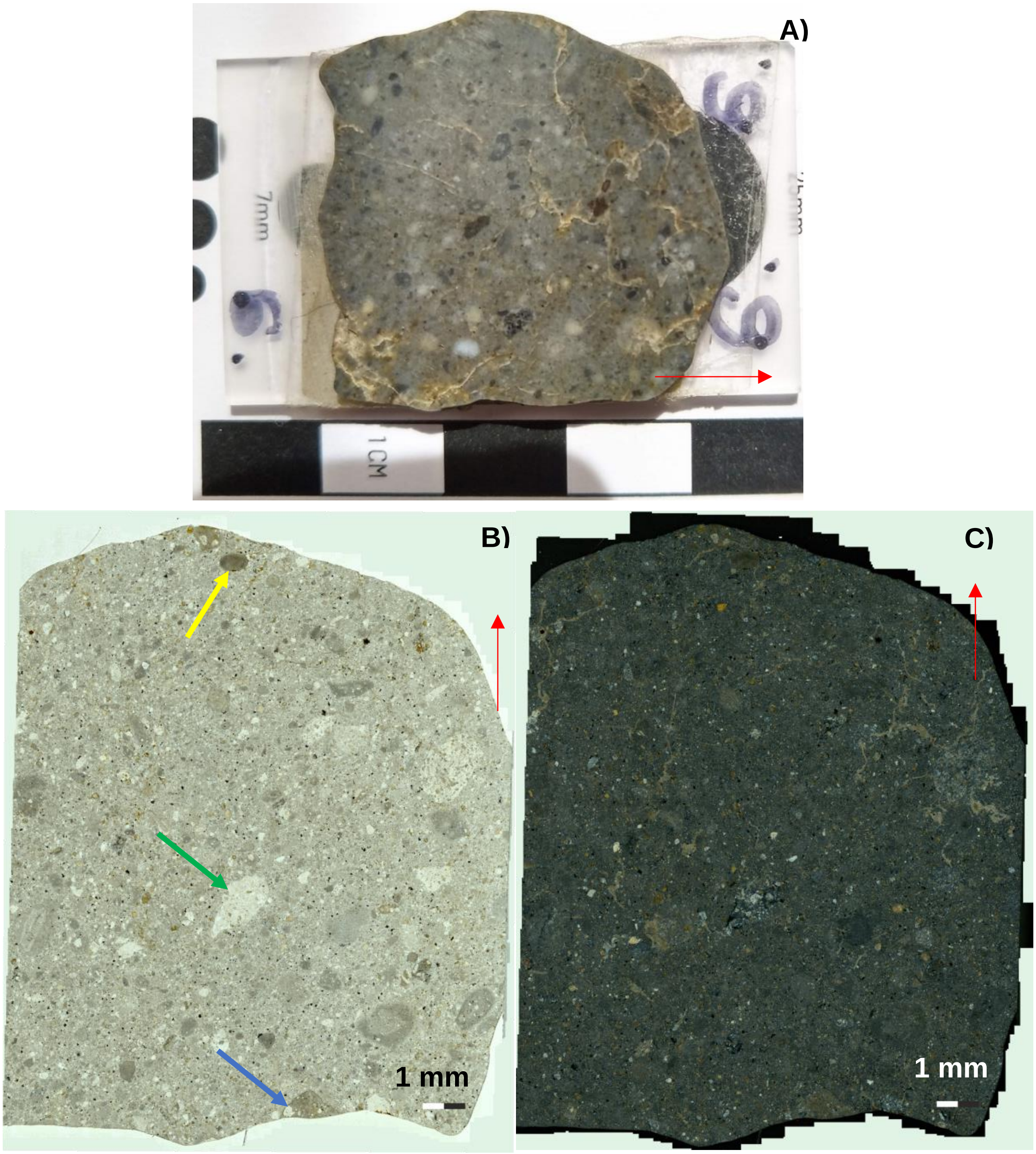

Fig. 3. NWA 15352 lunar feldspathic breccia. **A**. Thick section. **B**. Thin section in a plane polarized light (PPL). **C**. Thin section in XPL. The red arrow: indicates sample orientation, blue arrow: breccia clast, yellow arrow: melt clast, green arrow: anorthosite clast.

3 ANALYTICAL METHODS

Two slices with dimensions around ~43 x 27 x 1 mm were prepared for this study: one for a thin section and one for a thick section (Fig. 3). One slice was sent to Warsaw University for the thin section (~ 0.03 mm thick) preparation and was later analyzed at the Nature Research Centre, Vilnius, Lithuania using a polarized microscope and Scanning Electron Microscope (SEM). The thick section was polished, cut, and analyzed by a SEM and Secondary Ion Mass Spectrometry (SIMS) at Stockholm University and Swedish Museum of Natural History, Stockholm, Sweden.

3.1 Petrograpic analysis

The Nicon SZM 1500 polarized microscope with an integrated photosystem, together with a whole thin section digital image made by "Microvisioneer manualWSI" software, allowed the petrological analysis of the thin section. The distribution of clasts and minerals in the matrix, along with their size, shape, and mineralogical composition, are characterized. Mineral identification is confirmed by the scanning electron microscopy (SEM). The most interesting locations are chosen for further SEM analysis (Fig. 6).

3.2 SEM EDS analysis

The thin and thick sections were cleaned with isopropyl alcohol before being carbon coated for a chemical analysis with SEM. A backscattered electron (BSE) imaging and Energy Dispersive Spectrometry (EDS) analysis were performed with a Quanta 250 SEM at the Nature Research Center, Vilnius, Lithuania to identify the main minerals and their chemical composition. The cobalt standard was used for the SEM analysis. Chemical analysis was conducted by an electron beam with operating current of 1.1–1.2 nA and accelerating voltage of 10–20 kV at a working distance of 10 mm.

BSE images and X-ray elemental maps of the thick section were performed using a Hitachi TM1000 SEM instrument and accompanying Oxford Instruments Energy Dispersive X-ray Spectroscopy (EDS) detector at Swedish Museum of Natural History (Stockholm). The mapping and analysis of the samples were conducted with an electron beam accelerating voltage of 20 kV at a working distance of 10 mm. BSE images and X-ray element maps (Na, Mg, Al, Si, P, S, K, Ca, Cr, Ti, Fe, Ni, and Zr) were performed for fast imaging to choose interesting parts for future secondary ion mass spectrometer (SIMS) analysis.

The thick section was cut into three parts (NWA 15352L – left, NWA 15352R – right, and NWA 15352B - bottom) using a diamond disk saw (app. C, Fig. 26). One part (NWA 15352L) was mounted in EPOTEK epoxy resin and polished for a SEM and SIMS analysis. Detailed BSE and element maps (Si, P, S, K, and Zr) were performed with 207 field numbers and with a speed of 1 frame per 15 minutes for the NWA 15352L and NWA 15352R thick sections. These detailed BSE and element maps were then used to identify the location of phases for Pb-Pb dating by SIMS in the clasts; as well as for phosphates, K-rich glass and feldspar identification. These phases were identified based on regions of high-K, high-P, and high-Zr. Due to K and Zr overlapping, a Si map was used to distinguish between K-rich feldspar and zircon. A desktop SEM with the AZtecOne software was applied to make a close-up BSE and element images for each target.

3.3 SIMS analysis

The SIMS analysis was conducted using a CAMECA IMS 1280 ion microprobe at the NordSIMS facility, Swedish Museum of Natural History, Stockholm, equipped with a Hyperion source. The SIMS methodology was based on the analytical procedures detailed in work (Snape et al., 2016). Before the analysis, the thick section was coated with a 30 nm thick gold layer. The targets were analyzed with a -13 kV $^{16}O_2^-$ primary beam (10 kV secondary beam) at a working intensity of 3 nA. The $^{16}O_2^-$ primary source was used to emit Pb^+ and OU^+ cations from the sample surface. The area of the beam was 10 μm. BCR-2G basaltic glass standard was used to calibrate SIMS. Before each measurement, an area of 20 x 20 μm around the spot location was pre-sputtered for the 90s to remove the gold coating and minimize possible surface contamination. The mass spectrometer was operated at a nominal mass resolution of 4862 (M/ΔM), sufficient to resolve Pb from known molecular interferences. To measure Pb-isotopes the simultaneous multidetector mode was used. The instrument was operated in a 160x magnification regime. SEM images with the targets were acquired to determine the exact location of SIMS spots to avoid fractures or grain boundaries and prevent any likely sources of error in the measurements. After SIMS analysis the data were processed using in-house software developed at NordSIMS for the CAMECA IMS1280 analyses. Ages were calculated and the isochron plotted using the Excel add-in Isoplot software (version 4.15; Ludwig 2012). Calculates ages at the 95% confidence level.

4 RESULTS

Results include petrographic description, SEM BSE images, EDS mineral chemical, and SIMS Pb-Pb analyses. The data is presented in appendices: SEM BSE, SEM EDS, and SIMS (app. A, B and C respectively).

4.1 Petrography

The NWA 15352 sample is a lunar feldspathic breccia made of rock clasts, and mineral fragments set in a melt rock matrix. The surface of the sample is fractured and filled with secondary minerals (Fig. 3C). Some parts of the thin section surface are affected by terrestrial weathering and contain iron oxides and barite. The colors of clasts vary from light gray to dark gray where the matrix has a gray color and consists of fine-grained mineral fragments and melt (Fig. 4). The size of clasts varies from 0.1 mm to 3.5 mm (Fig. 5). Among mineral fragments, plagioclase, olivine, pyroxene, ilmenite, Cr-rich spinel, and sulfides (troilite) are identified. The accessory minerals are spinel, zircon, baddeleyite, and an FeNi metal.

4.1.1 Mineral fragments

Most minerals have an angular shape with sharp edges in contact with the matrix. The surface of minerals is fractured (Fig. 4). Some minerals are surrounded by opaque minerals. Fractures filled with opaque minerals can be found (Fig. 4). The size of minerals varies from very fine-grained (10 μm) to fine-grained (up to 700 μm). Plagioclase is the dominant mineral among the largest fragments.

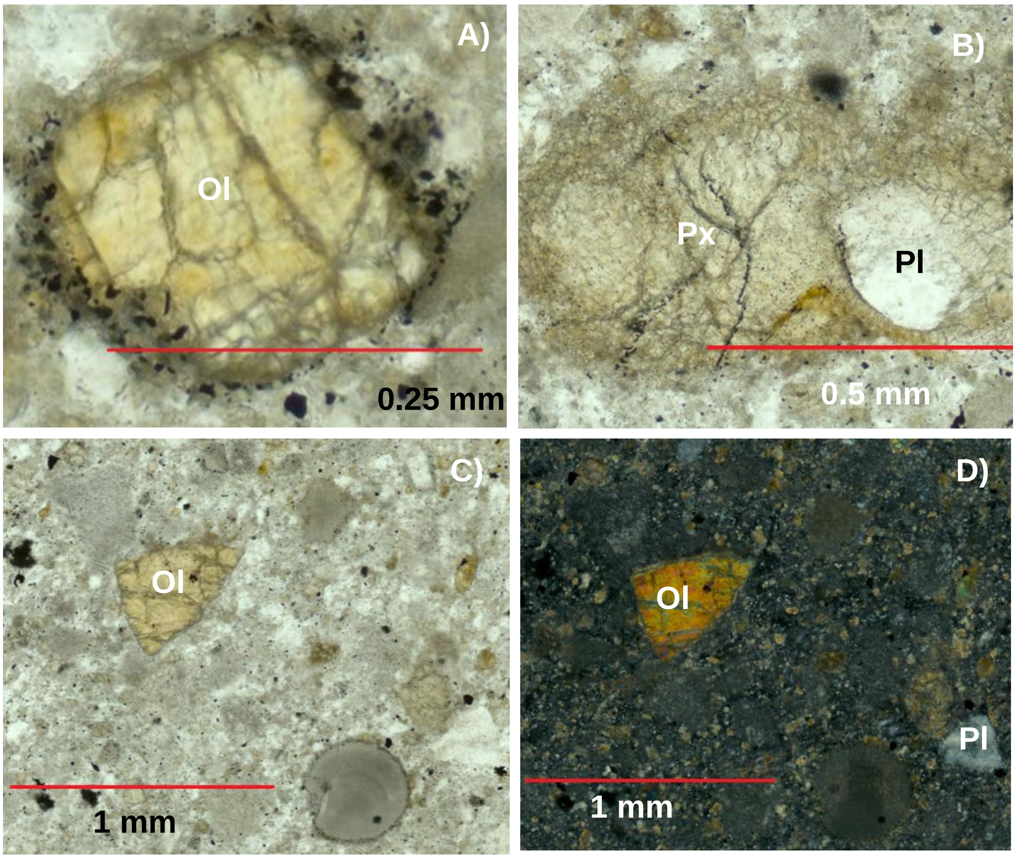

Fig. 4. Mineral fragments in the matrix. **A**. Fractured olivine (Ol) with opaque minerals near the edge, plane polarized light (PPL). **B**. Fractured pyroxene (Px) filled with opaque minerals and plagioclase (Pl), PPL. **C**. angular olivine (Ol) in the matrix, PPL. **D**. angular olivine (Ol) fragment in the matrix, XPL.

4.1.2 Rock (lithic) clasts

Several types of clasts were identified: anorthosite clasts, breccia clasts, and melt clasts (Fig. 5). Some clasts exhibit sharp contacts with the matrix, others have smooth contacts with the matrix. The plagioclase clasts vary in size between 1 mm and 3 mm. Most of these clasts have small portions of olivine and pyroxene (Fig. 5). In cross-polarized light (XPL), plagioclases have mosaic texture (Fig. 5 B). Breccia clasts are complex, consisting of fine-grained matrix with small rock fragments inside (mainly plagioclase) (Fig. 5 D). The largest of these clasts reaches 3 mm in size. Along with these clasts, the solidified melt clasts were recognized and have rounded or oval shape (Fig. 5 F). These clasts vary in size from 0.5 mm to 1 mm. Some of them are homogenous consisting of fine-grained matrix, others contain needle-shaped plagioclase minerals (Fig. 5 E).

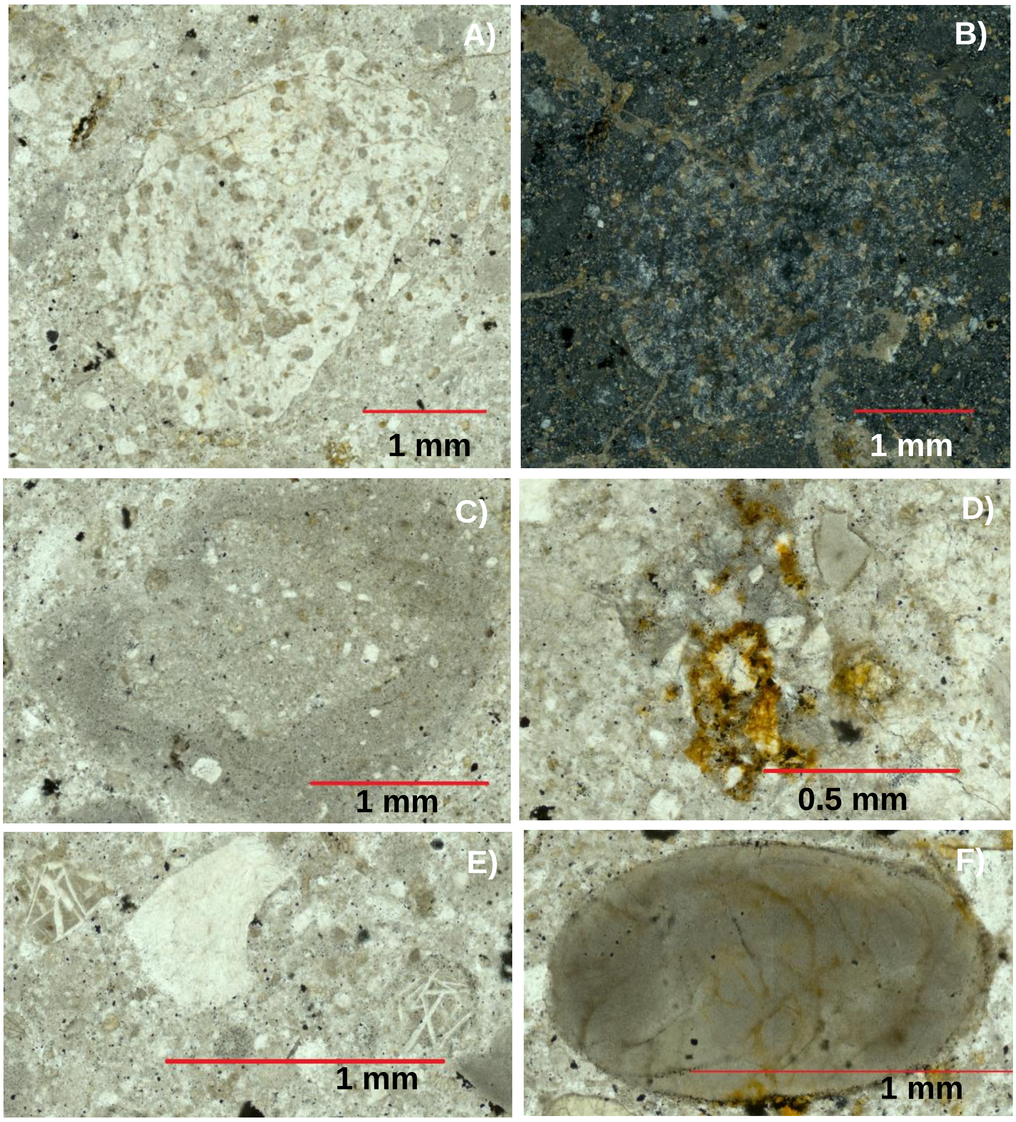

Fig. 5. Clasts in the matrix. **A**. Anorthosite clast in PPL, **B**. Anorthosite clast in XPL, **C**. Breccia clast in PPL, **D**. Breccia clast in PPL, **E**. Melt clast in PPL, **F**. Melt clast in PPL

4.2 Mineral chemistry (SEM analyses)

In total, 36 areas were selected for chemical analysis and mineral identification: 16 analyses from mineral fragments, and 20 from clasts (Fig. 6; Table 1). For 16 clasts, the average composition was determined (App. A, Tables 4 – 6). Mineral compositions totaling between 97 and 101 wt.% are considered reliable analytically. For the average composition of clasts, the totals are lower (96-100 wt. %) due to the highly fractured surface influencing the measurements.

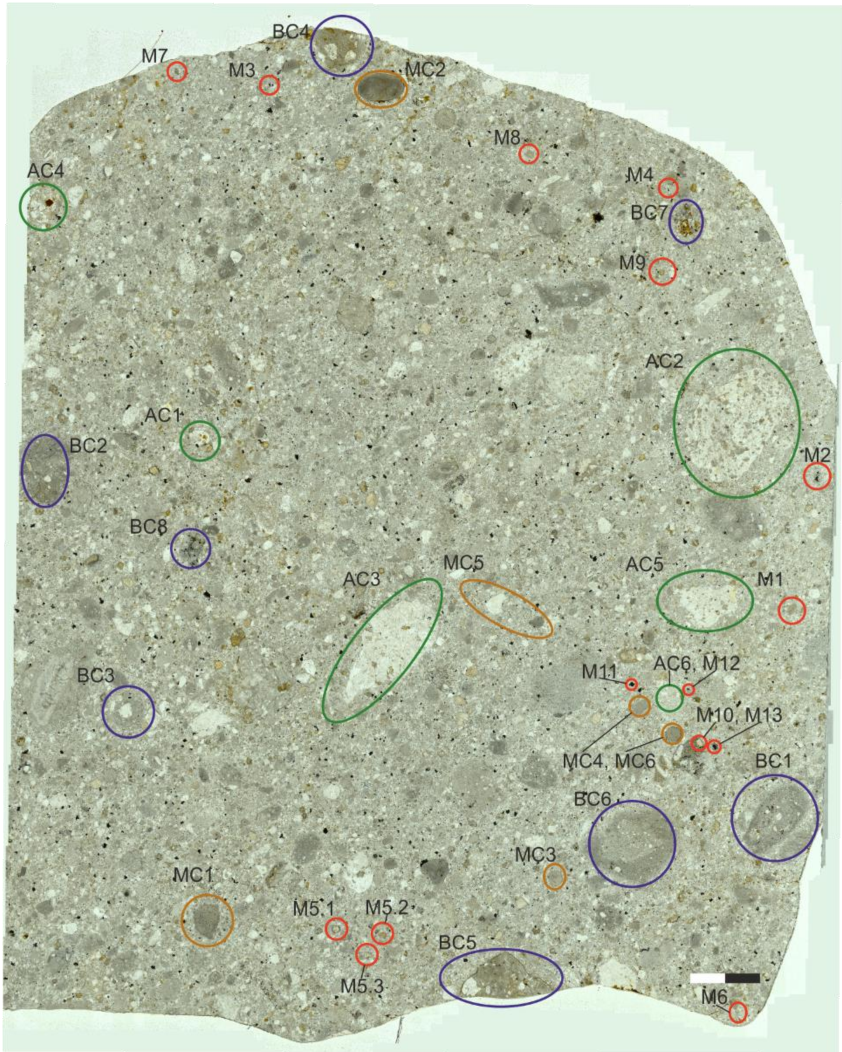

Fig. 6. Plane polarized light image of NWA 15352 with SEM analysis locations. Anorthosite clasts (AC) – green, breccia clasts (BC) – blue, melt clasts (MC) – light brown, mineral fragments (M) – red.

*Table 1. Feldspar, olivine and pyroxene compositions of different lithic clasts from NWA 15352. Mg# - Mg/(Mg+Fe)*100*

Clast type	Clast	Pl					Ol					Px				
		An	Ab	Or	An average	Pl Mg#	Fo	Fa	Tp	Fo average	Ol Mg#	En	Fs	Wo	Cpx Mg#	Opx Mg#
Anorthosite clast	AC1	95-96	4-5	-	96	48.50	60-79	21-40	0-0.44	70	60-79	57	30	13	-	65
Anorthosite clast	AC2	95-96	4-5	-	96	-	59-60	40	0.35-0.44	60	60	55-58	29-30	12-16	-	65-66
Anorthosite clast	AC3	85-98	2-13	0-1	92	-	60-62	38-39	0.28-0.52	61	61-62	45-61	17-32	8-37	66-72	66-74
Anorthosite clast	AC4	94-96	4-6	-	95	-	60-67	33-39	0.27-0.45	64	61-67	51-76	21-33	4-16	-	64-79
Anorthosite clast	AC5	95-97	3-5	-	96	-	59	40	0.36-0.54	59	60	58-60	31-33	7-11	-	65
Anorthosite clast	AC6	96	4	-	96	-	60	40	0.36	60	62	44-63	16-27	10-40	71-74	70
Breccia clast	BC1	93-94	6-7	-	94	0-46	60	39-40	0.29-0.45	60	60	57	31	13	65	-
Breccia clast	BC2	92-93	7-8	-	93	0-38	61	39	0.47	61	61	60	33	8	-	65
Breccia clast	BC3	95-98	2-5	-	97	-	60	39	0.36-0.48	60	60	35	31	34	-	67
Breccia clast	BC4	91-96	4-8	0-2	94	0-43	62	38	0.36	62	62	56	27	17	-	67
Breccia clast	BC5	94-98	2-6	0-1	96	0-44	64-76	24-36	0.0.31	70	64-76	43-60	17-31	9-40	66	72
Breccia clast	BC6	95-96	4-5	0-1	96	0-48	56-60	40-43	0-0.47	58	56-60	57-58	31-33	9-11	-	64-65
Breccia clast	BC7	90-97	3-9	-	94	0-64	61	38-39	0.34-0.40	61	61-62	49-64	21-32	4-30	67-70	66-68
Breccia clast	BC8	91-93	7-9	-	92	0-38	60	39	0.28-0.46	60	61	64-65	31	4-5	-	67-68
Melt clast	MC1	94	6	-	94	51-55	-	-	-	-	-	58	31	11	-	65
Melt clast	MC2	94-95	5-6	-	95	-	62	38	0.39	62	62	44-45	18-21	35-37	71-72	-
Melt clast	MC3	91-96	4-9	-	94	0-50	59	40-41	0.0.47	59	59-60	68-66	31-32	3-10	-	65-68
Melt clast	MC4	92	7	1	92	40.00	60-61	39	0.33-0.63	61	60-61	58-59	29-31	9-13	-	65-67
Melt clast	MC5	91-93	7-8	0-1	92	39-41	60	40	-	60	60	60-61	31	9	-	66
Melt clast	MC6	95-97	3-5	-	4	0-40	59	41	0.41	59	59	58-59	29-33	9-13	-	64-66

4.2.1 Mineral fragments in the matrix

The chemical composition of these minerals was obtained: plagioclase, olivine, pyroxene, ilmenite, spinel, Cr-rich spinel, Mg-rich spinel, and sulfide (troilite). Composition of all the studied mineral clasts are shown in app. A, Tables 28 – 39. Troilite and FeNi metals are affected by oxidation and give low wt.% values, thus for quantitative analysis, these minerals are not efficient.

Ca-rich plagioclase (An $_{89\text{-}97}$, Ab $_{3\text{-}9}$, Or $_{0\text{-}1}$; n=12) is the most abundant type of mineral fragments embedded in the matrix. The anorthite content in plagioclases varies from 89 to 97. The olivine (Fo $_{0\text{-}0.6}$, Fa $_{39\text{-}41}$, Tp $_{58\text{-}60}$; n=16) fragments show slight variations in chemical composition. The magnesium number Mg# ranges from 56 to 61 (app. A, Tables 28 – 39). Clinopyroxenes and orthopyroxenes are present. Some clinopyroxenes show compositional gradations being richer in Ca at the edges relative to their cores (Fig. 7 A, Table 31). The variation of composition of calculated end members in the clinopyroxene: En $_{0\text{-}50}$, Fs $_{1\text{-}46}$, Wo $_{23\text{-}45}$; n=7. Mg# ranges from 27 to 74 (Table 28 – 39). Orthopyroxene (En $_{52\text{-}82}$, Fs $_{0\text{-}35}$, Wo $_{2\text{-}42}$; n=10) also shows variation in chemical composition with the Mg# ranging from 61 to 86. Olivine and pyroxene have angular shape, and size varies in a wide range (10-300 μm). Apart from the mineral fragments mentioned above, less abundant minerals were identified, indicating more complex structures associated with secondary chemical reactions (Fig. 7).

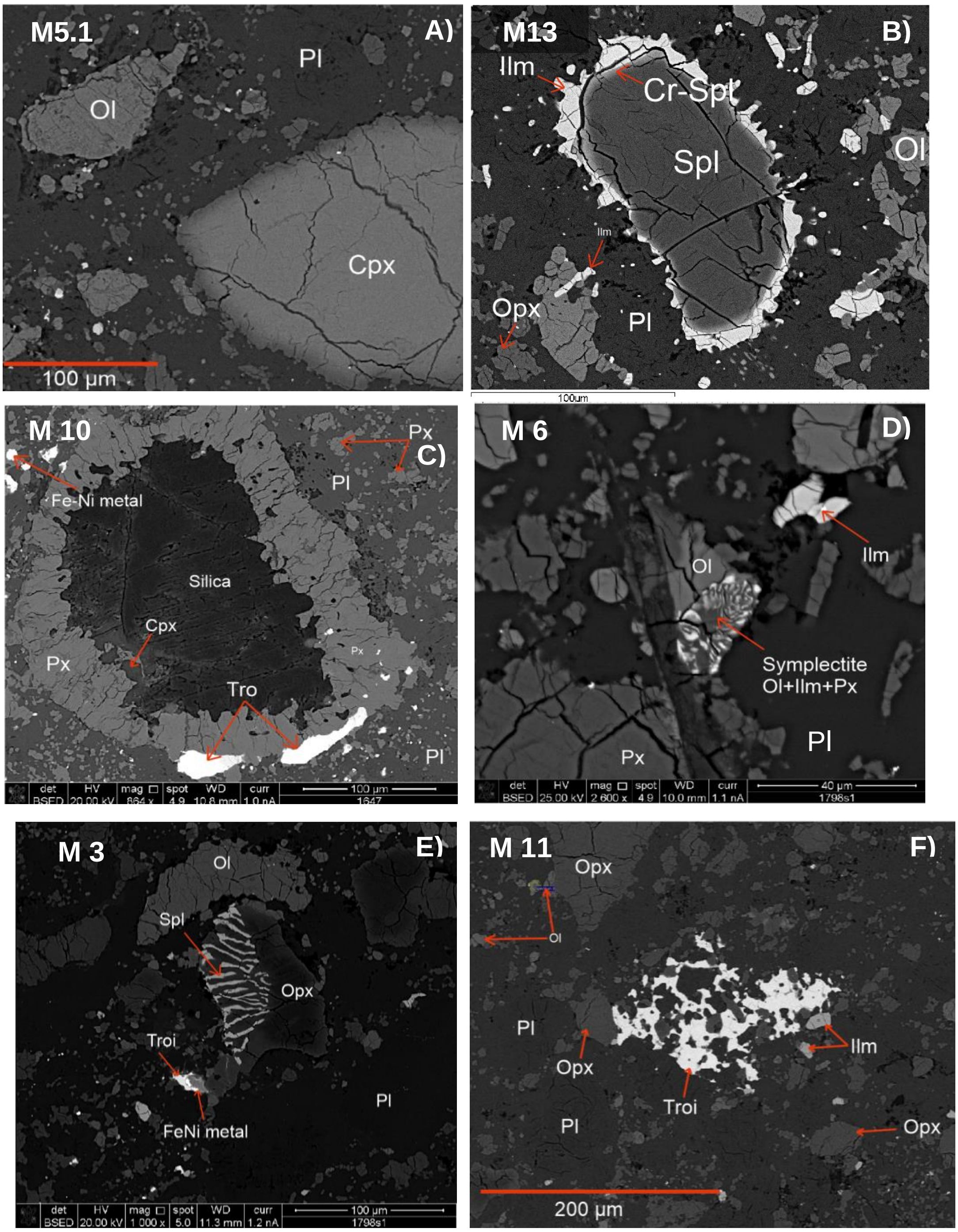

Fig. 7. Backscattered images (BSE) of mineral fragments (M). Plagioclase (Pl), olivine (Ol), pyroxene (Px), orthopyroxene (Opx), clinopyroxene (Cpx), spinel (Spl), Cr-rich spinel (Cr-Spl), ilmenite (Ilm), troilite (Troi), quartz (Qtz).

Some spinel fragments found in the matrix near the edge are enriched in Cr and surrounded by an ilmenite rim (Fig. 7 B; app. A, Table 39). The magnesium number in the spinel near the edge is lower (edge: Mg# 38, middle: Mg# 53) compared to the middle part (App. A, Table 39). Pyroxene with a silica melt inside was found (Fig. 7 C; app A, Table 36) as well as in a symplectite composed of olivine, ilmenite, and pyroxene (Fig. 7 D; app. A, Table 32), and exsolution with spinel and pyroxene (Fig. 7 E; app. A, Table 29). Sulfides (troilite) are common in the matrix usually forming large (~200 μm) mineral fragments compared with others (Fig. 7 F; app. A, Table 37).

4.2.2 Rock clasts

Compositions of all the studied rock clasts are shown in app. A, Tables 7 – 27. The summary of compositions is shown in Table 1. Anorthosite clasts consist of Ca-rich plagioclase (An_{85-98}, Ab_{2-13}, Or_{0-1}, n=19) (Table 1). Olivine consists of Fo_{59-79}, Fa_{21-40}, $Tp_{0-0.6}$; n= 22. The magnesium number varies between 60 and 79. Clinopyroxene consists of En_{46-58}, Fs_{17-30}, Wo_{13-37}; n=2. The magnesium number (Mg#) varies between 66 and 72. Orthopyroxene consists of En_{47-75}, Fs_{16-33}, Wo_{3-36}; n=17. The magnesium number varies between 64 and 79. Olivine and pyroxene are of euhedral-subhedral shape and vary in size between 50 μm and 250 μm (Fig. 8). Some pyroxene and olivine have a skeletal texture (Fig. 8 B).

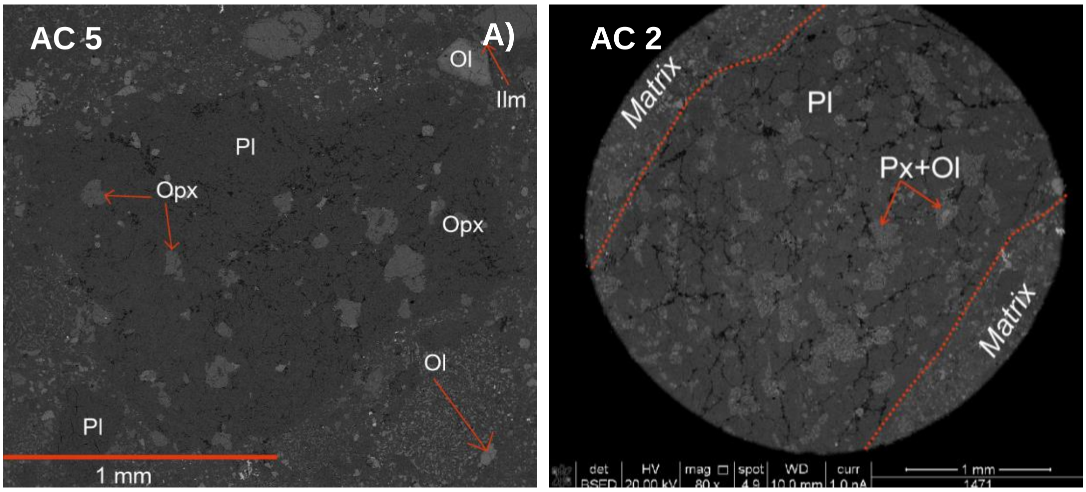

Fig. 8. Backscattered images (BSE) of anorthosite clasts (AC). Plagioclase (Pl), olivine (Ol), pyroxene (Px), orthopyroxene (Opx), and ilmenite (Ilm).

Melt clasts that are found in the matrix consist of anhedral, very fine-grained (~5-10 μm) olivine and pyroxene minerals together with plagioclase occupying the remaining space (Fig. 9 A – B). A few euhedral ilmenite minerals can be recognized (Fig. 9 B). Some melt clasts have a skeletal texture where olivine and pyroxene form needle-shaped, elongated, very fine-grained (10-50 μm) minerals (Fig. 9 A). Plagioclase in the melts clasts consists of An_{90-97}, Ab_{3-9}, Or_{0-1}; n=13. Melt clasts show more differences in chemical composition compared to the anorthosite clasts. In the melt clasts, magnesium number (Mg# 38-55) increases compared to the plagioclase clast Mg#=0 (Table 1). In the melt clasts olivine consists of Fo_{59-61}, Fa_{37-41} Tp_{0-1}; n= 11; Mg=59-61. Clinopyroxene (En_{44-45}, Fs_{18-21}, Wo_{35-37}; n=2; Mg#=71-72) was found only in MC 2 melt (app. A, Table 16). Orthopyroxene consists of En_{58-66}, Fs_{29-33} Wo_{4-13}; n=13; Mg#=64-68 (Table 1).

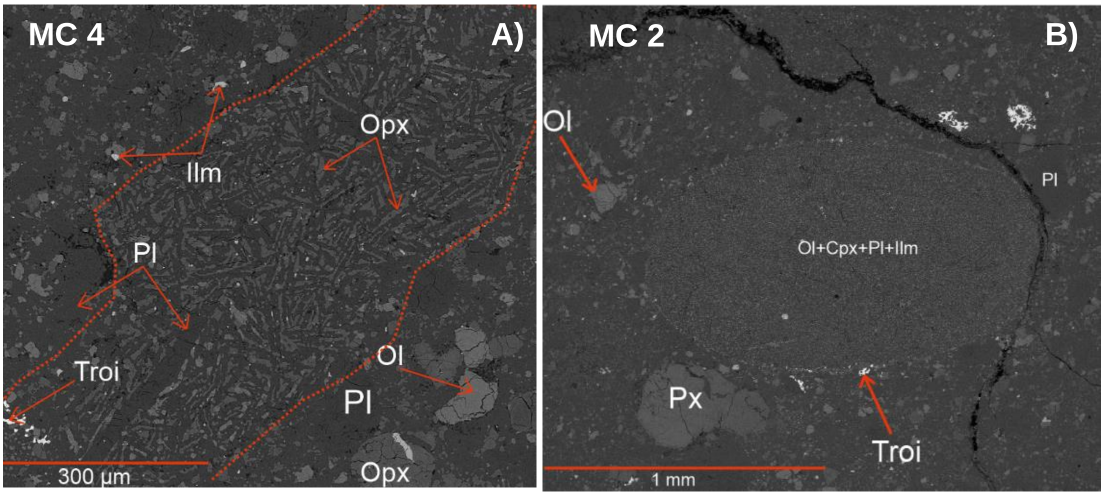

Fig. 9. Backscattered images (BSE) of melt clast (MC). Plagioclase (Pl), olivine (Ol), orthopyroxene (Opx), clinopyroxene (Cpx), ilmenite (Ilm), troilite (Troi).

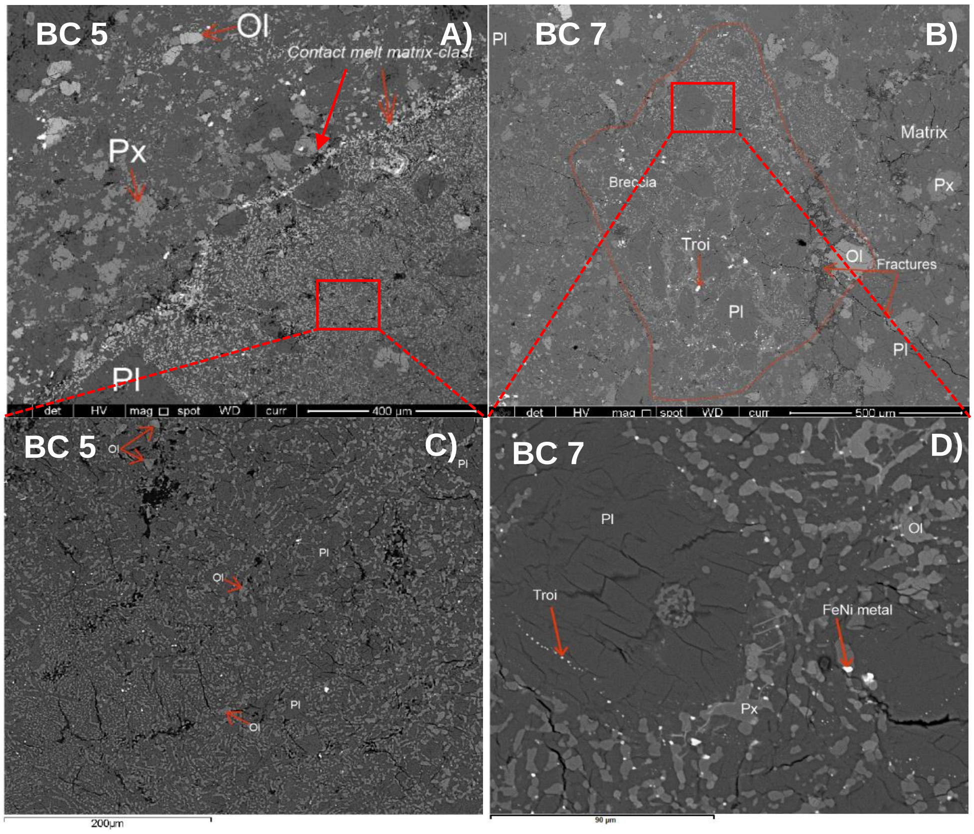

Fig. 10. Backscattered images (BSE) of breccia clasts (BC). Plagioclase (Pl), olivine (Ol), pyroxene (Px), ilmenite (Ilm).

Inside the breccia clasts, angular shaped plagioclase fragments are embedded in a fine grained (~10-30 µm) matrix composed of olivine, pyroxene, and plagioclase (Fig. 10). Plagioclase fragments vary in size between ~50 µm and ~150 µm. Plagioclase consists of An $_{90-97}$, Ab $_{2-7}$, Or $_{02}$; n=22 (Table 1). Olivine consists of Fo $_{56-75}$, Fa $_{24-43}$, Tp $_{0-1}$; n= 17; Mg#=56-76. Clinopyroxene consists of En $_{35-60}$, Fs $_{21-31}$, Wo $_{9-30}$; n=7; Mg#= 53-70. Orthopyroxene consists of En $_{43-64}$, Fs $_{16-32}$, Wo $_{4-40}$; n=11; Mg#= 64-72 (Table 1).

4.3 SIMS Pb-Pb age

For a SIMS Pb-Pb dating, only one clast was chosen from the NWA 15352L section that contains enough phases to ensure data quality and avoid large uncertainties. The other thick sections are shown in app. C, Fig 26. The clast is a basaltic clast containing phases (phosphate, K-rich glass, and plagioclase) that are rich in Pb necessary for Pb-Pb dating (Fig. 11).

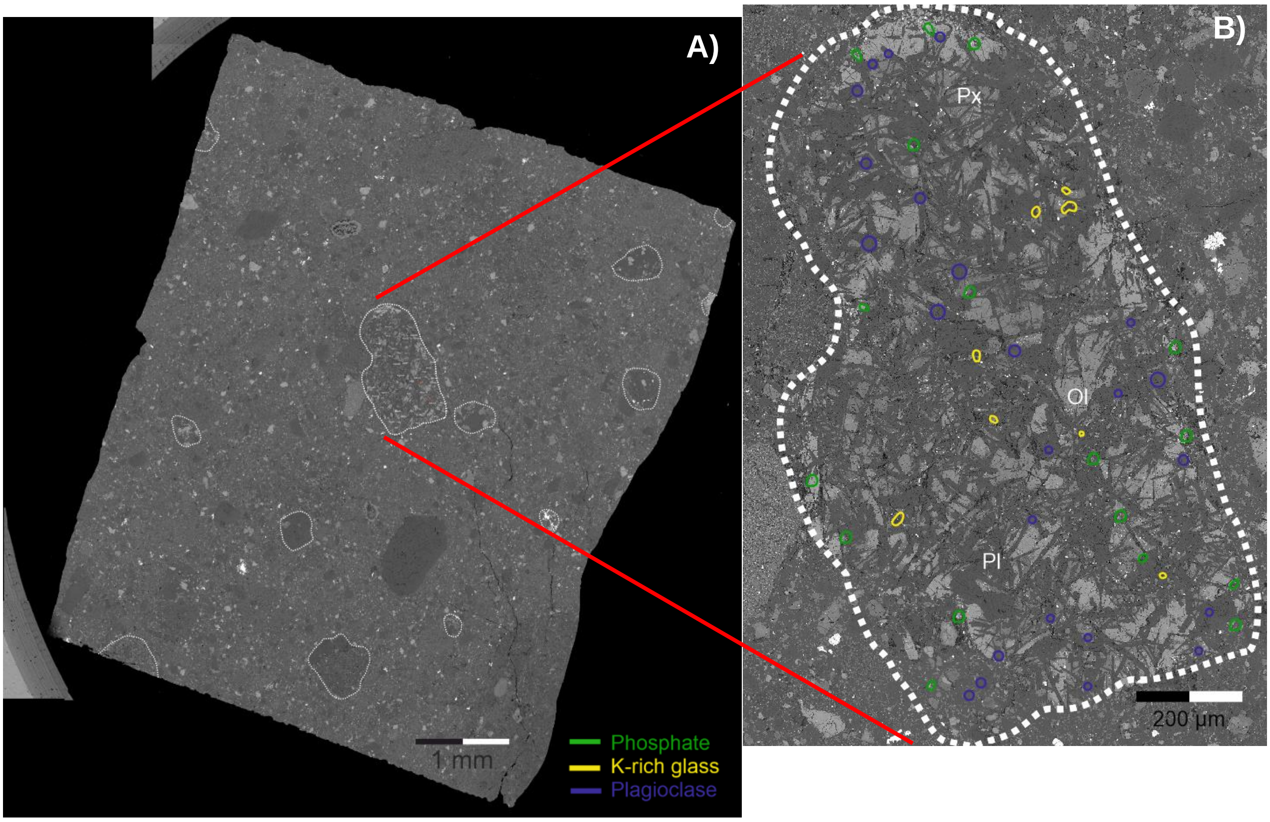

Fig. 11. **A**. BSE image of the NWA 15352L thick section with clasts. **B**. BSE image of basaltic clasts with targets used for the Pb-Pb dating (green – phosphate, yellow – K-rich glass and blue – plagioclase), white dash-lined area shows clasts embedded in the matrix.

The grain sizes in the clast are from 10 µm to 20 µm. Fifty-six Pb isotopic analyses were made in these phases. The data for each target in the clast was first filtered following the procedure described above (Snape et al., 2016) to remove analyses affected by the terrestrial contamination that could occur during the weathering before the sample was collected, sample preparation or polishing. Compared to the Apollo basalts, the investigated clast has more terrestrial Pb contamination (Snape et al., 2016). The SIMS Pb-Pb results for the grains of phases are shown in Table 2. A mean 3846 ± 44 Ma (2σ and MSWD = 0.93) $^{207}Pb/^{206}Pb$ age was calculated for the clast (Fig 12). The age corresponds to the Imbrium period (3.72-3.93 Ga; Neal et al., 2023).

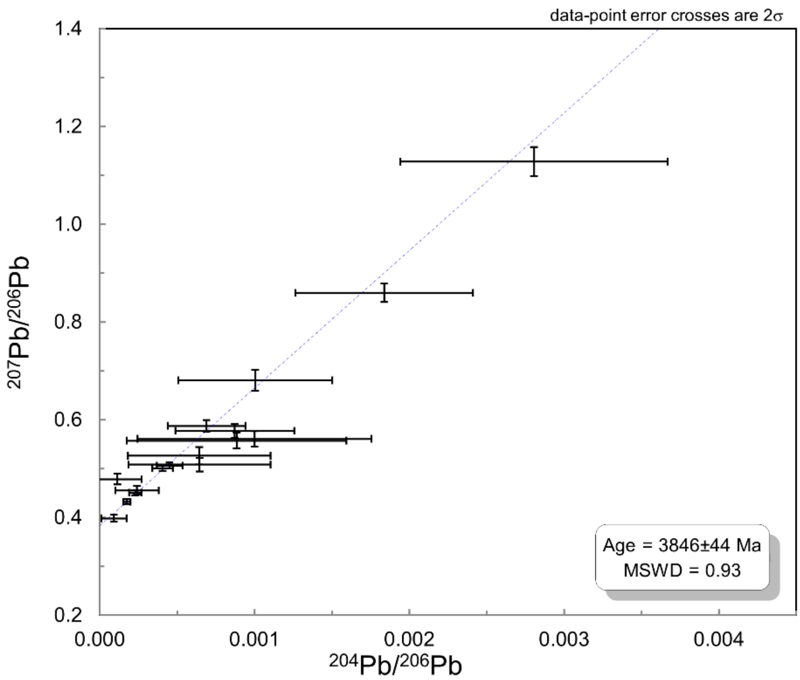

Fig. 12. Pb-Pb isochron determined by the SIMS for the basaltic clast. Error bars represent the 95% confidence level.

Table 2. SIMS Pb-Pb data for the phosphate, K-rich glass, and plagioclase minerals in a basalt clast.

Sample Name/analysed phase/analysis number	204 cps[a]	1se(%)[a]	206 cps	1se(%)	208Pb/206Pb[b]	1se(%)[b]	204Pb/206Pb[a,b]	1se(%)[a,b]	207Pb/206Pb[a]	1se(%)[a]	Phase
NWA152352,L Pb-iso_plag1	0.06	15.08	23.20	23.197	0.83822	1.18	0.00281	15.39	1.12784	1.31	Plagioclase
NWA152352,L Pb-iso_plag2	0.04	24.54	36.38	36.383	0.66148	1.81	0.00100	24.74	0.68070	1.58	Plagioclase
NWA152352,L Pb-iso_phos4	0.02	34.69	3.79	3.793	0.85958	1.94	0.00421	34.89	0.99725	1.89	Phosphate
NWA152352,L Pb-iso_plag8	0.02	35.36	23.62	23.617	1.23086	2.18	0.00064	35.83	0.52626	1.68	Plagioclase
NWA152352,L Pb-iso_plag9	0.03	32.89	15.22	15.221	0.84173	1.49	0.00200	33.62	0.51415	1.64	Plagioclase
NWA152352,L Pb-iso_plag16	0.01	50.00	2.86	2.863	1.01293	2.06	0.00354	50.25	0.50555	2.51	Plagioclase
NWA152352,L Pb-iso_phos9	0.07	15.43	38.14	38.143	1.09774	1.14	0.00184	15.60	0.85955	1.10	Phosphate
NWA152352,L Pb-iso_phos10	0.02	30.43	28.64	28.643	1.26506	1.23	0.00076	30.51	0.51246	1.35	Phosphate
NWA152352,L Pb-iso_phos11	0.01	25.00	42.14	42.140	0.83211	1.39	0.00035	25.03	0.43137	1.00	Phosphate
NWA152352,L Pb-iso_phos13	0.02	37.73	21.30	21.297	1.01814	1.31	0.00100	37.80	0.56075	1.41	Phosphate
NWA152352,L Pb-iso_phos15	0.01	40.00	13.62	13.620	0.88036	1.42	0.00088	40.10	0.55699	1.48	Phosphate
NWA152352,L Pb-iso_phos16	0.05	17.96	70.30	70.304	0.78772	1.32	0.00069	18.14	0.58723	1.01	Phosphate
NWA152352,L Pb-iso_phos17	0.02	28.87	88.57	88.571	1.40498	0.86	0.00024	28.95	0.45536	1.00	Phosphate
NWA152352,L Pb-iso_phos18	0.03	26.13	27.81	27.807	0.63576	1.27	0.00104	26.20	0.51793	1.25	Phosphate
NWA152352,L Pb-iso_phos19	0.02	31.62	2.92	2.919	1.10384	1.84	0.00578	32.05	0.77607	2.20	Phosphate
NWA152352,L Pb-iso_kglass1	0.22	8.61	958.42	958.420	0.70469	0.49	0.00023	8.67	0.45085	0.56	K-rich glass
NWA152352,L Pb-iso_kglass2	0.21	8.94	461.19	461.195	1.70686	1.12	0.00045	9.15	0.50605	0.62	K-rich glass
NWA152352,L Pb-iso_kglass3	0.01	68.60	49.34	49.337	0.87296	1.04	0.00011	68.69	0.47817	1.14	K-rich glass
NWA152352,L Pb-iso_kglass4	0.01	44.10	114.47	114.472	0.59181	1.02	0.00009	44.12	0.39810	0.88	K-rich glass
NWA152352,L Pb-iso_kglass5	0.35	5.99	2005.22	2005.219	0.76752	1.41	0.00018	6.24	0.43199	0.56	K-rich glass
NWA152352,L Pb-iso_kglass6	0.42	8.09	1057.52	1057.523	0.72964	0.52	0.00041	8.12	0.50095	0.57	K-rich glass
NWA152352,L Pb-iso_kglass7	0.02	35.36	23.54	23.541	0.79827	1.50	0.00064	35.50	0.50800	1.36	K-rich glass
NWA152352,L Pb-iso_kglass8	0.11	14.14	220.55	220.553	0.74292	0.81	0.00048	14.20	0.47939	0.86	K-rich glass
NWA152352,L Pb-iso_plag27	0.01	44.72	39.20	39.200	0.49725	1.38	0.00031	44.98	0.42048	1.26	Plagioclase
NWA152352,L Pb-iso_plag32	0.05	21.82	60.94	60.937	0.97527	1.23	0.00087	22.02	0.57729	1.23	Plagioclase

5 DISCUSION

5.1 Petrography and SEM results

Petrological investigations confirm that the meteorite NWA 15352 originates from the Moon. This confirmation is based on the following measurements and arguments:

1. Dominance of plagioclase with high Ca (An >90%), olivine, and pyroxene, and lacking minerals that contain water (Lucey et. al., 2006).
2. The presence of FeNi metals, as well as a high content of ilmenite, is rare in terrestrial rocks (Weyer et al., 2005).
3. The Fe/Mn atomic ratios of pyroxene plot close to the lunar line and are noticeably different from other planets, Earth or asteroids rocks (Fig. 13; Jolliff et al., 2006).

Fe/Mn ratio is commonly used as a fingerprint of meteorite origins. The ratio increases with a distance from the Sun, probably related to heating events in the early solar system (Papike et al., 2003).

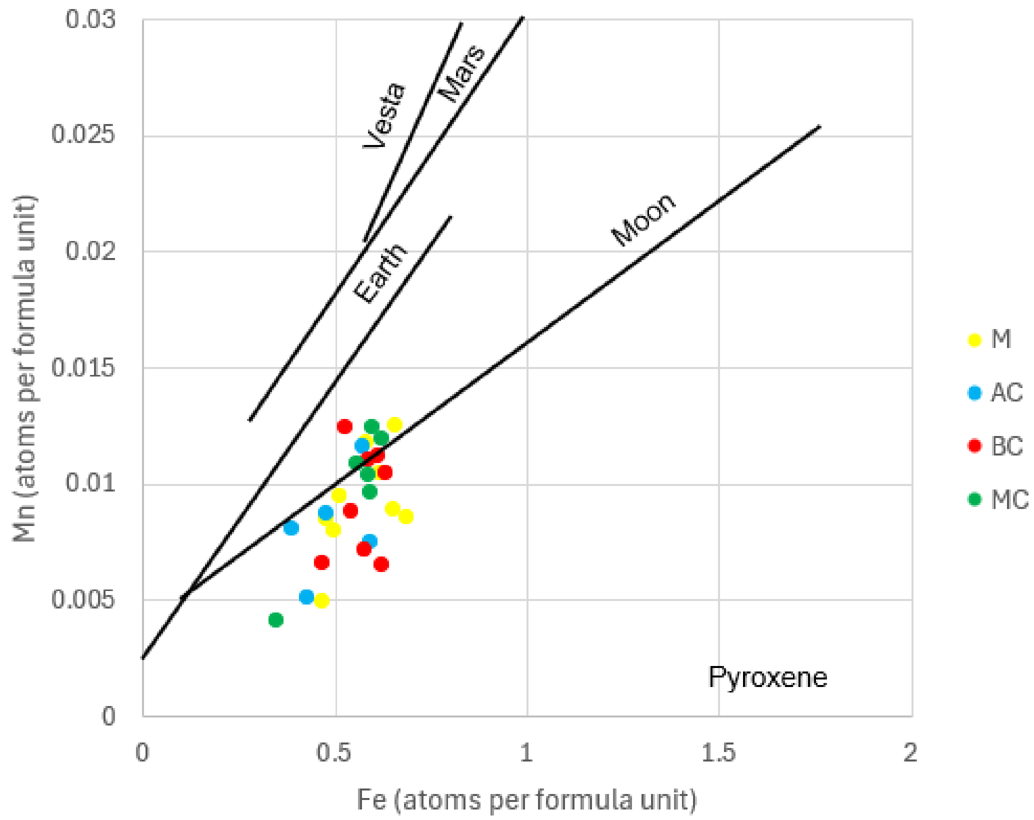

Fig. 13. Plot of Fe versus Mn (in atomic formula units) for clasts in the NWA 15352. Fe/Mn ratios support a lunar origin for this meteorite. M – mineral fragment, AC – anorthosite clast, BC – breccia clast, MC – melt clast (applied after Xia et al., 2021).

5.1.1 Fragment and microstructure interpretation of the NWA 15352

Detailed petrological and microstructure investigations by the polarizing and scanning electron microscopes reveal the textural and chemical complexity and show inhomogeneous distribution of different clasts. Features such as fractures on the sample surface, angular shaped rock clasts, and mineral fragments are common among other lunar meteorites (Taylor et al., 1991). They are the result of multiple meteorites impacts that shattered, crushed, and melted material on the Moon's surface and shallower depths. Based on the abundances of An content in plagioclase and Mg# content in mafic minerals (olivine and pyroxene), clasts and mineral fragments are closely related to the composition of ferroan anorthosite (FAN) suite (Fig. 14). These results indicate that all the clasts and fragments share similar origins as the FAN and belong to the lunar highlands representing ancient lunar crust that may have originated from the early crystallization and differentiation of the Lunar Magma Ocean (LMO) (Shearer, 2006). Abundant Ca-rich (An>90) plagioclase strongly supports this assumption because the highland anorthosites have distinguishable high An>90 values (Fig. 15).

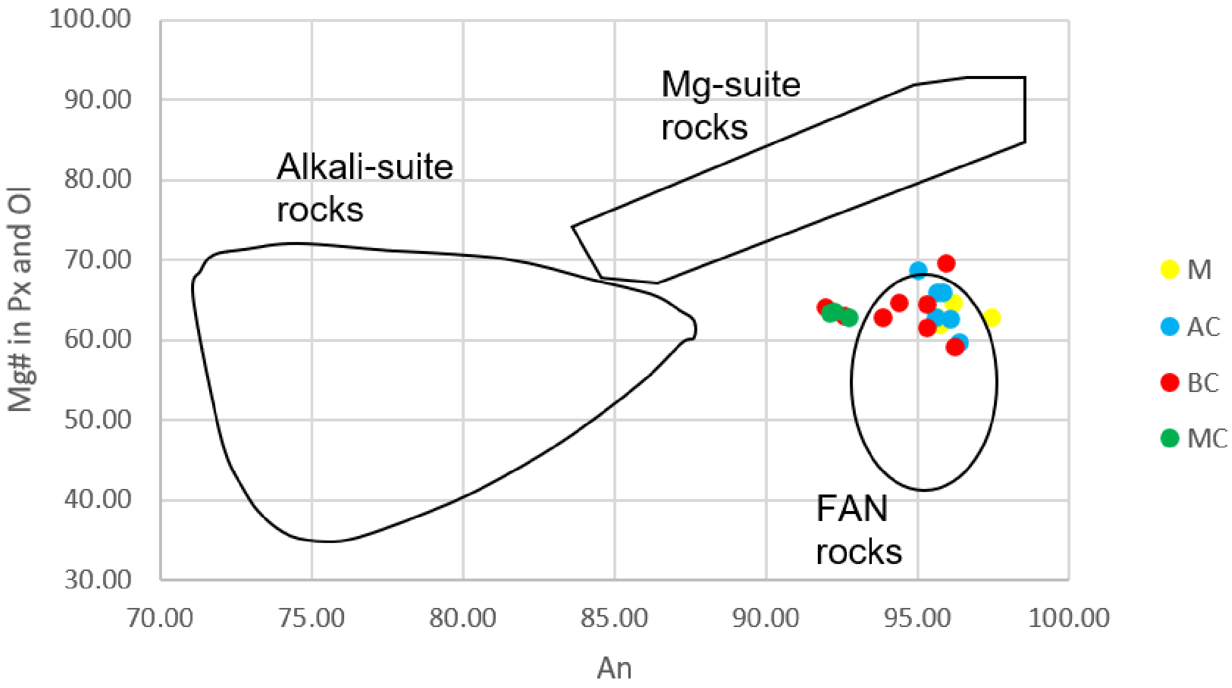

Fig. 14. Anorthosite content An# (Ca/[Ca+Na+K]) in plagioclase vs Mg# (Mg/[Mg+Fe]) in mafic minerals (olivine and pyroxene), FAN rocks – ferroan anorthosite (applied after Nagoaka et al., 2013).

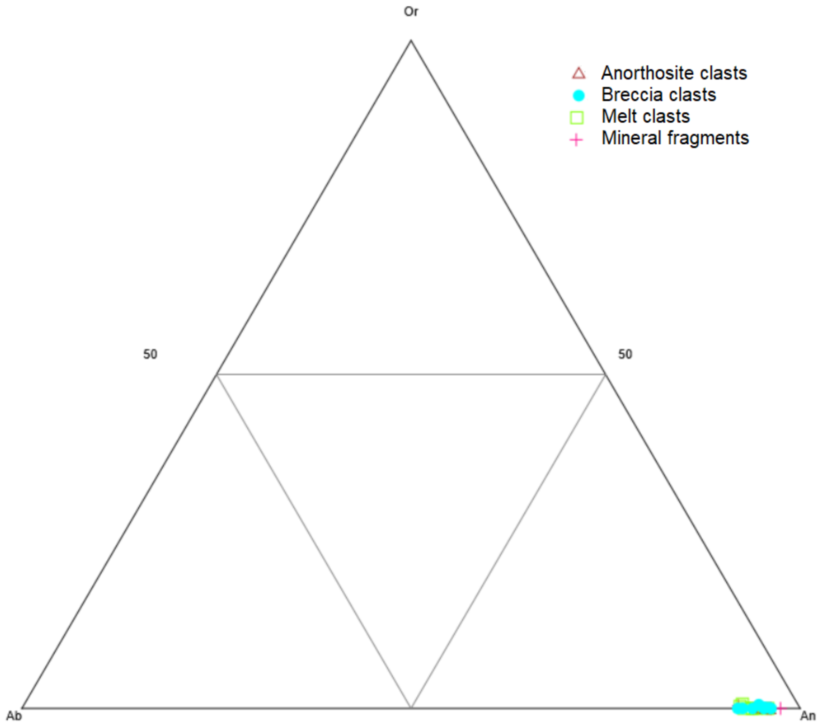

Fig. 15. Composition of feldspar in the mineral fragments and clasts.

The variation of Mg# in major mineral phases (Ol, Px and Pl) among the clasts (Table 1) may represent changes in composition of parent melt during crystallization processes or post-crystallization processes associated with impact events (Lucey et al., 2006). Pyroxenes and olivines show narrow range in chemical distribution (Fig. 16). Pyroxenes belong to the augite and pigeonite fields that are richer in Ca and Mg, while olivine composition varies less, probably due to its ability to crystallize first from the melt or the similarity in chemical composition to the parent magma source (Fig. 16). The NWA 15352 pyroxenes show similar chemical compositions with other lunar meteorite pyroxenes, i.e. NWA 773, NWA 6950, NWA 79848, Dhofar 1428 (Zeigler et al., 2007; Bao et al., 2020; Zeng et al., 2018, Xue et al., 2019).

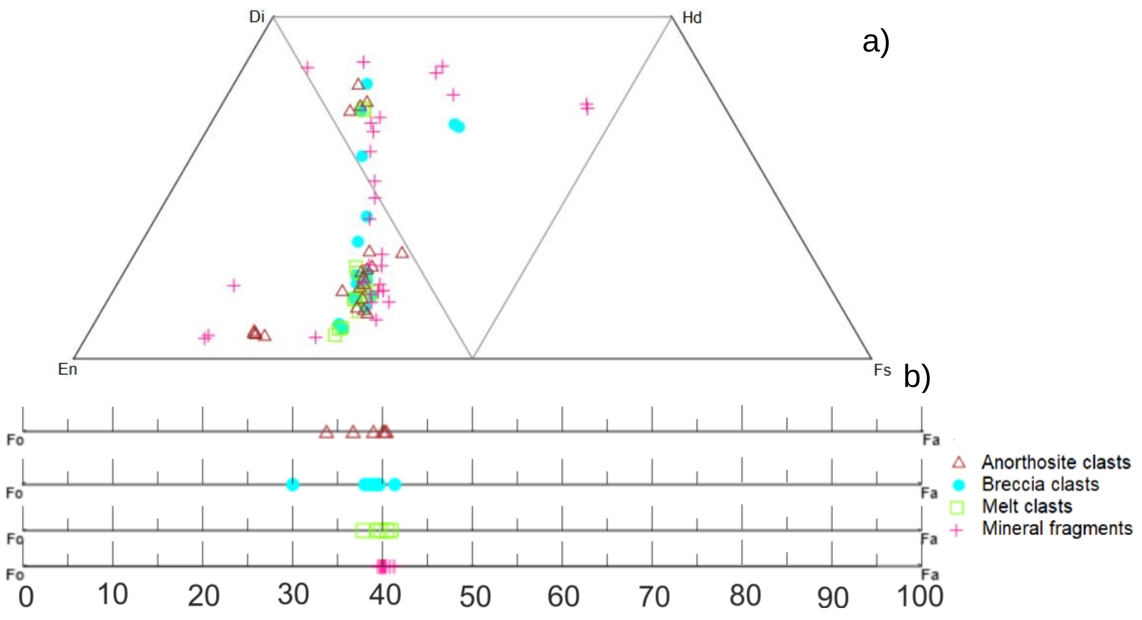

Fig. 16. Compositions of pyroxene (a) and olivine (b) in the mineral fragments and clasts in NWA 15352.

A Mg-rich spinel fragment in the matrix with a Cr-rich rim found in the NWA 15352 (Fig. 7B) may indicate that it comes from the upper mantle and has experienced later post-magmatic alteration related to a thermal event (Wittmann et al., 2019). There is a common agreement that the presence of Mg-rich spinel in a lunar sample may be associated with the basin forming impact event that excavated the deep seater material from the upper mantle by the basin forming impact (Wittmann et al., 2019). Large impacts responsible for the formation of impact basins (> 300 km in diameter (Wilhelms et al., 1987)) are likely big enough to excavate rocks from the upper mantle (e.g., Imbrium basin, which is 1123 km in diameter), at least in those areas where the crust is thin enough. For example, the average thickness of lunar crust is 34 km based on recent modeling of geophysical data from the GRAIL (Gravity Recovery and Interior Laboratory) spacecraft (Wieczorek et al., 2013). To excavate material from these depths, the crater diameter should be at least ~400 km (Cintala and Grieve 1998). Orbital remote sensing data also reveals wide occurrence of Mg-rich material exposed in central peaks of craters in both near and far sides of the Moon indicating exposed mantle rocks at the lunar surface (Saranya et al., 2018).

Based on Al# versus Mg plot, one spinel grain (M13, Fig. 7B) is situated in the PST (pink spinel troctolite) field (Fig. 17). According to other studies, Mg-spinels belonging to this field are interpreted as a result from the interaction between Mg-rich lunar mantle melt and the anorthosite crust (Chen et al., 2023), while Cr-spinel rims might form from the residual melt depleted in Mg and Al and enriched in Fe and Cr after the crystallization of the anorthite and Mg-rich olivine (Xia et al., 2024). The fact that Cr-spinel formation was not caused by the leading impact event is that these Cr-spinels are highly resistant to post-magmatic alterations, including metamorphism (Saranya et al., 2018). In general, these spinels give insights into understanding of the mantle and crust-mantle interaction processes and geodynamic evolution of the Moon. However, other studies have shown that Mg-rich spinel could crystallize from Mg-Al-rich melt produced by impact melting of Mg-rich anorthosite precursor (Lan et al., 2024). Fig. 17 gives a clue that spinels in the matrix and lithic fragments come from different sources. They are significantly enriched in Cr (Cr# 70) (Table 3). It may indicate an origin from mare basalts, because most spinels found in the mare basalt from Apollo samples tend to be rich in Cr (Papike et al., 1976).

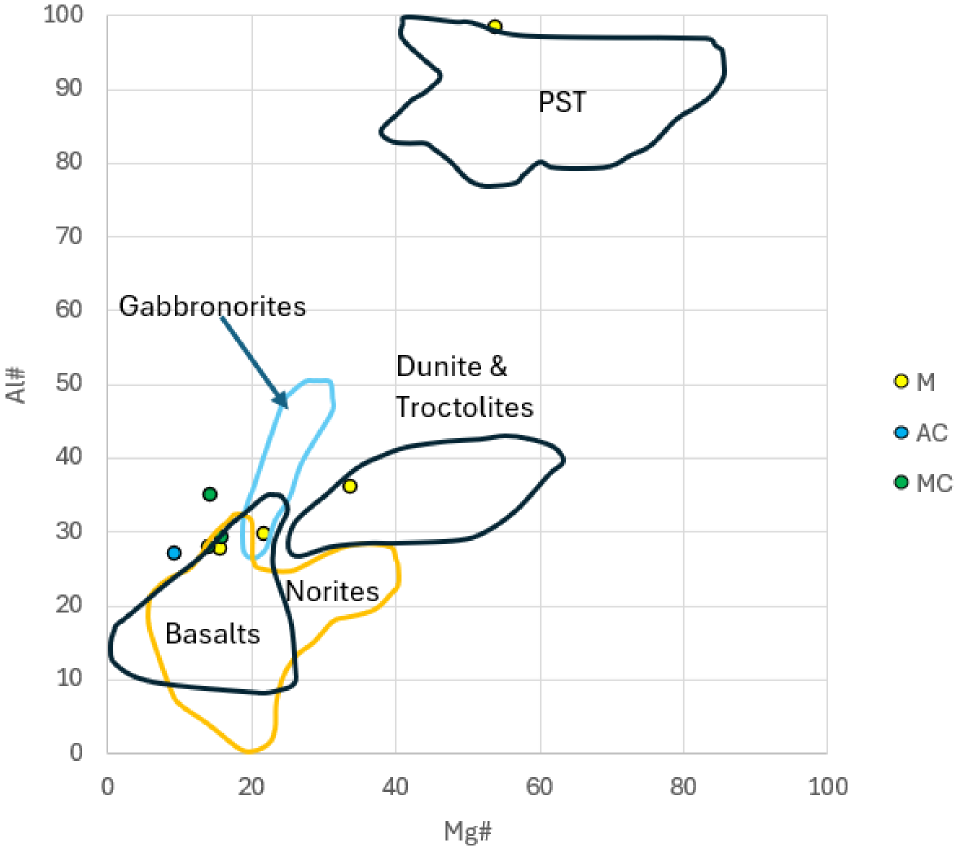

*Table 3. Mg# (Mg/(Mg+Fe)x100, Al#(Al/Al+Cr)x100 and Cr#(Cr+Al)*100 distribution between lithic clasts and mineral fragments. M – mineral fragment, AC – anorthosite clast, MC – melt clast.*

Name	Mg#	Al#	Cr#
M13	54.00	98.27	25.08
M8	21.98	29.54	70.46
M6	33.99	36.10	63.90
M3	15.82	27.68	72.32
AC1	9.51	26.96	73.04
MC6	14.15	27.74	72.26
MC4	14.34	34.93	65.07
MC1	15.92	29.16	70.84

Fig. 17. Mg# versus Al# of spinel in the NWA 15352. Mg# (afu [Mg/(Mg+Fe)]x100), Al# (afu [Al/Al+Cr)]x100), afu – atoms per formula unit (applied after Xia et al., 2025).

The presence of breccia melt, impact glass, and pure FeNi metal fragments in the melt matrix corresponds to regolith breccia characteristics, indicating that NWA 15352 might be a polymictic regolith breccia that has been formed through impact mixing of lunar lithologies in a near-surface regolith environment (Taylor et al., 1991). Additionally, petrological observations and chemical analysis confirm that NWA 15352 contains clasts from multiple sources that originated from both mare and lunar highlands (Figs. 14, and 17).

5.1.2 Shock effects of the NWA 15352

The detailed texture investigations provided clues indicating that the sample has experienced different degrees of separate shock events and partial remelting. The BC7 clast contains a small, rounded inclusion that might be the older breccia in a younger breccia (Fig. 10D). These breccia clasts contain mineral fragments that preserve information about older multiple generation impact events, giving much wider history about the sample.

Moreover, minerals can be used as natural barometry indicators, revealing how much pressure the rock experiences during the body impact. Based on classification for shock metamorphism, planar fractures of olivine and pyroxene and plagioclase mosaicism correspond to different degrees of shock effects (Fig. 4 and Fig. 5). Planar fractures appear in a 5 – 65 GPa range in olivine, while the plagioclase mosaicism indicates a 15 – 35 GPa range in plagioclase (Stöffler et al., 2017). If we follow progressive shock metamorphism with increasing pressure, textures will appear in this order: planar fractures → mosaicism. In this case, both minerals could indicate separate impact events. Whether plagioclases have clues indicating smaller or more distant impact events, olivines and pyroxenes indicate larger or closer impact events associated with higher pressure. Those mineral fragments that are rounded (e.g. Fig. 4 B) may have experienced high thermal events where the temperature was large enough to partially melt the mineral and can be associated with separate larger impact events or even the last impact event that is responsible for NWA 15352 final formation and ejection.

The BSE images reveal more clues about shock events. The symplectites found in the melt matrix (Fig. 7 D-E) might be a result of unstable minerals that breakdown when the pressure and temperature change. The most common theory suggests that these symplectites have formed during an impact event (Miao et al., 2014). Additionally, there are more processes of how symplectites might form. Some scientists argue that symplectites could crystallize from a residual magmatic melt together with some late-stage minerals such as plagioclase and phosphate (for example, mare basalts) (Oba et al., 2001; Miao et al., 2014). Since symplectites are found in the melt matrix in NWA 15352 far away from its original parent rock, their origin is unclear.

Other features indicating changes in pressure and temperature are quartz exsolutions in clinopyroxene found in one mineral clast (Fig. 7 C). According to Smyth (1980), silica exsolutions in clinopyroxene are a product of former supersilic clinopyroxene and appear in mafic and ultramafic rocks from the high-pressure environment (Haijun et al., 2015). Even though these Earth's analogues do not consider shock metamorphism, it's clear that changes in pressure and temperature are responsible for these features. The closest analogues were found in the Martian meteorite NWA 7533, where silica exsolutions are interpreted as cooling rate speedometers rather than shock indicators (Leroux et al., 2016).

To sum up, three types of lithic clasts (anorthosite clasts (AC), breccia clasts (BC) and melt clasts (MC)) identified in NWA 15352 show that they have formed at distinct times and, probably, their source locations were far away from each other before they all came together into one place and finally were ejected toward the Earth.

5.2 SIMS Pb-Pb age

The Pb-Pb isotope analysis conducted for the basalt clast in NWA 15352 provides a 3846 ± 44 Ma crystallization age and corresponds to the Imbrium period (3.72-3.93 Ga; Neal et al., 2023), which represents a time of Imbrium impact basin formation. Imbrium basin is located on the Moon near side – north hemisphere and can be visible from Earth by the naked eye (Fig. 19). These ages overlap (including ages uncertainties) with lunar basalt from the Apollo 11 and Apollo 17 rock samples and lunar basalt meteorite MIL 0535 that were dated by the same Pb-Pb method (Fig. 18). Even though ages are similar with the NWA 15352, the chemical composition of pyroxene shares similarities only with the Apollo 11 and Apollo 15 samples, but not with the MIL 05035 (Meyer et al., 2011; Zhang et al., 2010). It indicates that the MIL 05035 may have originated from a distinct region of provenance with unique basalt chemical properties.

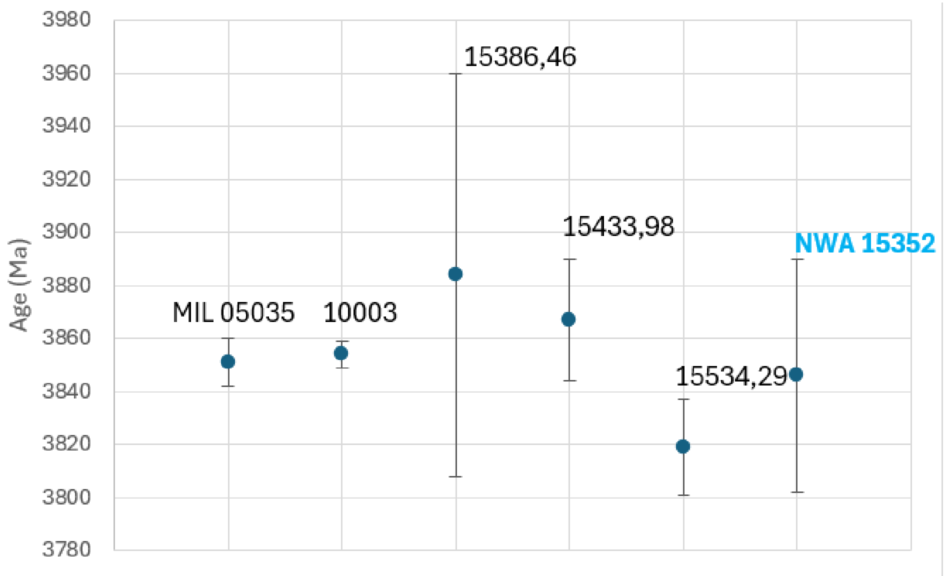

Fig. 18. Lunar basalt Pb-Pb ages (Apollo 11 basalts (10003), Apollo 15 basalts (15386,46; 15433,98; 15534,29)) including the NWA 15352. Error bars represent the 95% confidence level. Data from Snape et al., 2019; Snape et al., 2016; Fernandes et al., 2019; and MIL 05035 lunar basalt meteorite from Zhang et al., 2010.

5.3 Associations of the NWA 15352 with an impact event

Considering the NWA 15352 association with an impact event, it is important to note that basalt clast provides only crystallization ages, but not the age of an impact event. However, the obtained ages of 3846 ± 44 Ma are close to those corresponding to the impact event that formed the Imbrium basin (Nemchin et al., 2021). A large amount of released energy caused by a huge impact inevitably initiates magmatism that finally fills the basin with basalt lava and forms so called “mares”. Thus, basalts could indirectly indicate a huge impact associated with the formation of an impact basin. Moreover, there are discussions that all, or nearly all, the 3.9 Ga impact melt rocks are products of a single event, the Imbrium basin-forming impact (Cohen, 2010). However, due to significant large age uncertainties of the NWA 15352 meteorite it’s difficult to assign it to this event. The age of NWA 15352 also correlates with a Late Heavy Bombardment (LHB) event that had happened between ~3.8 and 4.1 Ga where most of the craters were formed. The majority of lunar rocks are scattered around this time interval indicating that all collected samples were formed during this LHB event (Tera et al., 1974). During this short period, the largest lunar basins were formed. These two events of the Imbrium basin and LHB formation are related to each other in a way that the LHB might be leading to the formation of impact basins.

In any case, ages show the time when the basalt clast was crystallized, but not the last impact event that formed the NWA 15352 as it is today. The Ar-Ar isotope analysis could be used and give clues about the last thermal event, usually associated with the last impact event. It would be helpful to look at the relative ages of mare basalts estimated using crater counting techniques (Hiesinger et al., 2011). The determined basalt clast ages of NWA 15352 overlap with the ages of the mare basalt bodies in Mare Serenitatis (3.81 Ga), Mare Marginis (3.80/3.88 Ga), Mare Australe (3.80-3.88 Ga) and the area that belongs to the Imbrium Fra Mauro Unit (3.85 Ga) where the Apollo 14 was landed (Fig. 19). Considering that the NWA 15352 contains clasts associated with lunar highlands (FAN) and basalt clasts associated with mare basalts, the most likely source region for the NWA 15352 is an area at the mare-highland boundary.

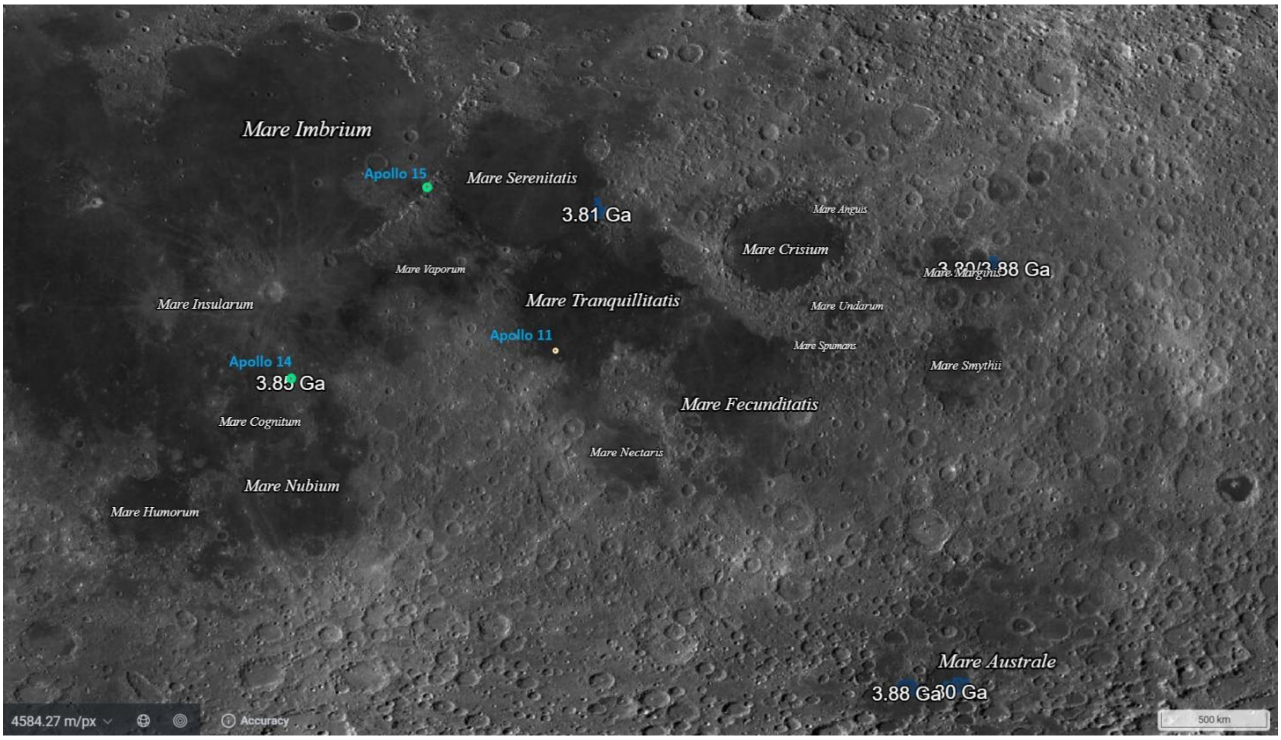

Fig. 19. Possible source locations of the basalt clast from NWA 15352 according to similar ages of the mare basalt units indicated in blue areas. The areas are estimated based on a crater size-frequency distribution model (Hiesinger et al., 2011). For data representation, https://quickmap.lroc.asu.edu/ was used.

Overall, it seems that NWA 15352 had a very complex history. The multiple impacts crushed, scattered through long distances, melted and mixed different rock lithologies. One clast has undergone several processes by forming a breccia clast, and probably is the oldest piece in the sample (Fig. 10 D). Other clasts were less affected by impacts and might have compositions closer to their parent rock sources, e.g. the anorthosite clasts or basalt clasts (Fig. 8 and Fig. 11). At some point, the impact clasts were included, indicating impact events large enough to melt a rock. The latest active processes are associated with a matrix melt formation, incorporating all clasts and mineral fragments.

5.4 Future insights

There are countless methods that can be applied for the NWA 15352, but only a few of them could provide the most relevant information:

A whole-rock chemical analysis could enable the comparison of the NWA 15352 to other meteorites with more confidence as well as the bulk composition could be used to compare with the remote sensing geochemical data (e.g., gamma ray spectroscopy data) to search for regions that are compositionally similar (Prettyman et al., 2006).

A trace element analysis in the basaltic clast of NWA 15352 would answer the question whether the basalt clasts contain KREEP elements and how many. The trace element analysis would additionally provide more insights into the sample origin. The KREEP abundances would be a strong argument that the sample came from somewhere in the PKT region, one of the Moon's near-side areas that are rich in KREEP elements (Fig. 1). Also, it would allow us to compare the trace element abundances with those from the Apollo samples and other lunar meteorites with more precision.

CONCLUSIONS

In this thesis, the results of detailed petrological and microstructure investigations of the meteorite NWA 15352 are presented performed. NWA 15352 is a lunar feldspathic breccia made of rock clasts and mineral fragments set in a melt rock matrix that represents common features among other lunar meteorites. Three types of clasts were identified: anorthosite clasts, breccia clasts, and melt clasts.

The presence of various types of clasts as well as pure FeNi metal fragments in a melt matrix shows similarities with a lunar regolith, confirming that NWA 15352 was formed through the impact mixing of different lunar lithologies. Fractures, angular shape of minerals, together with partially melted clasts in a matrix, indicate that NWA 15352 has experienced different degrees of multiple stage shock events associated with separate impact events.

The Pb-Pb isotope analysis for phosphates, plagioclase, and K-rich glass in NWA 15352 provides 3846 ± 44 Ma crystallization ages corresponding to the Imbrium period and might date Imbrium impact itself. These ages are contemporaneous with the ages of the Apollo 11 and Apollo 17 rock samples and the MIL 05035 ages. Compared with crater counting ages, the NWA 15352 overlaps with Mare Serenitatis, Mare Marginis, Mare Australe, and Fra Mauro Formation Unit near the Apollo 14 landing site.

Given the presence of clasts linked to the lunar highlands and basalt clasts associated with the mare basalts, the most probable source region for the NWA 15352 is an area at the boundary between mare and highland terrains. NWA 15352 was formed involving crushing, mixing, and remelting of different lithologies of lunar rocks, revealing its complex history.

ACKNOWLEDGEMENTS

First and foremost, I would like to thank Michail Ivanov, without his support, providing this precious lunar sample, all this thesis wouldn't be possible.

I would like to deeply thank my supervisors, Grazina Skridlaite and scientific advisor Victoria Peace, for supporting and guiding me on my MSc thesis topic and my first steps forward in this exciting study field, which opens doors to new opportunities. Many thanks to Victoria Peace; your contribution to my thesis is immeasurable. First, thank you for your response when I was seeking support to study the lunar sample, and for inviting me to conduct research at Stockholm University and Naturhistoriska Riksmuseet (NRM). Second, thank you for coordinating and organizing my research at the NRM, where I felt like a true scientist. Here, many thanks go to Martin Whitehouse for giving me the opportunity to use SEM and SIMS, such an amazing and complex machine. I would like to thank Cécile Deligny and your support in guiding me during those first days in the NRM and for all your support in helping with the SEM and SIMS analysis. Many thanks to Renaud Merle for finding his time to help me with SEM and SIMS analysis. Also, I would like to thank Laurynas Siliauskas for his effort and time teaching me to use SEM in the Nature Research Centre, Vilnius, and PhD student Olga Demina for your contribution.

Funding for the petrographic and SEM analyses performed at the Nature Research Center in Vilnius was provided by the Research Council of Lithuania (LMTLT), during the summer student internship program agreement No. P-SV-24-304.

REFERENCES

1. Bao, Z., Shi, Y., Anderson, J., Kennedy, A., Ke, Z., Gu, X., Wang, P., Che, X., Yuelan, K., Sun, H., & Wang, C. (2020). Petrography and chronology of lunar meteorite Northwest Africa 6950. Science China Information Sciences, 63(12), 1–10. https://doi.org/10.1007/s11432-019-2809-3Binder, A. B. (1998). Lunar Prospector: Overview. *Science, 281*(5382), 1475–1476.
2. Chandrana, S. R., Thesniya, P. M., Rajesh, V. J., & Govinda, A. (2018). Compositional diversity of lunar magmatic spinels: Implications for endogenic processes.
3. Cintala, M. J., & Grieve, R. A. F. (1998). Scaling impact melting and crater dimensions: Implications for the lunar cratering record—Errata. *Meteoritics & Planetary Science, 33*(6), 1343. https://doi.org/10.1111/j.1945-5100.1998.tb01320.x
4. Cohen, B. A. The impact history of the Moon. (2010). Space Science Office, VP62, NASA Marshall Space Flight Center.
5. Fernandes, V. A., Czaja, P., Fawcett, L., Fonseca, R. O. C., Khan, A., Liebske, C., Nemchin, A., Sliwinski, J., Snape, J., Whitehouse, M., & Willbold, M. (2019). Investigating volcanism within Imbrium and Serenitatis basins: A systematic study of basaltic regolith fragments. *2nd Annual Meeting of The Meteoritical Society 2019 (LPI Contribution No. 2157)*.
6. Gattacceca, J., McCubbin, F. M., Grossman, J. N., Schrader, D. L., Chabot, N. L., D'Orazio, M., Goodrich, C., Greshake, A., Gross, J., Joy, K. H., Komatsu, M., & Miao, B. (2023). The Meteoritical Bulletin, No. 111. *Meteoritics & Planetary Science*, *58*(4), 901–904. https://doi.org/10.1111/maps.13995
7. Grossman, J. N. (1994). The Meteoritical Bulletin, No. 76, 1994 January: The U.S. Antarctic Meteorite Collection. *Meteoritics, 29*(1), 100–143. https://doi.org/10.1111/j.1945-5100.1994.tb00661.x
8. Haijun, X., Junfeng, Z., Keqing, Z., & Liang, L. (2015). Quartz exsolution topotaxy in clinopyroxene from the UHP eclogite of Weihai, China. *Lithos*, *226*, 17–30. https://doi.org/10.1016/j.lithos.2015.02.010
9. Hiesinger, H., & Head, J. W. (2006). New views of lunar geoscience: An introduction and overview. *Reviews in Mineralogy and Geochemistry, 60*(1), 1–81.
10. Hiesinger, H., Head, J. W., Wolf, U., Jaumann, R., & Neukum, G. (2011). Ages and stratigraphy of lunar mare basalts: A synthesis. In *Recent Advances and Current Research Issues in Lunar Stratigraphy*.

11. Jolliff, B. L., Gillis, J. J., Haskin, L. A., Korotev, R. L., & Wieczorek, M. A. (2000). Major lunar crustal terranes: Surface expressions and crust–mantle origins. *Journal of Geophysical Research: Planets, 105*(E2), 4197–4216. https://doi.org/10.1029/1999JE001103
12. Jolliff, B. L., Wieczorek, M. A., Shearer, C. K., & Neal, C. R. (2006). *New views of the Moon*. Chantilly, VA: Mineralogical Society of America.
13. Korotev, R. L. (2005). Lunar geochemistry as told by lunar meteorites. *Geochimica et Cosmochimica Acta, 65*(4), 297–346.
14. Leroux, H., Jacob, D., Marinova, M., Hewins, R. H., Zanda, B., Pont, S., Lorand, J. P., & Humayun, M. (2016). Exsolution and shock microstructures of igneous pyroxene clasts in the Northwest Africa 7533 Martian meteorite. *Meteoritics & Planetary Science, 51*(5), 932–945.
15. Lucey, P. G. (2006). Understanding the lunar surface and space–Moon interactions. *Reviews in Mineralogy and Geochemistry, 60*(1), 83–219. https://doi.org/10.2138/rmg.2006.60.2
16. Ludwig, K. (2012). *User's manual for Isoplot version 3.75–4.15: A geochronological toolkit for Microsoft Excel*. Berkeley Geochronological Center Special Publication.
17. McKay, D. S., Heiken, G., Basu, A., Blanford, G., Simon, S., Reedy, R., French, B. M., & Papike, J. (1991). The lunar regolith. In G. H. Heiken, D. T. Vaniman, & B. M. French (Eds.), *Lunar sourcebook* (pp. 285–356). Cambridge University Press.
18. Meyer, C., Kerridge, J. F., Eugster, O., Kim, J. S. (2011). Lunar sample compendium: Elemental analysis of Apollo core samples. In *Proceedings of the 10th Lunar and Planetary Science Conference* (pp. 1425–1435).
19. Miao, B., Xie, L., Yao, J., Xia, Z., Chen, H., Ni, W., & Zhang, C. (2014). Lunar meteorites: Witnesses of the composition and evolution of the Moon. *Advances in Polar Science, 25*(2), 61–74. https://doi.org/10.13679/j.advps.2014.2.00061
20. Nagaoka, H., Karouji, Y., Arai, T., Ebihara, M., & Hasebe, N. (2013). Geochemistry and mineralogy of a feldspathic lunar meteorite (regolith breccia), Northwest Africa 2200. *Polar Science, 7*(3–4), 241–259. https://doi.org/10.1016/j.polar.2013.09.001
21. Neal, C., Gaddis, L., Jolliff, B., Lawrence, S., Mackwell, S., Shearer, C., & Valencia, S. (2023). *New view of the Moon 2*. De Gruyter. https://doi.org/10.1515/9781501519895
22. Nemchin, A. A., Long, T., Jolliff, B. L., Wan, Y., Snape, J. F., Zeigler, R., Grange, M. L., Liu, D., Whitehouse, M. J., Timms, N. E., & Jourdan, F. (2021). Ages of lunar impact breccias: Limits for timing of the Imbrium impact. *Geochemistry, 81*(1), 125683. https://doi.org/10.1016/j.chemer.2020.125683
23. Nozette, S., Rustan, P., Pleasance, L., Kordas, J., Lewis, I., Park, H.-S., Priest, R., Horan, D., Regeon, P., Lichtenberg, C. L., Shoemaker, E., Eliason, E., McEwen, A., Robinson, M.,

Spudis, P., Acton, C., Buratti, B., Duxbury, T., Baker, D., & Zuber, M. (1995). The Clementine mission to the Moon: Scientific overview. *Science, 266*(5192), 1835–1839. https://doi.org/10.1126/science.266.5192.1835

24. Oba, T., & Kobayashi, Y. (2001). The mineral assemblage of symplectites in lunar meteorite Asuka-881757. *Antarctic Meteorite Research, 14*, 21–27.
25. Papike, J. J., Karner, J. M., & Shearer, C. K. (2003). Letter: Determination of planetary basalt parentage: A simple technique using the electron microprobe. *American Mineralogist, 88*(2–3), 469–472. https://doi.org/10.2138/am-2003-2-323
26. Papike, J. J., Taylor, L. A., & Simon, S. B. (1976). Mare basalts: Crystal chemistry, mineralogy, and petrology. *Reviews of Geophysics and Space Physics, 14*(4), 475–540.
27. Shearer, C. K. (2006). Thermal and magmatic evolution of the Moon. *Reviews in Mineralogy and Geochemistry, 60*(1), 365–518. https://doi.org/10.2138/rmg.2006.60.4
28. Prettyman T. H., Hagerty J. J., Elphic R. C., Feldman W. C., Lawrence D. J., McKinney G. W., and Vaniman D. T. (2006). Elemental composition of the lunar surface: Analysis of gamma ray spectroscopy data from Lunar Prospector. Journal of Geophysical Research—Planets. 111:E12007, doi:10.1029/2005JE002656.
29. Saranya R. Chandrana , P. M. Thesniyab , V. J. Rajeshb and Ajit Govinda. (2018). Compositional diversity of lunar magmatic spinels: Implications for endogenic processes.
30. Shearer, C., & Papike, J. (2005). Early crustal building processes on the Moon: Models for the petrogenesis of the magnesian suite. *Geochimica et Cosmochimica Acta, 69*(14), 3445–3461. https://doi.org/10.1016/j.gca.2005.02.025
31. Smyth, J. R. (1980). Cation vacancies and the crystal chemistry of breakdown reactions in kimberlitic omphacite. *American Mineralogist, 65*(11–12), 1185–1191.
32. Snape, J. F., Nemchin, A. A., Bellucci, J. J., Whitehouse, M. J., Tartèse, R., Barnes, J. J., Anand, M., Crawford, I. A., & Joy, K. H. (2016). Lunar basalt chronology, mantle differentiation and implications for determining the age of the Moon. *Earth and Planetary Science Letters, 451*, 149–158. https://doi.org/10.1016/j.epsl.2016.07.026
33. Snape, J. F., Nemchin, A. A., Grange, M. L., Bellucci, J. J., Thiessen, F., & Whitehouse, M. J. (2016). Phosphate ages in Apollo 14 breccias: Resolving multiple impact events with high precision U-Pb SIMS analyses. *Geochimica et Cosmochimica Acta, 174*, 13–29.
34. Snape, J. F., Nemchin, A. A., Whitehouse, M. J., Merle, R. E., Hopkinson, T., & Anand, M. (2019). The timing of basaltic volcanism at the Apollo landing sites. *Geochimica et Cosmochimica Acta, 266*, 29–53. https://doi.org/10.1016/j.gca.2019.07.042

35. Spray, J. G. (2016). Lithification mechanisms for planetary regoliths: The glue that binds. *Annual Review of Earth and Planetary Sciences, 44*, 139–165. https://doi.org/10.1146/annurev-earth-060115-012203

36. Stöffler, D., Hamann, C., & Metzler, K. (2017). Shock metamorphism of planetary silicate rocks and sediments: Proposal for an updated classification system. *Meteoritics & Planetary Science, 53*(1), 5–49. https://doi.org/10.1111/maps.12912

37. Takeda, H., Mori, H., & Tagai, T. (1986). Mineralogy of Antarctic lunar meteorites and differentiated products of the lunar crust. *Proceedings of the 10th NIPR Symposium on Antarctic Meteorites, Memoirs of the National Institute of Polar Research*, (41), 45–57.

38. Taylor, G. J., Warren, P., Ryder, G., Delano, J., Pieters, C., & Lofgren, G. (1991). Lunar rocks. In G. H. Heiken, D. T. Vaniman, & B. M. French (Eds.), *Lunar sourcebook* (pp. 183–284). Cambridge University Press.

39. Tera, F., Papanastassiou, D. A., & Wasserburg, G. J. (1974). Isotopic evidence for a terminal lunar cataclysm. *Earth and Planetary Science Letters, 22*(1), 1–21.

40. Warren, P. H., & Wasson, J. T. (1979). The origin of KREEP. *Reviews of Geophysics, 17*(1), 73–88.

41. Weyer, S., Anbar, A. D., Brey, G. P., Münker, C., Mezger, K., & Woodland, A. B. (2005). Iron isotope fractionation during planetary differentiation. *Earth and Planetary Science Letters, 240*(2), 251–264.

42. Wieczorek, M. A., Neumann, G. A., Nimmo, F., Kiefer, W. S., Taylor, G. J., Melosh, H. J., Phillips, R. J., Solomon, S. C., Andrews-Hanna, J. C., Asmar, S. W., Konopliv, A. S., Lemoine, F. G., Smith, D. E., Watkins, M. W., Williams, J. G., & Zuber, M. T. (2013). The crust of the Moon as seen by GRAIL. *Science, 339*(6120), 671–675. https://doi.org/10.1126/science.1231530

43. Wilhelms, D. E., John, F., & Trask, N. J. (1987). *The geologic history of the Moon* (pp. 2330–7102). U.S. Geological Survey.

44. Wittmann, A., Korotev, R. L., Jolliff, B. L., & Carpenter, P. K. (2019). Spinel assemblages in lunar meteorites Graves Nunataks 06157 and Dhofar 1528: Implications for impact melting and equilibration in the Moon's upper mantle. *Meteoritics & Planetary Science, 54*(2), 379–394. https://doi.org/10.1111/maps.13217

45. Wood, J. A. (1970). Petrology of the lunar soil and geophysical implications. *Journal of Geophysical Research, 75*(32), 6497–6513.

46. Xia, Z., Miao, B., Zhang, C., Chen, H., Xie, L., Ranjith, P. M., Zhang, Y., & Si, B. (2021). Petrography and shock metamorphism of the lunar breccia meteorite NWA 13120. *Minerals, 11*(8), 899. https://doi.org/10.3390/min1108089
47. Xia, Z., Yang, B., Si, B., Chen, G., Wang, X., Chen, H., Zhang, C., & Miao, B. (2025). Petrogenesis of lunar granulitic breccia meteorites Northwest Africa 15062 and 15063. *Meteoritics & Planetary Science, 60*(1), 32–50. https://doi.org/10.1111/maps.14285
48. Xie, L. F., Chen, H. Y., Miao, B. K., Song, W. L., Xia, Z. P., Zhang, C. T., Chen, G. Z., Zhang, J. Y., Zhao, S. Z., & Gao, X. K. (2024). A possible origin of the lunar spinel-bearing lithologies as told by the meteorite NWA 13191. *American Mineralogist, 109*(3), 457–470. https://doi.org/10.2138/am-2022-8728
49. Xue, Z., Xiao, L., Neal, C. R., & Xu, Y. (2019). Oldest high-Ti basalt and magnesian crustal materials in feldspathic lunar meteorite Dhofar 1428. *Geochimica et Cosmochimica Acta, 266*, 74–108.
50. Zeigler, R. A., Barnes, J. J., Friedrich, J. M., Agee, C. B., Burgess, K. D., Corrigan, C. M., Gross, J., Joy, K. H., McCubbin, F. M., & Righter, K. (2023). Recommendation of a new lunar meteorite naming nomenclature.
51. Zeigler, R. A., Korotev, R. L., & Jolliff, B. L. (2007). Petrography, geochemistry, and pairing relationships of basaltic lunar meteorite stones NWA 773, NWA 2700, NWA 2727, NWA 2977, and NWA 3160. *Proceedings of the 38th Lunar and Planetary Science Conference*, 2109.
52. Zeng, X., Joy, K. H., Li, S., Pernet-Fisher, J. F., Li, X., Martin, D. J. P., Li, Y., & Wang, S. (2018). Multiple lithic clasts in lunar breccia Northwest Africa 7948 and implication for the lithologic components of lunar crust. *Meteoritics & Planetary Science, 53*(5), 1030–1050.
53. Zhang, A.-C., Hsu, W., Li, Q.-L., Liu, Y., Jiang, Y., & Tang, G. (2010). SIMS Pb/Pb dating of Zr-rich minerals in lunar meteorites Miller Range 05035 and LaPaz Icefield 02224: Implications for the petrogenesis of mare basalt. *Science China Earth Sciences, 53*(3), 327–334. https://doi.org/10.1007/s11430-010-0041-z
54. Zhou, Q. (2017). Lunar meteorites. In B. Cudnik (Ed.), *Encyclopedia of Lunar Science*. Springer. https://doi.org/10.1007/978-3-319-05546-6_58-1

APPENDICES

A. SEM EDS analysis

Table 4. Average composition (wt.%) in breccia clasts BC in NWA 15352.

	BC1		BC2		BC3		BC4		BC5		BC6		BC8	
	Average	Sd	Average	Sd	Average	Sd	Average	Sd	Average	Sd	Average	Sd	Average	Sd
No.	7		11		6		7		4		3		6	
SiO2	45.96	0.55	45.35	1.11	45.52	0.79	44.95	0.43	42.91	0.79	44.5	0.07	45.64	1.03
TiO2	0.65	0.14	0.54	0.22	0.37	0.12	0.35	0.19	0.05	0.1	0.54	0.19	0.18	0.15
Al2O3	26	1.08	25.91	0.67	25.77	0.7	24.86	0.56	25.92	1.36	25.13	0.53	27.21	0.93
Cr2O3	0.07	0.13	0.11	0.12	0.04	0.09	0.16	0.16	-	-	-	-	0.04	0.1
FeO	6.28	0.41	5.79	0.41	5.97	0.62	7.71	0.33	6.59	1.21	6.33	0.18	6.38	0.88
MnO	-	-	0.02	0.08	-	-	0.03	0.09	-	-	-	-	-	-
MgO	5.51	0.39	5.32	0.35	5.46	0.5	6.65	0.14	8	1.12	5.53	0.26	4.54	0.51
CaO	14.78	0.5	14.58	0.55	14.58	0.37	13.84	0.23	13.69	0.93	14.03	0.21	14.68	0.64
Na2O	0.51	0.05	0.52	0.09	0.47	0.1	0.63	0.05	0.42	0.03	0.39	0.12	0.11	0.09
K2O	0.1	0.07	0.08	0.08	0.14	0.07	0.11	0.08	0.06	0.07	0.13	0.11	-	-
P	-	-	-	-	-	-	-	-	-	-	-	-	-	-
S	0.19	0.18	0.19	0.16	-	-	0.07	0.11	0.07	0.11	-	-	0.86	0.47
Ni	-	-	-	-	-	-	-	-	-	-	-	-	0.04	0.11
Total	100.05		98.41		98.32		99.37		97.64		96.58		99.68	
Mg#	46.73	48.75	47.88	46.05	47.77	44.64	46.31	29.82	54.83	48.07	46.63	59.09	41.58	36.69

wt.% - weight percentages; No. Number of analyses. Sd - standar deviation. Mg# - Mg/(Mg+Fe)*100

Table 5. Average composition (wt.%) in melt clasts MC in NWA 15352.

	MC1		MC2		MC3		MC4		MC5		MC6	
	Average	Sd	Average	Sd	Average	Sd	Average	Sd	Average	Sd	Average	Sd
No.	11		11		3		8		6		3	
SiO2	48.7	0.63	42.48	0.99	47.4	0.23	46.15	0.54	46.86	0.47	47.66	0.40
TiO2	0.93	0.27	0.32	0.08	0.53	0.15	0.58	0.13	0.30	0.05	0.69	0.17
Al2O3	14.86	0.61	24.97	0.73	20.14	0.23	24.45	1.11	24.09	1.09	14.43	0.05
Cr2O3	0.64	0.24	0.14	0.14	0.07	0.15	0.08	0.11	-	-	0.27	0.04
FeO	13.05	0.52	10.19	0.60	9.52	0.6	6.99	0.57	6.65	0.59	12.96	0.17
MnO	0.15	0.14	0.04	0.10	-	-	-	-	0.07	0.10	0.26	0.04
MgO	12.25	0.33	7.99	0.33	9.02	0.31	6.39	0.55	6.24	0.61	12.08	0.14
CaO	10.02	0.42	13.37	0.47	11.21	0.21	13.16	0.43	13.45	0.32	9.37	0.06
Na2O	0.25	0.14	0.36	0.13	0.45	0.12	0.56	0.09	0.56	0.07	0.28	0.04
K2O	0.07	0.08	0.04	0.06	0.09	0.07	0.12	0.05	0.07	0.08	0.07	0.06
P	0.03	0.1	-	-	-	-	-	-	-	-	-	-
S			0.02	0.08	-	-	-	-	0.09	0.14	-	-
Ni	-	-	-	-	-	-	-	-	-	-	-	-
Total	100.95		99.92		98.43		98.49		98.38		98.07	
Mg#	48.42	38.82	43.93	35.46	48.65	34.07	47.77	49.21	48.39	50.82	48.24	44.17

wt.% - weight percentages; No. Number of analyses. Sd - standar deviation. Mg# - Mg/(Mg+Fe)*100

Table 6. Average composition (wt.%) in anorthosite clasts AC in NWA 15352.

	AC1		AC2		AC5		AC6	
	Average	Sd	Average	Sd	Average	Sd	Average	Sd
No.	3		9		4		9	
SiO2	42.01	0.77	44.02	1.54	43.13	0.62	43.08	0.43
TiO2	0.07	0.11	0.20	0.12	0.05	0.09	0.03	0.06
Al2O3	29.82	1.34	29.44	2.05	31.95	0.46	30.04	0.79
Cr2O3	-	-	-	-	-	-	0.02	0.05
FeO	3.42	1.45	3.62	1.04	1.75	0.5	3.44	2.76
MnO	-	-	-	-	0.05	0.1	1.06	1.60
MgO	5.29	2.72	3.14	0.99	1.57	0.54	3.55	0.95
CaO	16.09	1.53	16.84	1.16	17.05	0.38	16.59	0.61
Na2O	0.38	0.02	0.46	0.09	0.4	0.05	0.38	0.03
K2O	0.09	0.08	0.09	0.08	0.17	0.04	0.11	0.05
P	-	-	-	-	-	-	-	-
S	-	-	0.03	0.08	-	-	0.09	0.14
Ni	-	-	-	-	-	-	-	-
Total	97.17		97.83		96.12		98.38	
Mg#	60.73	65.23	46.46	48.88	47.29	51.92	50.79	25.69

wt.% - weight percentages; No. Number of analyses. Sd - standar deviation. Mg# - Mg/(Mg+Fe)*100

Table 7 Chemical compositions of minerals in the breccia clast BC in NWA 15352.

	BC 1									
wt.%	Pl			Ol					Cpx	
SiO2	45.06	45.45	SiO2	36.17	36.65	37.28	36.78	SiO2	52.49
TiO2	-	-	TiO2	-	0.25	-	-	TiO2	0.85
Al2O3	34.84	34.55	Al2O3	-	0.69	0.92	0.41	Al2O3	2.84
Cr2O3	-	-	Cr2O3	-	-	0.23	-	Cr2O3	0.34
FeO	0.37	0.24	FeO	34.83	33.67	33.3	34.27	FeO	18.72
MnO	-	-	MnO	0.25	0.34	0.38	0.36	MnO	0.23
MgO	0.18	-	MgO	29.58	28.83	28.71	28.82	MgO	19.57
CaO	19.3	18.66	CaO	0.27	0.44	0.64	0.25	CaO	6.01
Na2O	0.64	0.73	Na2O	-	-	-	-	Na2O	-
K2O	-	-	K2O	-	-	-	-	K2O	-
Total	100.39	99.63	Total	101.11	100.88	101.45	100.91	Total	101.06
Si	2.08	2.10	Si	0.99	1.00	1.01	1.01	Si	1.93
Al	1.89	1.88	Ti	0.00	0.01	0.00	0.00	Ti	0.02
Ti	0.00	0.00	Al	0.00	0.02	0.03	0.01	Al	0.12
Fe++	0.01	0.01	Cr	0.00	0.00	0.00	0.00	Cr	0.01
Mn	0.00	0.00	Fe++	0.80	0.77	0.76	0.78	Fe++	0.58
Mg	0.01	0.00	Mn	0.01	0.01	0.01	0.01	Mn	0.01
Ca	0.95	0.93	Mg	1.21	1.17	1.16	1.18	Mg	1.07
Na	0.06	0.07	Ni	0.00	0.00	0.00	0.00	Ca	0.24
K	0.00	0.00	Ca	0.01	0.01	0.02	0.01	Na	0.00
Total	5.01	4.99	Total	3.02	2.99	2.99	2.99	Total	3.98
Mg*	46.44	0.00	Mg*	60.22	60.42	60.59	59.99	Mg*	65.08
Or	0.00	0.00	Fo	60.05	60.18	60.31	59.74	En	56.90
Ab	5.66	6.61	Fa	39.66	39.42	39.24	39.84	Fs	30.54
An	94.34	93.39	Tp	0.29	0.40	0.45	0.42	Wo	12.56

wt.% - weight percentages; BC - breccia clast; Pl -Plagioclase - Plagioclase formula cations/ 8 oxygen; Ol - Olivine; Olivine formula cations/ 4 oxygen; Cpx- Clinopyroxene, Clinopyroxene formula cations/ 6 oxygen; Mg# - molar Mg/(Fe+Mg)*100

Table 8 Chemical compositions of minerals in breccia clast BC in NWA 15352.

	BC 2							
wt.%	Pl			Ol		Opx		Troi
SiO2	46.15	46.2	SiO2	36.63	SiO2	52.42	SiO2	0.59
TiO2	-	-	TiO2	-	TiO2	0.67	TiO2	-
Al2O3	33.76	33.96	Al2O3	0.56	Al2O3	1.37	Al2O3	0.28
Cr2O3	-	-	Cr2O3	-	Cr2O3	0.58	Cr2O3	-
FeO	0.69	0.62	FeO	33.08	FeO	20.22	FeO	56.06
MnO	-	-	MnO	0.4	MnO	0.33	MnO	-
MgO	0.24	-	MgO	29.39	MgO	20.64	MgO	-
CaO	18.74	18.86	CaO	0.36	CaO	3.63	CaO	0.69
Na2O	0.79	0.87	Na2O	-	Na2O	-	Na2O	-
K2O	-	-	K2O	-	K2O	-	K2O	-
Ni	-	-	Ni	-	Ni	-	Ni	0.77
S	-	-	S	-	S	-	S	38.78
Total	100.35	100.51	Total	100.42	Total	99.86	Total	97.17
Si	2.12	2.12	Si	1.00	Si	1.96		
Al	1.83	1.84	Ti	0.00	Ti	0.02		
Ti	0.00	0.00	Al	0.02	Al	0.06		
Fe++	0.03	0.02	Cr	0.00	Cr	0.02		
Mn	0.00	0.00	Fe++	0.76	Fe++	0.63		
Mg	0.02	0.00	Mn	0.01	Mn	0.01		
Ca	0.92	0.93	Mg	1.20	Mg	1.15	Ni	0.09
Na	0.07	0.08	Ni	0.00	Ca	0.15	Fe	6.64
K	0.00	0.00	Ca	0.01	Na	0.00	S	8.00
Total	4.99	4.99	Total	3.00	Total	3.99	Total	14.73
Mg*	38.27	0.00	Mg*	61.30	Mg*	64.53		
Or	0.00	0.00	Fo	61.01	En	59.67		
Ab	7.09	7.70	Fa	38.52	Fs	32.79		
An	92.91	92.30	Tp	0.47	Wo	7.54		

wt.% - weight percentages; BC - breccia clast; Pl -Plagioclase - Plagioclase formula cations/ 8 oxygen; Ol - Olivine; Olivine formula cations/ 4 oxygen; Opx- Orthopyroxene, Orthopyroxene formula cations/ 6 oxygen; Troi - Troilite, Troilite formula 8 sulfur; Mg# - molar Mg/(Fe+Mg)*100

Table 9 Chemical compositions of minerals in breccia clast BC in NWA 15352.

	BC 3													
wt.%	Pl			Ol			Cpx			Opx		Ilm		
SiO2	43.4	44.19	SiO2	36.44	36.34	SiO2	49.66	50.13	SiO2	53.26	SiO2	0	0.4	0.29
TiO2	-	-	TiO2	-	-	TiO2	0.87	0.92	TiO2	0.61	TiO2	52.79	53.18	51.72
Al2O3	36.27	34.77	Al2O3	-	-	Al2O3	1.94	1.86	Al2O3	1.13	Al2O3	0.26	0	0.33
Cr2O3	-	-	Cr2O3	-	-	Cr2O3	0.55	0.74	Cr2O3	-	Cr2O3	0.55	0.49	0.73
FeO	-	0.23	FeO	34.03	34.12	FeO	18.15	18.7	FeO	18.23	FeO	39.49	39.12	39.04
MnO	-	-	MnO	0.41	0.31	MnO	0.25	0.45	MnO	0.33	MnO	0.32	0.58	0.35
MgO	-	-	MgO	29.02	29.21	MgO	11.67	11.64	MgO	20.37	MgO	4.92	4.84	5.08
CaO	19.8	19.28	CaO	0.16	0.31	CaO	15.87	15.8	CaO	5.93	CaO	0.24	0.25	0.66
Na2O	0.24	0.6	Na2O	-	-	Na2O	-	-	Na2O	-	Na2O	-	-	-
K2O	-	-	K2O	-	-	K2O	-	-	K2O	-	K2O	-	-	-
Total	99.71	99.07	Total	100.06	100.29	Total	98.96	100.24	Total	99.86	Total	98.57	98.86	98.20
Si	2.01	2.06	Si	1.01	1.00	Si	1.93	1.93	Si	1.98	Si	0.00	0.02	0.01
Al	1.98	1.91	Ti	0.00	0.00	Ti	0.03	0.03	Ti	0.02	Ti	1.96	1.96	1.92
Ti	0.00	0.00	Al	0.00	0.00	Al	0.09	0.08	Al	0.05	Al	0.02	0.02	0.03
Fe++	0.00	0.01	Cr	0.00	0.00	Cr	0.02	0.02	Cr	0.00	Cr	0.02	0.00	0.02
Mn	0.00	0.00	Fe++	0.79	0.79	Fe++	0.59	0.60	Fe++	0.57	Fe++	1.63	1.60	1.61
Mg	0.00	0.00	Mn	0.01	0.01	Mn	0.01	0.01	Mn	0.01	Mn	0.01	0.02	0.01
Ca	0.98	0.96	Mg	1.19	1.20	Mg	0.68	0.67	Mg	1.13	Mg	0.36	0.35	0.37
Na	0.02	0.05	Ni	0.00	0.00	Ca	0.66	0.65	Ca	0.24	Ca	0.01	0.01	0.03
K	0.00	0.00	Ca	0.00	0.01	Na	0.00	0.00	Na	0.00	Na	0.00	0.00	0.00
Total	5.00	5.01	Total	3.00	3.01	Total	3.99	3.99	Total	3.98	Total	4.01	3.99	4.01
Mg*	0.00	0.00	Mg*	60.32	60.42	Mg*	53.41	52.60	Mg*	66.58	Mg*	18.18	18.07	18.83
Or	0.00	0.00	Fo	60.03	60.20	En	35.09	34.76	En	58.44				
Ab	2.15	5.33	Fa	39.49	39.44	Fs	30.61	31.33	Fs	29.34				
An	97.85	94.67	Tp	0.48	0.36	Wo	34.30	33.91	Wo	12.23				

wt.% - weight percentages; BC - breccia clast; Pl-Plagiocalse, Plagioclase formula cations/8 oxygen; Opx-Orthopyroxene, Cpx-Clinopyroxene, Orthopyroxene and Clinopyroxene formula cations/ 6 oxygen; Qtz-Quartz; Ilm-Ilmenite, formula cations/6 oxygen; Mg# - molar Mg/(Fe+Mg)*100

Table 10 Chemical compositions of minerals in breccia clast BC in NWA 15352.

	BC 4						
wt.%	Pl				Ol		Opx
SiO2	44.93	44.62	44.55	SiO2	37.27	SiO2	51.55
TiO2	-	-	-	TiO2	-	TiO2	0.68
Al2O3	33.5	35.22	35.31	Al2O3	1.18	Al2O3	1.47
Cr2O3	-	-	-	Cr2O3	-	Cr2O3	0.37
FeO	0.61	-	0.27	FeO	31.15	FeO	16.62
MnO	0.2	-	-	MnO	0.29	MnO	0.39
MgO	0.26	-	-	MgO	28.4	MgO	19.21
CaO	17.83	19	19.32	CaO	0.62	CaO	8.2
Na2O	0.83	0.39	0.43	Na2O	-	Na2O	-
K2O	0.28	-	-	K2O	-	K2O	-
P	-	-	-	P	0.41	P	-
Total	98.44	99.23	99.88	Total	99.32	Total	98.49
Si	2.11	2.07	2.06	Si	1.03	Si	1.95
Al	1.86	1.93	1.93	Ti	0.00	Ti	0.02
Ti	0.00	0.00	0.00	Al	0.04	Al	0.07
Fe++	0.02	0.00	0.01	Cr	0.00	Cr	0.01
Mn	0.01	0.00	0.00	Fe++	0.72	Fe++	0.53
Mg	0.02	0.00	0.00	Mn	0.01	Mn	0.01
Ca	0.90	0.95	0.96	Mg	1.17	Mg	1.08
Na	0.08	0.04	0.04	Ni	0.00	Ca	0.33
K	0.00	0.00	0.00	Ca	0.02	Na	0.00
Total	5.01	4.98	4.99	Total	2.97	Total	3.99
Mg*	43.17	0.00	0.00	Mg*	61.91	Mg*	67.32
Or	1.69	0.00	0.00	Fo	61.69	En	55.80
Ab	7.64	3.58	3.87	Fa	37.95	Fs	27.08
An	90.67	96.42	96.13	Tp	0.36	Wo	17.12

wt.% - weight percentages; BC - breccia clast; Pl -Plagioclase - Plagioclase formula cations/ 8 oxygen; Ol - Olivine; Olivine formula cations/ 4 oxygen; Opx-Orthopyroxene, formula cations/ 6 oxygen; Mg# - molar Mg/(Fe+Mg)*100

Table 11 Chemical compositions of minerals in breccia clast BC in NWA 15352.

BC 5 inner part

wt.%	Pl					Ol
SiO2	44.31	44.23	43.52	43.74	SiO2	38.94
TiO2	-	-	-		TiO2	-
Al2O3	35.41	34.66	35.41	34.66	Al2O3	-
Cr2O3	-	-	-		Cr2O3	-
FeO	0.4	0.4	0.4	0.56	FeO	22.21
MnO	-	-	-		MnO	-
MgO	-	-	-		MgO	38.66
CaO	19.97	19.42	20.09	19.73	CaO	0.33
Na2O	0.47	0.55	0.26	0.5	Na2O	-
K2O	-	-	-		K2O	-
Total	100.56	99.26	99.68	99.19	Total	100.14
Si	2.04	2.06	2.03	2.05	Si	1.01
Al	1.93	1.91	1.94	1.91	Ti	0.00
Ti	0.00	0.00	0.00	0.00	Al	0.00
Fe++	0.02	0.02	0.02	0.02	Cr	0.00
Mn	0.00	0.00	0.00	0.00	Fe++	0.48
Mg	0.00	0.00	0.00	0.00	Mn	0.00
Ca	0.99	0.97	1.00	0.99	Mg	1.50
Na	0.04	0.05	0.02	0.05	Ni	0.00
K	0.00	0.00	0.00	0.00	Ca	0.01
Total	5.01	5.01	5.02	5.02	Total	3.00
Mg*	0.00	0.00	0.00	0.00	Mg*	75.63
Or	0.00	0.00	0.75	0.00	Fo	75.63
Ab	4.09	4.88	2.27	4.38	Fa	24.37
An	95.91	95.12	96.98	95.62	Tp	0.00

BC 5 outer part

	Pl			Ol		Opx			Cpx	
SiO2	43.5	44.79	SiO2	37.12	SiO2	51.18	50.77	SiO2	52.15	51.71
TiO2	-	-	TiO2	-	TiO2	1.15	1.49	TiO2	0.49	0.86
Al2O3	35.48	34.45	Al2O3	0.65	Al2O3	2.2	1.84	Al2O3	1.34	1.13
Cr2O3	-		Cr2O3	-	Cr2O3	0.61	0.61	Cr2O3	-	0.32
FeO	0.29	0.39	FeO	30.65	FeO	10.23	11.09	FeO	19.21	18.67
MnO	-	-	MnO	0.26	MnO	-	-	MnO	0.42	0.41
MgO	-	0.17	MgO	30.92	MgO	14.87	15.93	MgO	20.78	20.61
CaO	19.76	19.08	CaO	0.36	CaO	19.29	17.56	CaO	4.11	5.34
Na2O	0.21	0.66	Na2O	-	Na2O	-	-	Na2O	-	-
K2O	-	-	K2O	-	K2O	-	-	K2O	-	-
Total	99.24	99.54	Total	99.96	Total	99.53	99.29	Total	98.5	99.05
Si	2.03	2.08	Si	1.01	Si	1.92	1.91	Si	1.97	1.95
Al	1.95	1.89	Ti	0.00	Ti	0.03	0.04	Ti	0.01	0.02
Ti	0.00	0.00	Al	0.02	Al	0.10	0.08	Al	0.06	0.05
Fe++	0.01	0.02	Cr	0.00	Cr	0.02	0.02	Cr	0.00	0.01
Mn	0.00	0.00	Fe++	0.70	Fe++	0.32	0.35	Fe++	0.61	0.59
Mg	0.00	0.01	Mn	0.01	Mn	0.00	0.00	Mn	0.01	0.01
Ca	0.99	0.95	Mg	1.25	Mg	0.83	0.89	Mg	1.17	1.16
Na	0.02	0.06	Ni	0.00	Ca	0.77	0.71	Ca	0.17	0.22
K	0.00	0.00	Ca	0.01	Na			Na		
Total	5.00	5.00	Total	2.99	Total	3.99	4.00	Total	3.99	4.00
Mg*	0.00	43.72	Mg*	64.27	Mg*	72.15	71.91	Mg*	65.85	66.31
Or	0.00	0.00	Fo	64.07	En	43.14	45.81	En	60.21	59.02
Ab	1.89	5.89	Fa	35.62	Fs	16.65	17.89	Fs	31.23	29.99
An	98.11	94.11	Tp	0.31	Wo	40.22	36.30	Wo	8.56	10.99

wt.% - weight percentages; BC - breccia clast; Pl -Plagioclase - Plagioclase formula cations/ 8 oxygen; Ol - Olivine; Olivine formula cations/ 4 oxygen; Opx-Orthopyroxene, Cpx-Clinopyroxene, Orthopyroxene and Clinopyroxene formula cations/ 6 oxygen

Mg* - molar Mg/(Fe+Mg)*100

Table 12 Chemical compositions of minerals in breccia clast BC in NWA 15352.

BC 6 inner part

wt.%	Pl				Ol			Opx
SiO2	44.67	44.07	44.19	SiO2	36.53	36.63	SiO2	51.58
TiO2	-	-	-	TiO2	-	-	TiO2	0.72
Al2O3	34.7	34.84	34.19	Al2O3	0.26	0.29	Al2O3	1.65
Cr2O3	-	-	-	Cr2O3	-	-	Cr2O3	0.4
FeO	0.57	0.38	0.4	FeO	34.43	34.24	FeO	19.09
MnO	-	-	-	MnO	-	0.4	MnO	0.41
MgO	0.16	-	0.21	MgO	28.44	28.54	MgO	19.82
CaO	19.56	19.83	19.03	CaO	0.23	0.46	CaO	5.5
Na2O	0.58	0.56	0.47	Na2O	-	-	Na2O	-
K2O	-	-	0.13	K2O	-	-	K2O	-
ZrO2	-	-	-	ZrO2	-	-	ZrO2	-
S	-	-	-	S	-	-	S	-
Total	100.24	99.68	98.62	Total	99.89	100.56	Total	99.17
Si	2.07	2.05	2.07	Si	1.01	1.01	Si	1.94
Al	1.89	1.91	1.89	Ti	0.00	0.00	Ti	0.02
Ti	0.00	0.00	0.00	Al	0.01	0.01	Al	0.07
Fe++	0.02	0.01	0.02	Cr	0.00	0.00	Cr	0.01
Mn	0.00	0.00	0.00	Fe++	0.80	0.79	Fe++	0.60
Mg	0.01	0.00	0.01	Mn	0.00	0.01	Mn	0.01
Ca	0.97	0.99	0.96	Mg	1.17	1.17	Mg	1.11
Na	0.05	0.05	0.04	Ni	0.00	0.00	Ca	0.22
K	0.00	0.00	0.00	Ca	0.01	0.01	Na	0.00
Total	5.01	5.02	5.00	Total	2.99	3.00	Total	4.00
Mg*	33.35	0.00	48.34	Mg*	59.56	59.78	Mg*	64.92
Or	0.00	0.00	0.77	Fo	59.56	59.49	En	57.48
Ab	5.09	4.86	4.25	Fa	40.44	40.03	Fs	31.06
An	94.91	95.14	94.98	Tp	0.00	0.47	Wo	11.46

BC 6 outer part

	Pl		Ol				Opx		Troi
SiO2	44.38	SiO2	36.51	34.74	36.64	SiO2	52.41	SiO2	0.22
TiO2	-	TiO2	-	-	-	TiO2	0.52	TiO2	-
Al2O3	35.74	Al2O3	0.96	1.09	0.4	Al2O3	1.04	Al2O3	0.15
Cr2O3	-	Cr2O3	-	-	-	Cr2O3	0.31	Cr2O3	-
FeO	0.47	FeO	35.02	35.43	35.56	FeO	20.76	FeO	61.65
MnO	-	MnO	0.38	0.21		MnO	-	MnO	-
MgO	-	MgO	27.85	25.75	28.1	MgO	20.6	MgO	-
CaO	19.96	CaO	0.64	0.47	0.26	CaO	4.56	CaO	0.25
Na2O	0.42	Na2O	-	-	-	Na2O	-	Na2O	-
K2O	-	K2O	-	-	-	K2O	-	K2O	-
ZrO2	-	ZrO2	-	-	-	ZrO2	-	ZrO2	0.52
S	-	S	-	-	-	S	-	S	37.39
Total	100.97	Total	101.36	97.69	100.96	Total	100.20	Total	100.18
Si	2.04	Si	1.00	0.99	1.01	Si	1.96		
Al	1.94	Ti	0.00	0.00	0.00	Ti	0.01		
Ti	0.00	Al	0.03	0.04	0.01	Al	0.05		
Fe++	0.02	Cr	0.00	0.00	0.00	Cr	0.01		
Mn	0.00	Fe++	0.80	0.85	0.82	Fe++	0.65		
Mg	0.00	Mn	0.01	0.01	0.00	Mn	0.00		
Ca	0.98	Mg	1.13	1.10	1.15	Mg	1.15	Zr	0.05
Na	0.04	Ni	0.01	0.01	0.01	Ca	0.18	Fe	7.57
K	0.00	Ca	0.02	0.01	0.01	Na	0.00	S	8.00
Total	5.01	Total	3.01	3.00	3.00	Total	4.00	Total	15.63
Mg*	0.00	Mg*	58.64	56.44	58.49	Mg*	63.88		
Or	0.00	Fo	58.38	56.29	58.49	En	57.99		
Ab	3.67	Fa	41.17	43.44	41.51	Fs	32.78		
An	96.33	Tp	0.45	0.26	0.00	Wo	9.23		

wt.% - weight percentages; BC - breccia clast; Pl -Plagioclase - Plagioclase formula cations/ 8 oxygen; Ol - Olivine; Olivine formula cations/ 4 oxygen; Opx- Orthopyroxene, Orthopyroxene formula cations/ 6 oxygen;
Troi - Troilite, Troilite formula 8 sulfur; Mg# - molar Mg/(Fe+Mg)*100

Table 13 Chemical compositions of minerals in breccia clast BC in NWA 15352

	BC 7																	
wt.%	Pl							Ol			Cpx			Opx				Troi
SiO2	43.53	44.44	44.62	45.91	43.68	43.92	SiO2	36.54	36.28	SiO2	49.76	51.60	SiO2	52.64	52.95	52.58	SiO2	0.72
TiO2	-	-	-	-	-	-	TiO2	-	-	TiO2	1.48	1.11	TiO2	0.67	0.54	0.75	TiO2	-
Al2O3	34.66	35.62	34.67	31.94	35.19	35.38	Al2O3	-	0.33	Al2O3	3.98	2.50	Al2O3	1.12	0.90	1.07	Al2O3	0.44
Cr2O3	-	-	-	-	-	-	Cr2O3	-	-	Cr2O3	0.65	0.48	Cr2O3	0.34	0.35	0.51	Cr2O3	-
FeO	0.29	0.24	0.33	1.20	0.60	0.31	FeO	33.65	32.72	FeO	15.79	13.31	FeO	19.97	19.19	19.21	FeO	54.74
MnO	-	-	-	-	-	-	MnO	0.34	0.29	MnO	0.37	0.28	MnO	0.00	0.43	0.32	MnO	-
MgO	-	-	-	1.18	0.20		MgO	29.17	29.34	MgO	17.76	17.14	MgO	22.75	21.19	22.53	MgO	0.23
CaO	19.30	19.23	19.21	17.77	18.93	19.74	CaO	0.30	0.42	CaO	9.73	14.42	CaO	2.18	4.37	2.49	CaO	0.52
Na2O	0.42	0.45	0.54	1.02	0.29	0.36	Na2O	-	-	Na2O	-	-	Na2O	-	-	-	Na2O	-
K2O	-	-	-	-	-	-	K2O	-	-	K2O	-	-	K2O	-	-	-	K2O	-
Ni	-	-	-	-	-	-	Ni	-	-	Ni	-	-	Ni	-	-	-	Ni	0.52
Si	-	-	-	-	-	-	Si	-	-	Si	-	-	S	-	-	-	S	40.12
Total	98.20	99.98	99.37	99.02	98.89	99.71	Total	100.00	99.38	Total	99.52	100.84	Total	99.67	99.92	99.46	Total	97.29
Si	2.05	2.05	2.08	2.15	2.04	2.04	Si	1.01	1.00	Si	1.87	1.91	Si	1.95	1.97	1.95		
Al	1.93	1.94	1.90	1.76	1.94	1.94	Ti	0.00	0.00	Ti	0.04	0.03	Ti	0.02	0.02	0.02		
Ti	0.00	0.00	0.00	0.00	0.00	0.00	Al	0.00	0.01	Al	0.18	0.11	Al	0.05	0.04	0.05		
Fe++	0.01	0.01	0.01	0.05	0.02	0.01	Cr	0.00	0.00	Cr	0.02	0.01	Cr	0.01	0.01	0.01		
Mn	0.00	0.00	0.00	0.00	0.00	0.00	Fe++	0.78	0.76	Fe++	0.50	0.41	Fe++	0.62	0.60	0.60		
Mg	0.00	0.00	0.00	0.08	0.01	0.00	Mn	0.01	0.01	Mn	0.01	0.01	Mn	0.00	0.01	0.01		
Ca	0.98	0.95	0.96	0.89	0.95	0.98	Mg	1.20	1.21	Mg	0.99	0.95	Mg	1.26	1.17	1.25	Ni	0.06
Na	0.04	0.04	0.05	0.09	0.03	0.03	Ni	0.00	0.00	Ca	0.39	0.57	Ca	0.09	0.17	0.10	Fe	6.27
K	0.00	0.00	0.00	0.00	0.00	0.00	Ca	0.01	0.01	Na	0.00	0.00	Na	0.00	0.00	0.00	S	8.00
Total	5.00	5.00	5.00	5.02	5.00	5.01	Total	3.00	3.00	Total	3.99	4.00	Total	4.00	3.99	3.99	Total	14.32
Mg*	0.00	0.00	0.00	63.67	37.27	0.00	Mg*	60.72	61.52	Mg*	66.72	69.66	Mg*	67.00	66.31	67.64		
Or	0.00	0.00	0.00	0.00	0.00	0.00	Fo	60.47	61.31	En	52.84	49.01	En	64.05	60.38	64.20		
Ab	3.79	4.06	4.84	9.41	2.70	3.19	Fa	39.13	38.35	Fs	26.35	21.35	Fs	31.54	30.67	30.71		
An	96.21	95.94	95.16	90.59	97.30	96.81	Tp	0.40	0.34	Wo	20.81	29.64	Wo	4.41	8.95	5.10		

wt.% - weight percentages; BC - breccia clast; Pl -Plagioclase - Plagioclase formula cations/ 8 oxygen; Ol - Olivine; Olivine formula cations/ 4 oxygen; Opx- Orthopyroxene, Cpx-Clinopyroxene Orthopyroxene and Clinopyroxene formula cations/ 6 oxygen;
Troi - Troilite, Troilite formula 8 sulfur; Mg# - molar Mg/(Fe+Mg)*100

Table 14 Chemical compositions (wt.%) of minerals in breccia clast BC in NWA 15352.

	BC 8									
wt.%	Pl			Ol			Opx			Fe-Ni
SiO2	45.50	45.39	SiO2	37.62	36.71	SiO2	53.42	52.89	SiO2	0.18
TiO2	-	-	TiO2	-		TiO2	0.69	0.64	TiO2	-
Al2O3	33.91	34.34	Al2O3	-	0.35	Al2O3	0.95	1.14	Al2O3	0.27
Cr2O3	-	-	Cr2O3	-		Cr2O3	0.37	0.43	Cr2O3	-
FeO	0.66	0.39	FeO	33.90	33.84	FeO	20.09	19.75	FeO	87.14
MnO	-	-	MnO	0.39	0.24	MnO	0.36	-	MnO	-
MgO	0.23	-	MgO	29.15	29.19	MgO	23.00	23.02	MgO	-
CaO	18.69	18.66	CaO	0.25	0.29	CaO	2.27	2.17	CaO	0.20
Na2O	0.83	0.97	Na2O	-	-	Na2O	-	-	Na2O	-
K2O	-	-	K2O	-	-	K2O	-	-	K2O	-
F	-	-	F	-	-	F	-	-	F	0.99
Ni	-	-	Ni	-	-	Ni	-	-	Ni	9.00
Total	99.82	99.75	Total	101.32	100.62	Total	101.15	100.06	Total	97.78
Si	2.11	2.10	Si	1.02	1.01	Si	1.96	1.95		
Al	1.85	1.87	Ti	0.00	0.00	Ti	0.02	0.02		
Ti	0.00	0.00	Al	0.00	0.01	Al	0.04	0.05		
Fe++	0.03	0.02	Cr	0.00	0.00	Cr	0.01	0.01		
Mn	0.00	0.00	Fe++	0.77	0.77	Fe++	0.62	0.61		
Mg	0.02	0.00	Mn	0.01	0.01	Mn	0.01	0.00		
Ca	0.93	0.93	Mg	1.18	1.19	Mg	1.26	1.27		
Na	0.07	0.09	Ni	0.00	0.00	Ca	0.09	0.09	Ni	0.09
K	0.00	0.00	Ca	0.01	0.01	Na	0.00	0.00	Fe	0.91
Total	5.00	5.00	Total	2.99	3.00	Total	3.98	3.98	Total	1.00
Mg*	38.32	0.00	Mg*	60.52	60.60	Mg*	67.11	67.51		
Or	0.00	0.00	Fo	60.25	60.43	En	64.06	64.56		
Ab	7.44	8.60	Fa	39.30	39.29	Fs	31.39	31.07		
An	92.56	91.40	Tp	0.46	0.28	Wo	4.54	4.37		

wt.% - weight percentages; BC - breccia clast; Pl -Plagioclase - Plagioclase formula cations/ 8 oxygen; Ol - Olivine; Olivine formula cations/ 4 oxygen; Opx- Orthopyroxene, Orthopyroxene formula cations/ 6 oxygen; Fe-Ni - iron-nickel metal, normalized to 1.0 cations ; Mg# - molar Mg/(Fe+Mg)*100

Table 15 Chemical compositions of melt clast IM in NWA 15352.

	MC 1						
wt.%	Pl			Opx		Cr-rich_ Spl	
SiO2	44.78	45.59	SiO2	52.32	SiO2	0.67	0.94
TiO2	-	-	TiO2	0.79	TiO2	14.52	14.95
Al2O3	33.29	31.58	Al2O3	2.05	Al2O3	8.25	8.14
Cr2O3	-	-	Cr2O3	0.45	Cr2O3	29.87	28.41
FeO	1.37	2.53	FeO	19.02	FeO	39.84	40.33
MnO	-	-	MnO	0.33	MnO	0.00	0.51
MgO	0.93	1.46	MgO	20.10	MgO	4.23	4.35
CaO	18.21	16.87	CaO	5.42	CaO	0.42	0.31
Na2O	0.67	0.60	Na2O	-	Na2O	-	-
K2O	-	-	K2O	-	K2O	-	-
V	-	-	V	-	V	0.80	0.79
Total	99.25	98.63	Total	100.48	Total	98.60	98.73
Si	2.09	2.15	Si	1.94	Si	0.02	0.03
Al	1.83	1.75	Ti	0.02	Ti	0.39	0.40
Ti	0.00	0.00	Al	0.09	Al	0.34	0.34
Fe++	0.05	0.10	Cr	0.01	Cr	0.83	0.79
Mn	0.00	0.00	Fe++	0.59	Fe++	1.18	1.19
Mg	0.06	0.10	Mn	0.01	Mn	0.00	0.02
Ca	0.91	0.85	Mg	1.11	Mg	0.22	0.23
Na	0.06	0.05	Ca	0.22	Ca	0.02	0.01
K	0.00	0.00	Na	0.00	Na	0.00	0.00
Total	5.02	5.01	Total	3.99	Total	3.00	3.01
Mg*	54.75	50.70	Mg*	65.32	Mg*	15.92	16.13
Or	0.00	0.00	En	57.98			
Ab	6.24	6.05	Fs	30.78			
An	93.76	93.95	Wo	11.24			

wt.% - weight percentages; MC - melt clast; Pl-Plagiocalse, Plagioclase formula cations/8 oxygen; Opx-Orthopyroxene, Orthopyroxene formula cations/ 6 oxygen; Cr-rich Spl -Chromium-rich Spinel, Spinel formua cations/6; Mg# - molar Mg/(Fe+Mg)*100

Table 16 Chemical compositions of minerals in melt clast MC in NWA 15352.

	MC 2						
wt.%	Pl			Ol		Cpx	
SiO2	44.07	43.98	SiO2	36.74	SiO2	51.23	51.62
TiO2	-	-	TiO2	-	TiO2	1.45	1.39
Al2O3	34.8	34.19	Al2O3	0.31	Al2O3	1.85	2.04
Cr2O3	-	-	Cr2O3	-	Cr2O3	0.48	0.39
FeO	0.62	0.65	FeO	32.46	FeO	11.22	11.17
MnO	-	-	MnO	0.33	MnO	0.26	-
MgO	-	-	MgO	29.88	MgO	15.81	15.58
CaO	19.17	19.13	CaO	0.39	CaO	17.81	17.36
Na2O	0.57	0.71	Na2O	-	Na2O	-	-
K2O	-	-	K2O	-	K2O	-	-
Total	99.23	98.66	Total	100.11	Total	100.11	99.55
Si	2.06	2.07	Si	1.01	Si	1.91	1.93
Al	1.92	1.89	Ti	0.00	Ti	0.04	0.04
Ti	0.00	0.00	Al	0.01	Al	0.08	0.09
Fe++	0.02	0.03	Cr	0.00	Cr	0.01	0.01
Mn	0.00	0.00	Fe++	0.74	Fe++	0.35	0.35
Mg	0.00	0.00	Mn	0.01	Mn	0.01	0.00
Ca	0.96	0.96	Mg	1.22	Mg	0.88	0.87
Na	0.05	0.06	Ni	0.00	Ca	0.71	0.70
K	0.00	0.00	Ca	0.01	Na	0.00	0.00
Total	5.01	5.02	Total	3.00	Total	4.00	3.98
Mg*	0.00	0.00	Mg*	62.14	Mg*	71.52	71.32
Or	0.00	0.00	Fo	61.90	En	45.29	44.10
Ab	5.11	6.29	Fa	37.71	Fs	18.03	20.58
An	94.89	93.71	Tp	0.39	Wo	36.67	35.32

wt.% - weight percentages; MC - melt clast; Pl -Plagioclase - Plagioclase formula cations/ 8 oxygen; Ol - Olivine; Olivine formula cations/ 4 oxygen; Cpx- Clinopyroxene, Clinopyroxene formula cations/ 4 oxygen; Mg# - molar Mg/(Fe+Mg)*100

Table 17 Chemical compositions of minerals in melt clast MC in NWA 15352.

	MC 3													
wt.%	Pl					Ol				Opx				Ilm
SiO2	47.14	46.21	45.43	44.31	SiO2	37.28	36.38	37.01	SiO2	51.70	53.34	53.38	SiO2	2.38
TiO2	-	-	-	-	TiO2	-	-	-	TiO2	0.60	0.58	0.32	TiO2	48.51
Al2O3	29.87	32.80	34.15	35.46	Al2O3	-	-	0.24	Al2O3	1.17	0.93	0.73	Al2O3	1.60
Cr2O3	0.20	-	-	-	Cr2O3	-	-	-	Cr2O3	0.32	0.39	0.29	Cr2O3	0.61
FeO	3.81	0.87	0.70	0.36	FeO	34.69	34.65	34.41	FeO	19.85	19.79	20.59	FeO	40.62
MnO	-	-	-	-	MnO	-	0.40	0.32	MnO	0.31	0.37	0.46	MnO	0.37
MgO	2.18	0.33	-	-	MgO	28.43	28.68	28.30	MgO	20.69	23.43	21.72	MgO	3.69
CaO	15.87	18.63	19.16	19.91	CaO	0.35	0.40	0.51	CaO	5.05	1.72	3.44	CaO	1.26
Na2O	0.88	0.82	0.98	0.46	Na2O	-	-	-	Na2O	-	-	-	Na2O	-
K2O	-	-	-	-	K2O	-	-	-	K2O	-	-	-	K2O	-
P	-	-	-	-	P	-	-	-	P	1.13	-	-	P	-
Total	99.95	99.66	100.42	100.50	Total	100.75	100.51	100.79	Total	100.82	100.55	100.93	Total	99.04
Si	2.20	2.14	2.10	2.04	Si	1.02	1.00	1.01	Si	1.94	1.96	1.97	Si	0.12
Al	1.64	1.79	1.86	1.93	Ti	0.00	0.00	0.00	Ti	0.02	0.02	0.01	Ti	1.78
Ti	0.00	0.00	0.00	0.00	Al	0.00	0.00	0.01	Al	0.05	0.04	0.03	Al	0.09
Fe++	0.15	0.03	0.03	0.01	Cr	0.00	0.00	0.00	Cr	0.01	0.01	0.01	Cr	0.02
Mn	0.00	0.00	0.00	0.00	Fe++	0.79	0.80	0.79	Fe++	0.62	0.61	0.64	Fe++	1.66
Mg	0.15	0.02	0.00	0.00	Mn	0.00	0.01	0.01	Mn	0.01	0.01	0.01	Mn	0.02
Ca	0.79	0.93	0.95	0.98	Mg	1.16	1.18	1.16	Mg	1.16	1.28	1.20	Mg	0.27
Na	0.08	0.07	0.09	0.04	Ni	0.00	0.01	0.01	Ca	0.20	0.07	0.14	Ca	0.07
K					Ca	0.01	0.01	0.00	Na	0.00	0.00	0.00	Na	0.00
Total	5.02	5.00	5.02	5.01	Total	2.99	3.01	2.98	Total	4.01	4.00	4.00	Total	4.02
Mg*	50.49	40.34	0.00	0.00	Mg*	59.37	59.61	59.45	Mg*	65.01	67.85	65.28	Mg*	13.94
Or	0.00	0.00	0.00	0.00	Fo	59.37	59.33	59.23	En	58.36	65.51	60.77		
Ab	9.12	7.38	8.47	4.01	Fa	40.63	40.20	40.39	Fs	31.41	31.04	32.25		
An	90.88	92.62	91.53	95.99	Tp	0.00	0.47	0.38	Wo	10.24	3.46	6.92		

wt.% - weight percentages; MC - melt clast; Pl -Plagioclase - Plagioclase formula cations/ 8 oxygen; Ol - Olivine; Olivine formula cations/ 4 oxygen; Opx- Orthopyroxene, Orthopyroxene formula cations/ 6 oxygen; Ilm-Ilmenite, formula cations/6 oxygen; Mg# - molar Mg/(Fe+Mg)*100

Table 18 Chemical compositions of minerals in melt clast MC in NWA 15352.

	MC 4									
wt.%	Pl		Ol				Opx			Cr-rich Spl
SiO2	45.01	SiO2	36.26	35.82	36.42	SiO2	51.58	50.63	SiO2	6.35
TiO2	-	TiO2	-	-	-	TiO2	0.67	1.15	TiO2	16.36
Al2O3	33.93	Al2O3	0.37	-	-	Al2O3	5.74	2.34	Al2O3	8.56
Cr2O3	-	Cr2O3	-	-	-	Cr2O3	0.31	0.63	Cr2O3	23.77
FeO	0.50	FeO	33.27	33.38	32.94	FeO	16.89	18.86	FeO	39.82
MnO	-	MnO	0.28	0.53	0.45	MnO	0.29	0.40	MnO	0.34
MgO	0.19	MgO	28.86	28.58	28.32	MgO	19.14	20.02	MgO	3.74
CaO	18.60	CaO	0.38	0.34	0.26	CaO	6.17	4.34	CaO	1.49
Na2O	0.79	Na2O	-	-	-	Na2O	-	-	Na2O	-
K2O	0.11	K2O	-	-	-	K2O	-	-	K2O	-
Total	99.13	Total	99.42	98.65	98.39	Total	100.79	98.37	Total	100.43
Si	2.10	Si	1.01	1.00	1.02	Si	1.88	1.92	Si	0.21
Al	1.87	Ti	0.00	0.00	0.00	Ti	0.02	0.03	Ti	0.41
Ti	0.00	Al	0.01	0.00	0.00	Al	0.25	0.10	Al	0.33
Fe++	0.02	Cr	0.00	0.00	0.00	Cr	0.01	0.02	Cr	0.62
Mn	0.00	Fe++	0.77	0.78	0.77	Fe++	0.52	0.60	Fe++	1.10
Mg	0.01	Mn	0.01	0.01	0.01	Mn	0.01	0.01	Mn	0.01
Ca	0.93	Mg	1.19	1.19	1.18	Mg	1.04	1.13	Mg	0.18
Na	0.07	Ni	0.00	0.01	0.01	Ca	0.24	0.18	Ca	0.05
K	0.01	Ca	0.01	0.01	0.01	Na	0.00	0.00	Na	0.00
Total	5.01	Total	3.00	3.01	2.99	Total	3.97	3.99	Total	2.91
Mg*	40.38	Mg*	60.73	60.42	60.52	Mg*	66.89	65.42	Mg*	14.34
Or	0.65	Fo	60.53	60.04	60.19	En	57.91	59.37		
Ab	7.09	Fa	39.14	39.33	39.27	Fs	28.67	31.38		
An	92.26	Tp	0.33	0.63	0.54	Wo	13.42	9.25		

wt.% - weight percentages; MC - melt clast; Pl -Plagioclase - Plagioclase formula cations/ 8 oxygen; Ol - Olivine; Olivine formula cations/ 4 oxygen;
Opx- Orthopyroxene, Orthopyroxene formula cations/ 4 oxygen; Cr-rich Spl-Chromium-rich Spinel, Spinel formua cations/6; Mg# - molar Mg/(Fe+Mg)*100

Table 19 Chemical compositions of minerals in melt clast MC in NWA 15352.

	MC 5						
wt.%	Pl			Ol		Opx	
SiO2	45.11	45.39	SiO2	36.65	SiO2	53.00	52.77
TiO2	-	-	TiO2	-	TiO2	0.61	0.52
Al2O3	33.39	34.30	Al2O3	-	Al2O3	0.87	1.12
Cr2O3	-	-	Cr2O3	-	Cr2O3	0.33	0.37
FeO	0.65	0.60	FeO	33.52	FeO	19.29	19.22
MnO	-	-	MnO	-	MnO	0.46	0.33
MgO	0.23	0.23	MgO	28.41	MgO	21.27	20.95
CaO	17.86	18.36	CaO	0.31	CaO	4.24	4.25
Na2O	0.88	0.76	Na2O	-	Na2O	-	-
K2O	0.11	-	K2O	-	K2O	-	-
S	-	-	S	-	S	0.22	-
Total	98.23	99.64	Total	98.89	Total	100.07	99.53
Si	2.12	2.10	Si	1.02	Si	1.97	1.97
Al	1.85	1.87	Ti	0.00	Ti	0.02	0.01
Ti	0.00	0.00	Al	0.00	Al	0.04	0.05
Fe++	0.03	0.02	Cr	0.00	Cr	0.01	0.01
Mn	0.00	0.00	Fe++	0.78	Fe++	0.60	0.60
Mg	0.02	0.02	Mn	0.00	Mn	0.01	0.01
Ca	0.90	0.91	Mg	1.18	Mg	1.18	1.16
Na	0.08	0.07	Ni	0.00	Ca	0.17	0.17
K	0.01	0.00	Ca	0.01	Na	0.00	0.00
Total	5.00	4.99	Total	2.99	Total	3.99	3.99
Mg*	38.68	40.59	Mg*	60.18	Mg*	66.28	66.02
Or	0.67	0.00	Fo	60.18	En	60.53	60.22
Ab	8.13	6.97	Fa	39.82	Fs	30.80	30.99
An	91.20	93.03	Tp	0.00	Wo	8.67	8.78

wt.% - weight percentages; MC - melt clast; Pl -Plagioclase - Plagioclase formula cations/ 8 oxygen; Ol - Olivine; Olivine formula cations/ 4 oxygen;
Opx- Orthopyroxene, Orthopyroxene formula cations/ 4 oxygen; Mg# - molar Mg/(Fe+Mg)*100

Table 20 Chemical compositions of minerals in melt clast MC in NWA 15352.

	MC 6											
wt.%	Pl			Ol		Opx				Ilm		Cr-rich Spl
SiO2	43.63	43.54	SiO2	35.55	SiO2	51.95	51.95	52.24	SiO2	9.90	SiO2	2.30
TiO2	-	-	TiO2	-	TiO2	0.67	0.62	0.55	TiO2	41.87	TiO2	18.35
Al2O3	34.54	34.67	Al2O3	0.23	Al2O3	4.19	1.49	2.04	Al2O3	2.00	Al2O3	6.12
Cr2O3	-		Cr2O3	-	Cr2O3	0.26	0.38	0.35	Cr2O3	1.61	Cr2O3	23.76
FeO	0.56	0.50	FeO	34.10	FeO	17.19	19.88	19.87	FeO	34.91	FeO	43.81
MnO	-	-	MnO	0.34	MnO	0.27	0.28	0.37	MnO	0.43	MnO	0.27
MgO	0.00	0.19	MgO	27.57	MgO	19.05	20.18	20.24	MgO	7.57	MgO	4.05
CaO	19.45	19.47	CaO	0.26	CaO	5.77	4.37	4.73	CaO	1.31	CaO	0.50
Na2O	0.57	0.36	Na2O	-	Na2O	-	-	-	Na2O	-	Na2O	-
K2O			K2O	-	K2O	-	-	-	K2O	-	K2O	-
Total	98.75	98.73	Total	98.05	Total	99.35	99.15	100.39	Total	99.60	Total	99.16
Si	2.05	2.05	Si	1.01	Si	1.93	1.95	1.94	Si	0.45	Si	0.08
Al	1.91	1.92	Ti	0.00	Ti	0.02	0.02	0.02	Ti	1.43	Ti	0.48
Ti	0.00	0.00	Al	0.01	Al	0.18	0.07	0.09	Al	0.06	Al	0.25
Fe++	0.02	0.02	Cr	0.00	Cr	0.01	0.01	0.01	Cr	0.11	Cr	0.66
Mn	0.00	0.00	Fe++	0.81	Fe++	0.53	0.63	0.62	Fe++	1.33	Fe++	1.28
Mg	0.00	0.01	Mn	0.01	Mn	0.01	0.01	0.01	Mn	0.02	Mn	0.01
Ca	0.98	0.98	Mg	1.16	Mg	1.05	1.13	1.12	Mg	0.51	Mg	0.21
Na	0.05	0.03	Ni	0.00	Ca	0.23	0.18	0.19	Ca	0.06	Ca	0.02
K	0.01	0.00	Ca	0.01	Na	0.00	0.00	0.00	Na	0.00	Na	0.00
Total	5.02	5.01	Total	3.00	Total	3.96	3.99	3.99	Total	3.97	Total	2.98
Mg*	0.00	40.38	Mg*	59.04	Mg*	66.39	64.41	64.49	Mg*	27.88	Mg*	14.15
Or	0.00	0.00	Fo	58.80	En	58.01	58.54	58.18				
Ab	5.04	3.24	Fa	40.79	Fs	29.36	32.35	32.67				
An	94.96	96.76	Tp	0.41	Wo	12.63	9.11	9.77				

wt.% - weight percentages; MC - melt clast; Pl -Plagioclase - Plagioclase formula cations/ 8 oxygen; Ol - Olivine; Olivine formula cations/ 4 oxygen; Opx- Orthopyroxene, Orthopyroxene formula cations/ 4 oxygen; Cr-rich Spl-Chromium-rich Spinel, Spinel formua cations/6; Ilm-Ilmenite, formula cations/6 oxygen Mg# - molar Mg/(Fe+Mg)*100

Table 21 Chemical compositions of minerals in anorthosite clast AC in NWA 15352.

	AC 1											
wt.%	Pl			Mg-rich Ol	Ol			Opx		Cr-rich Spl		Troi
SiO2	44.7	45.1	SiO2	39.48	36.73	36.66	SiO2	53.24	SiO2	1.29	SiO2	0.21
TiO2	-	-	TiO2	-	-	-	TiO2	0.58	TiO2	18.26	TiO2	-
Al2O3	34.93	35.87	Al2O3	0.54	0.22	-	Al2O3	0.74	Al2O3	6.09	Al2O3	0.15
Cr2O3	-	-	Cr2O3	-	-	-	Cr2O3	0.28	Cr2O3	24.59	Cr2O3	-
FeO	1.00	0.35	FeO	19.08	34.52	34.09	FeO	19.04	FeO	44.8	FeO	61.74
MnO	-	-	MnO	-	0.21	0.37	MnO	0.24	MnO	0.59	MnO	-
MgO	0.53	0.18	MgO	40.13	29.04	28.7	MgO	20.03	MgO	2.64	MgO	-
CaO	19.14	19.85	CaO	0.32	0.27	0.37	CaO	6.51	CaO	0.73	CaO	0.17
Na2O	0.46	0.52	Na2O	-	-	-	Na2O	-	Na2O	-	Na2O	-
K2O	-	-	K2O	-	-	-	K2O	-	K2O	-	K2O	-
S	-	-	S	-	-	-	S	-	S	-	S	36.84
Total	100.76	101.87	Total	99.55	100.99	100.19	Total	100.66	Total	98.99	Total	99.11
Si	2.06	2.05	Si	1.01	1.01	1.01	Si	1.97	Si	0.05		
Al	1.90	1.92	Ti	0.00	0.00	0.00	Ti	0.02	Ti	0.49		
Ti	0.00	0.00	Al	0.02	0.01	0.00	Al	0.03	Al	0.25		
Fe++	0.04	0.01	Cr	0.00	0.00	0.00	Cr	0.01	Cr	0.69		
Mn	0.00	0.00	Fe++	0.41	0.79	0.79	Fe++	0.59	Fe++	1.33		
Mg	0.04	0.01	Mn	0.00	0.00	0.01	Mn	0.01	Mn	0.02		
Ca	0.94	0.97	Mg	1.54	1.18	1.18	Mg	1.11	Mg	0.14		
Na	0.04	0.05	Ni	0.00	0.00	0.00	Ca	0.26	Ca	0.03	Fe	7.70
K	0.00	0.00	Ca	0.01	0.01	0.01	Na	0.00	Na	0.00	S	8.00
Total	5.01	5.01	Total	2.99	3.00	3.00	Total	3.99	Total	2.99	Total	15.70
Mg*	48.58	47.83	Mg*	78.95	60.00	60.02	Mg*	65.22	Mg*	9.51		
Or	0.00	0.00	Fo	78.95	59.85	59.75	En	56.60				
Ab	4.17	4.53	Fa	21.05	39.90	39.81	Fs	30.18				
An	95.83	95.47	Tp	0.00	0.25	0.44	Wo	13.22				

wt.% - weight percentages; AC - anorthosite clast; Pl - Plagioclase; Plagioclase formula cations/ 8 oxygen; Ol - Olivine and Mg-rich Ol - Magnesium rich olivine; Olivine formula cations/ 4 oxygen; Cr-rich Spl - chromium rich spinel; Spinel formula cations/4 oxygen; Cpx- Clinopyroxene, Clinopyroxene formula cations/ 4 oxygen; Troi - Troilite; Troilite formula 8 sulfur, Mg# - molar Mg/(Fe+Mg)*100

Table 22 Chemical compositions of minerals in anorthosite clast AC in NWA 15352.

	AC 2								
wt.%	Pl				Ol			Opx	
SiO2	44.67	44.04	44.26	SiO2	36.10	36.51	SiO2	50.63	51.82
TiO2	-	-	-	TiO2	-	-	TiO2	1.57	0.98
Al2O3	35.09	35.08	35.13	Al2O3	0.28	0.29	Al2O3	2.79	1.40
Cr2O3	-	-	-	Cr2O3	-	-	Cr2O3	0.52	0.28
FeO	0.00	0.50	0.24	FeO	34.55	33.91	FeO	17.62	18.78
MnO	-	-	-	MnO	0.37	0.29	MnO	0.48	0.25
MgO	-	-	-	MgO	28.72	28.48	MgO	18.64	20.04
CaO	19.49	19.29	18.76	CaO	0.33	0.46	CaO	7.47	5.78
Na2O	0.48	0.48	0.50	Na2O	-	-	Na2O	-	-
K2O	-	-	-	K2O	-	-	K2O	-	-
Total	99.73	99.39	98.89	Total	100.35	99.94	Total	99.72	99.33
Si	2.07	2.05	2.07	Si	1.00	1.01	Si	1.90	1.94
Al	1.92	1.93	1.93	Ti	0.00	0.00	Ti	0.04	0.03
Ti	0.00	0.00	0.00	Al	0.01	0.01	Al	0.12	0.06
Fe++	0.00	0.02	0.01	Cr	0.00	0.00	Cr	0.02	0.01
Mn	0.00	0.00	0.00	Fe++	0.80	0.78	Fe++	0.55	0.59
Mg	0.00	0.00	0.00	Mn	0.01	0.01	Mn	0.02	0.01
Ca	0.97	0.96	0.94	Mg	1.18	1.17	Mg	1.04	1.12
Na	0.04	0.04	0.05	Ni	0.00	0.00	Ca	0.30	0.23
K	0.00	0.00	0.00	Ca	0.01	0.01	Na	0.00	0.00
Total	4.99	5.01	4.99	Total	3.01	3.00	Total	3.99	3.99
Mg*	0.00	0.00	0.00	Mg*	59.71	59.96	Mg*	65.35	65.54
Or	0.00	0.00	0.00	Fo	59.45	59.75	En	55.00	57.70
Ab	4.27	4.31	4.60	Fa	40.11	39.90	Fs	29.16	30.34
An	95.73	95.69	95.40	Tp	0.44	0.35	Wo	15.84	11.96

wt.% - weight percentages; AC - anorthosite clast; Pl -Plagioclase, Plagioclase formula cations/ 8 oxygen; Ol - Olivine; Olivine formula cations/ 4 oxygen; Opx- Orthopyroxene, Orthopyroxene formula cations/ 6 oxygen; Mg# - molar Mg/(Fe+Mg)*100

Table 23 Chemical compositions of minerals in anorthosite clast AC in NWA 15352.

AC 3.1

wt.%	Pl	Pl		Cpx		Opx
SiO2	43.58	43.99	SiO2	51.37	SiO2	52.68
TiO2	-	-	TiO2	1.36	TiO2	0.83
Al2O3	36.34	36.41	Al2O3	1.64	Al2O3	0.95
Cr2O3	-	-	Cr2O3	0.46	Cr2O3	0.38
FeO	-	-	FeO	10.6	FeO	18.94
MnO	-	-	MnO	-	MnO	0.34
MgO	-	-	MgO	15.58	MgO	20.45
CaO	20.01	20.1	CaO	17.67	CaO	5.11
Na2O	0.25	0.32	Na2O	-	Na2O	-
K2O	-	-	K2O	-	K2O	-
Total	100.18	100.82	Total	98.68	Total	99.68
Si	2.01	2.02	Si	1.94	Si	1.97
Al	1.98	1.97	Ti	0.04	Ti	0.02
Ti	0.00	0.00	Al	0.07	Al	0.04
Fe++	0.00	0.00	Cr	0.01	Cr	0.01
Mn	0.00	0.00	Fe++	0.33	Fe++	0.59
Mg	0.00	0.00	Mn	0.00	Mn	0.01
Ca	0.99	0.99	Mg	0.88	Mg	1.14
Na	0.02	0.03	Ca	0.71	Ca	0.20
K	0.00	0.00	Na	0.00	Na	0.00
Total	5.01	5.01	Total	3.98	Total	3.98
Mg*	0.00	0.00	Mg*	72.38	Mg*	65.81
Or	0.00	0.00	En	45.52	En	58.85
Ab	2.21	2.80	Fs	17.37	Fs	30.58
An	97.79	97.20	Wo	37.11	Wo	10.57

AC 3.2

	Pl	Pl		Ol	Ol	Ol		Cpx		Opx		Ilm
SiO2	44.44	44.37	SiO2	36.69	36.88	37.03	SiO2	51.31	SiO2	52.94	SiO2	4.55
TiO2	-	-	TiO2	-	-	-	TiO2	0.87	TiO2	0.62	TiO2	48
Al2O3	35.16	35.24	Al2O3	-	-	0.27	Al2O3	1.33	Al2O3	1.79	Al2O3	0.58
Cr2O3	-	-	Cr2O3	-	-	-	Cr2O3	0.56	Cr2O3	0.68	Cr2O3	0.97
FeO	-	0.22	FeO	32.82	32.74	33.3	FeO	18.28	FeO	10.2	FeO	37.64
MnO	-	-	MnO	0.44	0.47	0.27	MnO	0.24	MnO	0.27	MnO	0.4
MgO	-	-	MgO	29.23	30.06	29.09	MgO	19.91	MgO	16.39	MgO	6.51
CaO	19.46	19.71	CaO	0.22	0.42	0.42	CaO	6.17	CaO	17.6	CaO	1.33
Na2O	0.59	0.56	Na2O	-	-	-	Na2O	-	Na2O	-	Na2O	-
K2O	-	-	K2O	-	0.12	-	K2O	-	K2O	-	K2O	-
Total	99.65	100.1	Total	99.4	100.69	100.38	Total	98.67	Total	100.49	Total	99.98
Si	2.06	2.05	Si	1.01	1.01	1.01	Si	1.94	Si	1.95	Si	0.21
Al	1.92	1.92	Ti	0.00	0.00	0.00	Ti	0.02	Ti	0.02	Ti	1.70
Ti	0.00	0.00	Al	0.00	0.00	0.01	Al	0.06	Al	0.08	Al	0.03
Fe++	0.00	0.01	Cr	0.00	0.00	0.00	Cr	0.02	Cr	0.02	Cr	0.04
Mn	0.00	0.00	Fe++	0.76	0.75	0.76	Fe++	0.58	Fe++	0.31	Fe++	1.48
Mg	0.00	0.00	Mn	0.01	0.01	0.01	Mn	0.01	Mn	0.01	Mn	0.02
Ca	0.97	0.98	Mg	1.20	1.22	1.19	Mg	1.12	Mg	0.90	Mg	0.46
Na	0.05	0.05	Ni	0.00	0.01	0.01	Ca	0.25	Ca	0.69	Ca	0.07
K	0.00	0.00	Ca	0.00	0.00	0.00	Na		Na		Na	0.00
Total	5.00	5.01	Total	2.99	2.99	2.98	Total	4.00	Total	3.98	Total	4.01
Mg*	0.00	0.00	Mg*	61.36	62.08	60.90	Mg*	66.00	Mg*	74.12	Mg*	23.57
Or	0.00	0.00	Fo	61.04	61.74	60.70	En	57.54	En	47.15		
Ab	5.20	4.89	Fa	38.44	37.71	38.98	Fs	29.64	Fs	16.46		
An	94.80	95.11	Tp	0.52	0.55	0.32	Wo	12.82	Wo	36.39		

wt.% - weight percentages; AC - anorthosite clast; Pl - Plagioclase formula cations/ 8 oxygen; Ol - Olivine; Olivine formula cations/ 4 oxygen; Opx- Orthopyroxene, Cpx-Clinopyroxene Orthopyroxene and Clinopyroxene formula cations/ 6 oxygen;
Ilm-Ilmenite, formula cations/6 oxygen; Mg# - molar Mg/(Fe+Mg)*100

Table 24 Chemical compositions of minerals in anorthosite clast AC in NWA 15352.

	AC 3.3								AC 3.4				
wt.%	Pl			Ol			Opx		Pl		Opx		Ilm
SiO2	44.13	43.57	SiO2	36.54	35.97	SiO2	53.10	SiO2	47.44	SiO2	51.91	SiO2	0.22
TiO2	-	-	TiO2	-	-	TiO2	0.54	TiO2	-	TiO2	0.57	TiO2	52.63
Al2O3	35.83	36.02	Al2O3	-	-	Al2O3	0.90	Al2O3	32.77	Al2O3	3.94	Al2O3	0.22
Cr2O3	-	-	Cr2O3	-	-	Cr2O3	0.32	Cr2O3	-	Cr2O3	0.25	Cr2O3	0.72
FeO	-	-	FeO	33.82	33.87	FeO	19.73	FeO	0.42	FeO	18.30	FeO	39.10
MnO	-	-	MnO	0.36	0.24	MnO	0.28	MnO	-	MnO	-	MnO	0.25
MgO	-	-	MgO	29.09	29.30	MgO	21.17	MgO	-	MgO	18.70	MgO	4.83
CaO	19.97	19.68	CaO	0.27	0.33	CaO	3.69	CaO	17.55	CaO	6.35	CaO	0.49
Na2O	0.38	0.37	Na2O	-	-	Na2O	-	Na2O	1.49	Na2O	-	Na2O	-
K2O	-	-	K2O	-	-	K2O	-	K2O	0.20	K2O	-	K2O	-
Total	100.31	99.64	Total	100.08	99.71	Total	99.73	Total	99.87	Total	100.02	Total	98.46
Si	2.04	2.02	Si	1.01	1.00	Si	1.98	Si	2.19	Si	1.92	Si	0.01
Al	1.95	1.97	Ti	0.00	0.00	Ti	0.02	Al	1.78	Ti	0.02	Ti	1.95
Ti	0.00	0.00	Al	0.00	0.00	Al	0.04	Ti	0.00	Al	0.17	Al	0.01
Fe++	0.00	0.00	Cr	0.00	0.00	Cr	0.01	Fe++	0.02	Cr	0.01	Cr	0.03
Mn	0.00	0.00	Fe++	0.78	0.79	Fe++	0.61	Mn	0.00	Fe++	0.57	Fe++	1.61
Mg	0.00	0.00	Mn	0.01	0.01	Mn	0.01	Mg	0.00	Mn	0.00	Mn	0.01
Ca	0.99	0.98	Mg	1.20	1.21	Mg	1.17	Ca	0.87	Mg	1.03	Mg	0.35
Na	0.03	0.03	Ni	0.00	0.00	Ca	0.15	Na	0.13	Ca	0.25	Ca	0.03
K	0.00	0.00	Ca	0.01	0.01	Na	0.00	K	0.01	Na	0.00	Na	0.00
Total	5.01	5.01	Total	3.00	3.01	Total	3.98	Total	5.00	Total	3.97	Total	3.99
Mg*	0.00	0.00	Mg*	60.53	60.67	Mg*	65.67	Mg*	0.00	Mg*	64.56	Mg*	18.05
Or	0.00	0.00	Fo	60.27	60.50	En	60.68	Or	1.16	En	55.77		
Ab	3.33	3.29	Fa	39.30	39.22	Fs	31.72	Ab	13.16	Fs	30.62		
An	96.67	96.71	Tp	0.42	0.28	Wo	7.60	An	85.67	Wo	13.61		

wt.% - weight percentages; AC - anorthosite clast; Pl - Plagioclase formula cations/ 8 oxygen; Ol - Olivine; Olivine formula cations/ 4 oxygen; Opx- Orthopyroxene, formula cations/ 6 oxygen;
Ilm-Ilmenite, formula cations/6 oxygen; Mg# - molar Mg/(Fe+Mg)*100

Table 25 Chemical compositions of minerals in anorthosite clast AC in NWA 15352.

AC 4

wt.%	Pl			
SiO2	44.28	45.03	44.28	45.03
TiO2	-	-	-	-
Al2O3	35.11	35.05	35.11	35.05
Cr2O3	-	-	-	-
FeO	-	0.46	-	0.46
MnO	-	-	-	-
MgO	-	-	-	-
CaO	19.55	19.31	19.55	19.31
Na2O	0.40	0.72	0.40	0.72
K2O	-	-	-	-
Total	99.34	100.57	99.34	100.57
Si	2.06	2.07	2.06	2.07
Al	1.93	1.90	1.93	1.90
Ti	0.00	0.00	0.00	0.00
Fe++	0.00	0.02	0.00	0.02
Mn	0.00	0.00	0.00	0.00
Mg	0.00	0.00	0.00	0.00
Ca	0.97	0.95	0.97	0.95
Na	0.04	0.06	0.04	0.06
K	0.00	0.00	0.00	0.00
Total	5.00	5.01	5.00	5.01
Mg*	0.00	0.00	0.00	0.00
Or	0.00	0.00	0.00	0.00
Ab	3.57	6.32	3.57	6.32
An	96.43	93.68	96.43	93.68

	Ol							
SiO2	36.93	36.97	37.41	36.60	36.48	36.88	36.99	39.03
TiO2	-	-	-	-	-	-	0.21	-
Al2O3	-	-	0.44	-	0.35	0.40	-	1.48
Cr2O3	-	-	-	-	0.23	-	-	-
FeO	30.77	31.73	30.37	33.51	31.30	33.25	32.09	27.51
MnO	0.37	0.39	0.33	0.23	0.23	0.40	0.25	0.27
MgO	31.03	31.60	30.43	29.06	29.71	28.86	31.21	31.11
CaO	0.23	0.24	0.35	0.21	0.30	0.31	0.25	0.68
Na2O	-	-	-	-	-	-	-	-
K2O	-	-	-	-	-	-	-	0.14
Total	99.33	100.93	99.33	99.61	98.60	100.10	101.00	100.22
Si	1.01	1.00	1.02	1.01	1.01	1.01	1.00	1.04
Ti	0.00	0.00	0.00	0.00	0.00	0.00	0.00	0.00
Al	0.00	0.00	0.01	0.00	0.01	0.01	0.00	0.05
Cr	0.00	0.00	0.00	0.00	0.01	0.00	0.00	0.00
Fe++	0.70	0.72	0.69	0.77	0.72	0.76	0.72	0.61
Mn	0.01	0.01	0.01	0.01	0.01	0.01	0.01	0.01
Mg	1.27	1.27	1.24	1.20	1.22	1.18	1.26	1.23
Ni	0.00	0.00	0.00	0.00	0.01	0.01	0.01	0.00
Ca	0.01	0.01	0.01	0.01	0.01	0.01	0.01	0.02
Total	3.00	3.01	2.98	3.00	2.99	2.99	3.00	2.96
Mg*	64.26	63.97	64.11	60.72	62.86	60.75	63.42	66.85
Fo	63.98	63.69	63.86	60.56	62.68	60.46	63.24	66.63
Fa	35.59	35.87	35.75	39.17	37.04	39.07	36.47	33.05
Tp	0.43	0.45	0.39	0.27	0.28	0.48	0.29	0.33

	Opx						
SiO2	52.28	53.88	54.04	55.07	51.61	54.95	54.23
TiO2	0.44	0.68	0.79	0.00	0.61	0.73	0.46
Al2O3	1.32	1.12	1.37	1.10	1.57	1.39	1.12
Cr2O3	0.00	0.45	0.62	0.61	0.59	0.42	0.46
FeO	20.79	13.44	13.48	14.50	20.31	13.68	13.49
MnO	0.36	0.23	0.26	0.31	0.30	0.23	0.28
MgO	20.87	27.16	27.19	27.22	17.42	28.10	27.72
CaO	3.29	1.96	1.88	1.78	7.42	2.01	2.15
Na2O	-	-	-	-	-	-	-
K2O	-	-	-	-	-	-	-
Total	99.35	98.92	99.63	100.59	99.83	101.51	99.91
Si	1.96	1.96	1.95	1.97	1.95	1.94	1.95
Ti	0.01	0.02	0.02	0.00	0.02	0.02	0.01
Al	0.06	0.05	0.06	0.05	0.07	0.06	0.05
Cr	0.00	0.01	0.02	0.02	0.02	0.01	0.01
Fe++	0.65	0.41	0.41	0.43	0.64	0.40	0.41
Mn	0.01	0.01	0.01	0.01	0.01	0.01	0.01
Mg	1.17	1.47	1.46	1.45	0.98	1.48	1.49
Ca	0.13	0.08	0.07	0.07	0.30	0.08	0.08
Na	0.00	0.00	0.00	0.00	0.00	0.00	0.00
Total	4.00	4.00	3.99	4.00	3.99	4.00	4.01
Mg*	64.15	78.27	78.24	76.99	60.46	78.55	78.55
En	59.80	75.22	75.31	74.30	51.02	75.50	75.26
Fs	33.42	20.88	20.95	22.20	33.37	20.62	20.55
Wo	6.78	3.90	3.74	3.49	15.62	3.88	4.20

wt.% - weight percentages; AC - anorthosite clast; P - Plagioclase formula cations/ 8 oxygen; Ol - Olivine; Olivine formula cations/ 4 oxygen; Opx- Orthopyroxene, Orthopyroxene formula cations/ 6 oxygen; Mg# - molar Mg/(Fe+Mg)*100

Table 26 Chemical compositions of minerals in anorthosite clast AC in NWA 15352.

	AC 5											
wt.%	Pl					Ol				Opx		
SiO2	43.76	43.65	43.46	43.9	SiO2	36.35	35.39	35.8	SiO2	53.19	52.45	52.7
TiO2	-	-	-	-	TiO2	-	-	-	TiO2	0.46	0.6	0.46
Al2O3	34.98	35.15	35.28	35.42	Al2O3	1.04	-	0.43	Al2O3	0.81	1.07	0.96
Cr2O3	-	-	-	-	Cr2O3	-	-	-	Cr2O3	-	-	-
FeO	0.17	0.27	0.28	0.21	FeO	33.56	34.32	33.86	FeO	20.19	19.29	20.29
MnO	-	-	-	-	MnO	0.3	0.34	0.45	MnO	0.33	0.33	0.36
MgO	-	-	-	-	MgO	27.78	28.47	28.23	MgO	21.19	20.39	21.17
CaO	19.9	20.14	20.29	20.23	CaO	0.5	0.61	0.34	CaO	4.44	5.41	3.56
Na2O	0.37	0.47	0.55	0.42	Na2O	-	-	-	Na2O	-	-	-
K2O	-	-	-	-	K2O	-	-	-	K2O	-	-	-
Total	99.18	99.68	99.86	100.18	Total	99.53	99.13	99.11	Total	100.61	99.54	99.5
Si	2.04	2.03	2.02	2.03	Si	1.01	0.99	1.00	Si	1.97	1.96	1.97
Al	1.93	1.93	1.94	1.93	Ti	0.00	0.00	0.00	Ti	0.01	0.02	0.01
Ti	0.00	0.00	0.00	0.00	Al	0.03	0.00	0.01	Al	0.04	0.05	0.04
Fe++	0.01	0.01	0.01	0.01	Cr	0.00	0.00	0.00	Cr	0.00	0.00	0.00
Mn	0.00	0.00	0.00	0.00	Fe++	0.78	0.81	0.79	Fe++	0.63	0.60	0.63
Mg	0.00	0.00	0.00	0.00	Mn	0.01	0.01	0.01	Mn	0.01	0.01	0.01
Ca	1.00	1.01	1.01	1.00	Mg	1.15	1.19	1.18	Mg	1.17	1.14	1.18
Na	0.03	0.04	0.05	0.04	Ni	0.00	0.01	0.00	Ca	0.18	0.22	0.14
K	0.00	0.00	0.00	0.00	Ca	0.01	0.02	0.01	Na	0.00	0.00	0.00
Total	5.01	5.02	5.03	5.02	Total	2.99	3.03	3.00	Total	4.00	4.00	4.00
Mg*	0.00	0.00	0.00	0.00	Mg*	59.61	59.66	59.78	Mg*	65.17	65.33	65.03
Or	0.00	0.00	0.00	0.00	Fo	59.39	59.42	59.46	En	59.34	58.09	60.29
Ab	3.26	4.05	4.68	3.62	Fa	40.24	40.18	40.00	Fs	31.72	30.83	32.93
An	96.74	95.95	95.32	96.38	Tp	0.36	0.40	0.54	Wo	8.94	11.08	7.29

wt.% - weight percentages; AC - anorthosite clast; Pl - Plagioclase formula cations/ 8 oxygen; Ol - Olivine; Olivine formula cations/ 4 oxygen;
Opx- Orthopyroxene, Orthopyroxene formula cations/ 4 oxygen; Mg# - molar Mg/(Fe+Mg)*100

Table 27 Chemical compositions of minerals anorthosite clast AC in NWA 15352.

	AC 6									
wt.%	Pl			Ol			Cpx			Opx
SiO2	44.54	43.91	SiO2	36.61	36.39	SiO2	51.87	52.03	SiO2	53.13
TiO2	-	-	TiO2	-	-	TiO2	1.17	1.14	TiO2	0.55
Al2O3	35.37	35.3	Al2O3	-	-	Al2O3	1.97	1.48	Al2O3	0.56
Cr2O3	-	-	Cr2O3	-	-	Cr2O3	0.46	0.44	Cr2O3	0.35
FeO	0.32	0.21	FeO	33.81	33.86	FeO	9.65	10.96	FeO	16.9
MnO	-	-	MnO	0.3	0.3	MnO	0.29	0.22	MnO	0.26
MgO	-	-	MgO	28.5	28.6	MgO	15.37	15.22	MgO	21.75
CaO	19.31	19.63	CaO	0.18	0.34	CaO	19.47	17.98	CaO	4.96
Na2O	0.44	0.49	Na2O	-	-	Na2O	-	-	Na2O	-
K2O	-	-	K2O	-	-	K2O	-	-	K2O	-
Total	99.98	99.54	Total	99.4	99.49	Total	100.25	99.47	Total	98.46
Si	2.06	2.04	Si	1.02	1.01	Si	1.93	1.95	Si	1.99
Al	1.93	1.94	Ti	0.00	0.00	Ti	0.03	0.03	Ti	0.02
Ti	0.00	0.00	Al	0.00	0.00	Al	0.09	0.07	Al	0.02
Fe++	0.01	0.01	Cr	0.00	0.00	Cr	0.01	0.01	Cr	0.01
Mn	0.00	0.00	Fe++	0.78	0.79	Fe++	0.30	0.34	Fe++	0.53
Mg	0.00	0.00	Mn	0.01	0.01	Mn	0.01	0.01	Mn	0.01
Ca	0.96	0.98	Mg	1.18	1.18	Mg	0.85	0.85	Mg	1.21
Na	0.04	0.04	Ni	0.00	0.00	Ca	0.77	0.72	Ca	0.20
K	0.00	0.00	Ca	0.01	0.01	Na	0.00		Na	
Total	5.00	5.01	Total	2.99	3.00	Total	3.99	3.98	Total	3.98
Mg*	0.00	0.00	Mg*	60.05	60.09	Mg*	73.95	71.23	Mg*	69.64
Or	0.00	0.00	Fo	59.83	59.88	En	44.20	44.38	En	62.51
Ab	3.96	4.32	Fa	39.81	39.76	Fs	15.57	17.93	Fs	27.25
An	96.04	95.68	Tp	0.36	0.36	Wo	40.24	37.69	Wo	10.25

wt.% - weight percentages; AC - anorthosite clast; Pl - Plagioclase formula cations/ 8 oxygen; Ol - Olivine; Olivine formula cations/ 4 oxygen;
Opx- Orthopyroxene, Cpx-Clinopyroxene; Orthopyroxene and Clinopyroxene formula cations/ 6 oxygen; Mg# - molar Mg/(Fe+Mg)*100

Table 28 Chemical compositions (wt.%) of mineral fragments in matrix NWA 15352.

	M 1					M 2									
wt.%	Ol			Cpx			Opx			Ilm			Troi		
SiO2	36.22	36.61	SiO2	52.31	52.21	SiO2	52.77	52.36	SiO2	-	-	SiO2	0.50	0.24	0.59
TiO2	-	-	TiO2	1.30	1.04	TiO2	0.35	0.56	TiO2	52.25	51.28	TiO2	-	-	-
Al2O3	0.41	0.28	Al2O3	2.09	1.50	Al2O3	0.63	0.57	Al2O3	0.32	0.30	Al2O3	0.15	0.21	0.22
Cr2O3	-	-	Cr2O3	0.53	0.48	Cr2O3	0.37	0.27	Cr2O3	0.73	1.03	Cr2O3	-	-	-
FeO	34.17	34.50	FeO	12.46	12.84	FeO	20.69	21.23	FeO	38.93	39.43	FeO	57.34	57.75	56.86
MnO	0.47	0.32	MnO	-	-	MnO	0.47	0.32	MnO	0.35	0.42	MnO	-	-	-
MgO	28.15	28.84	MgO	15.85	15.26	MgO	19.84	19.80	MgO	4.62	4.87	MgO	0.20	-	-
CaO	0.28	0.33	CaO	16.71	17.05	CaO	4.78	4.88	CaO	0.17	-	CaO	0.25	0.21	0.25
Na2O	-	-	Na2O	-	-	Na2O	-	-	Na2O	-	-	Na2O	-	-	-
K2O	-	-	K2O	-	-	K2O	-	-	K2O	-	-	K2O	-	-	-
Total	99.71	100.87	Total	101.26	100.39	Total	99.68	99.98	Total	97.37	97.35	S	39.18	39.15	38.64
												Ni	0.32	-	-
												ZrO2	0.87	0.61	0.74
Si	1.01	1.00	Si	1.93	1.95	Si	1.98	1.97	Si	0.00	0.00	Total	98.81	98.17	97.30
Ti	0.00	0.00	Ti	0.04	0.03	Ti	0.01	0.02	Ti	1.96	1.92				
Al	0.01	0.01	Al	0.09	0.07	Al	0.03	0.03	Al	0.02	0.02				
Cr	0.00	0.00	Cr	0.02	0.01	Cr	0.01	0.01	Cr	0.03	0.04				
Fe++	0.79	0.79	Fe++	0.38	0.40	Fe++	0.65	0.67	Fe++	1.62	1.64				
Mn	0.01	0.01	Mn	0.00	0.00	Mn	0.01	0.01	Mn	0.01	0.02				
Mg	1.16	1.18	Mg	0.87	0.85	Mg	1.11	1.11	Mg	0.34	0.36	Ni	0.04	0.00	0.00
Ni	0.00	0.00	Ca	0.66	0.68	Ca	0.19	0.20	Ca	0.01	0.00	Fe	6.72	6.77	6.76
Ca	0.01	0.01	Na	0.00	0.00	Na	0.00	0.00	Na	0.00	0.00	S	8.00	8.00	8.00
Total	2.99	3.00	Total	3.98	3.98	Total	3.99	4.00	Total	3.99	4.01	Total	14.76	14.77	14.76
Mg*	59.49	59.85	Mg*	69.40	67.93	Mg*	63.09	62.44	Mg*	17.46	18.05				
Fo	59.16	59.62	En	45.48	43.96	En	56.88	56.22							
Fa	40.28	40.00	Fs	20.06	20.75	Fs	33.27	33.82							
Tp	0.56	0.38	Wo	34.46	35.30	Wo	9.85	9.96							

wt.% - weight percentages; M - Mineral fragment; Ol - Olivine; Olivine formula cations/ 4 oxygen; Opx-Orthopyroxene, Cpx-Clinopyroxene, Orthopyroxene and Clinopyroxene formula cations/ 6 oxygen; Ilm-Ilmenite, formula cations/6 oxygen; Troi - Troilite, Troilite formula 8 sulfur; Mg# - molar Mg/(Fe+Mg).

Table 29 Chemical compositions (wt.%) of mineral fragments in matrix NWA 15352.

	M 3						
wt.%	Ol		Opx		Cr-rich Spl		Troi
SiO2	36.81	SiO2	54.49	SiO2	3.6	SiO2	0.32
TiO2	-	TiO2	0.79	TiO2	17.17	TiO2	-
Al2O3	-	Al2O3	1.22	Al2O3	6.08	Al2O3	0.16
Cr2O3	-	Cr2O3	0.54	Cr2O3	23.68	Cr2O3	-
FeO	33.89	FeO	9.89	FeO	41.83	FeO	59.57
MnO	-	MnO	-	MnO	0.5	MnO	-
MgO	28.49	MgO	28.05	MgO	4.41	MgO	-
CaO	0.32	CaO	5.6	CaO	0.9	CaO	0.4
Na2O	-	Na2O	-	Na2O	-	Na2O	-
K2O	-	K2O	-	K2O	-	K2O	-
S	-	S	-	S	0.28	S	36.38
Ni	-	Ni	-	Ni	-	Ni	0.76
ZrO2	-	ZrO2	-	ZrO2	-	ZrO2	0.76
Total	99.51	Total	100.58	Total	98.45	Total	98.35
Si	1.02	Si	1.93	Si	0.13		
Ti	0.00	Ti	0.02	Ti	0.45		
Al	0.00	Al	0.05	Al	0.25		
Cr	0.00	Cr	0.02	Cr	0.65		
Fe++	0.78	Fe++	0.29	Fe++	1.22		
Mn	0.00	Mn	0.00	Mn	0.01		
Mg	1.18	Mg	1.48	Mg	0.23	Ni	0.09
Ni	0.00	Ca	0.21	Ca	0.03	Fe	7.52
Ca	0.01	Na	0.00	Na	0.00	S	8.00
Total	2.99	Total	4.01	Total	2.97	Total	15.61
Mg*	59.98	Mg*	83.49	Mg*	15.82		
Fo	59.98	En	74.56				
Fa	40.02	Fs	14.75				
Tp	0.00	Wo	10.70				

wt.% - weight percentages; M - Mineral fragment; Ol - Olivine; Olivine formula cations/ 4 oxygen; Opx-Orthopyroxene, Orthopyroxene formula cations/ 6 oxygen; Cr-rich Spl-Chromium-rich Spinel, Spinel formua cations/6; Troi - Troilite, Troilite formula 8 sulfur; Mg# - molar Mg/(Fe+Mg)*100

Table 30 Chemical compositions (wt.%) of mineral fragments in matrix NWA 15352.

	M 4								
wt.%	Pl		Ol		Cpx		Opx		Troi
SiO2	43.68	SiO2	36.56	SiO2	51.37	SiO2	53.35	SiO2	0.15
TiO2	-	TiO2	0.25	TiO2	1.18	TiO2	0.55	TiO2	-
Al2O3	35.28	Al2O3	0.36	Al2O3	1.75	Al2O3	1.11	Al2O3	-
Cr2O3	-	Cr2O3	-	Cr2O3	0.38	Cr2O3	0.4	Cr2O3	-
FeO	0.57	FeO	33.16	FeO	14.95	FeO	18.06	FeO	57.87
MnO	-	MnO	0.44	MnO	0.27	MnO	0.33	MnO	-
MgO	-	MgO	28.53	MgO	16.69	MgO	23.97	MgO	-
CaO	19.25	CaO	0.28	CaO	12.25	CaO	1.53	CaO	0.23
Na2O	0.42	Na2O	-	Na2O	-	Na2O	-	Na2O	-
K2O	-	K2O	-	K2O	-	K2O	-	K2O	-
S	-	S	-	S	-	S	-	S	39.65
Ni	-	Ni	-	Ni	-	Ni	-	Ni	-
ZrO2	-	ZrO2	-	ZrO2	-	ZrO2	-	ZrO2	0.69
Total	99.2	Total	99.58	Total	98.84	Total	99.30	Total	98.59
Si	2.04	Si	1.01	Si	1.94	Si	1.97		
Al	1.94	Ti	0.01	Ti	0.03	Ti	0.02		
Ti	0.00	Al	0.01	Al	0.08	Al	0.05		
Fe++	0.02	Cr	0.00	Cr	0.01	Cr	0.01		
Mn	0.00	Fe++	0.77	Fe++	0.47	Fe++	0.56		
Mg	0.00	Mn	0.01	Mn	0.01	Mn	0.01		
Ca	0.96	Mg	1.18	Mg	0.94	Mg	1.32	Ni	0
Na	0.04	Ni	0.00	Ca	0.50	Ca	0.06	Fe	6.70
K	0.00	Ca	0.01	Na	0.00	Na	0.00	S	8.00
Total	5.01	Total	2.99	Total	3.98	Total	3.99	Total	14.70
Mg*	0.00	Mg*	60.54	Mg*	66.56	Mg*	70.29		
Or	0.00	Fo	60.22	En	49.26	En	68.09		
Ab	3.80	Fa	39.26	Fs	24.75	Fs	28.78		
An	96.20	Tp	0.53	Wo	25.99	Wo	3.12		

wt.% - weight percentages; M-Mineral fragments; P - Plagioclase formula cations/ 8 oxygen; Ol - Olivine; Olivine formula cations/ 4 oxygen; Opx- Orthopyroxene, Cpx-Clinopyroxene Orthopyroxene and Clinopyroxene formula cations/ 6 oxygen; Troi - Troilite, Troilite formula 8 sulfur; Mg# - molar Mg/(Fe+Mg)*100

Table 31 Chemical compositions (wt.%) of mineral fragments in matrix NWA 15352.

	M 5.1					M 5.2				M 5.3	
wt.%	Cpx					Opx				Ol	
SiO2	47.87	47.71	49.48	52.48	SiO2	55.13	52.70	55.26	SiO2	36.14	36.28
TiO2	1.07	1.06	1.12	0.40	TiO2	0.28	0.44	0.27	TiO2	-	
Al2O3	1.24	1.23	1.35	1.33	Al2O3	0.97	1.56	1.08	Al2O3	-	0.22
Cr2O3	0.26	0.33	0.29	0.22	Cr2O3	0.23	0.29	0.25	Cr2O3	-	
FeO	26.44	26.75	16.80	9.23	FeO	9.79	5.10	10.06	FeO	34.20	33.90
MnO	0.50	0.42	0.27	0.18	MnO	-	0.15	0.15	MnO	0.42	0.19
MgO	5.55	5.63	11.11	14.81	MgO	30.16	17.61	30.22	MgO	28.91	28.49
CaO	16.82	16.58	18.03	21.31	CaO	1.52	21.12	1.75	CaO	0.31	0.28
Na2O	-	-	-	-	Na2O	-	-	-	Na2O	-	-
K2O	-	-	-	-	K2O	-	-	-	K2O	-	-
ZrO2	-	-	0.17	-	ZrO2	-	-	-	ZrO2	-	-
Ni	-	-	-	-	Ni	-	-	-	Ni	-	0.20
Total	99.75	99.71	99.71	99.96	Total	98.08	98.97	99.04	Total	99.98	99.56
Si	1.93	1.93	1.93	1.96	Si	1.98	1.95	1.97	Si	1.00	1.01
Ti	0.03	0.03	0.03	0.01	Ti	0.01	0.01	0.01	Ti	0.00	0.00
Al	0.06	0.06	0.06	0.06	Al	0.04	0.07	0.05	Al	0.00	0.01
Cr	0.01	0.01	0.01	0.01	Cr	0.01	0.01	0.01	Cr	0.00	0.00
Fe++	0.89	0.90	0.55	0.29	Fe++	0.29	0.16	0.30	Fe++	0.79	0.79
Mn	0.02	0.01	0.01	0.01	Mn	0.00	0.00	0.00	Mn	0.01	0.00
Mg	0.33	0.34	0.65	0.82	Mg	1.61	0.97	1.60	Mg	1.19	1.18
Ca	0.73	0.72	0.75	0.85	Ca	0.06	0.84	0.07	Ni	0.00	0.00
Na	0.00	0.00	0.00	0.00	Na	0.00	0.00		Ca	0.01	0.01
Total	4.00	4.01	4.00	4.00	Total	3.99	4.00	4.00	Total	3.01	3.00
Mg*	27.23	27.28	54.10	74.10	Mg*	84.60	86.02	84.26	Mg*	60.11	59.97
En	17.09	17.30	33.17	41.95	En	82.08	49.40	81.41	Fo	59.82	59.84
Fs	45.68	46.10	0.28	0.15	Fs	14.95	8.03	0.15	Fa	39.69	39.94
Wo	37.23	36.61	38.69	43.38	Wo	2.97	42.58	3.39	Tp	0.49	0.23

wt.% - weight percentages; M - Mineral fragment; Ol - Olivine; Olivine formula cations/ 4 oxygen; Opx-Orthopyroxene, Cpx-Clinopyroxene, Orthopyroxene and Clinopyroxene formula cations/ 6 oxygen; Mg# - molar Mg/(Fe+Mg)*100

Table 32 Chemical compositions (wt.%) of mineral fragments in matrix NWA 15352.

	M 5.3				M 6			
wt.%	Cpx		Opx		Ol			Cr_rich Spl
SiO2	50.83	SiO2	50.91	SiO2	36.09	36.09	SiO2	18.89
TiO2	0.77	TiO2	0.80	TiO2	-	-	TiO2	11.60
Al2O3	1.86	Al2O3	2.51	Al2O3	-	0.28	Al2O3	5.62
Cr2O3	0.58	Cr2O3	0.69	Cr2O3	-	-	Cr2O3	14.83
FeO	12.72	FeO	16.36	FeO	33.71	33.50	FeO	35.91
MnO	0.30	MnO	0.35	MnO	0.30	0.35	MnO	0.26
MgO	15.59	MgO	17.98	MgO	28.56	28.38	MgO	10.37
CaO	15.73	CaO	9.71	CaO	0.45	0.47	CaO	1.87
Na2O	-	Na2O	-	Na2O	-	-	Na2O	-
K2O	-	K2O	-	K2O	-	-	K2O	-
ZrO2	-	ZrO2	-	ZrO2	-	-	ZrO2	-
Ni	-	Ni	-	Ni	-	-	Ni	-
V	-	V	-	V	-	-	V	0.52
Total	98.38	Total	99.31	Total	99.11	99.07	Total	99.87
Si	1.93	Si	1.92	Si	1.01	1.01	Si	0.58
Ti	0.02	Ti	0.02	Ti	0.00	0.00	Ti	0.27
Al	0.08	Al	0.11	Al	0.00	0.01	Al	0.20
Cr	0.02	Cr	0.02	Cr	0.00	0.00	Cr	0.36
Fe++	0.40	Fe++	0.51	Fe++	0.79	0.78	Fe++	0.92
Mn	0.01	Mn	0.01	Mn	0.01	0.01	Mn	0.01
Mg	0.88	Mg	1.01	Mg	1.19	1.18	Mg	0.47
Ca	0.64	Ca	0.39	Ni	0.00	0.00	Ca	0.06
Na	0.00	Na	0.00	Ca	0.01	0.01	Na	0.00
Total	3.99	Total	4.00	Total	3.01	3.00	Total	2.87
Mg*	68.60	Mg*	66.21	Mg*	60.17	60.17	Mg*	33.99
En	45.81	En	52.67	Fo	59.95	59.91		
Fs	20.97	Fs	26.89	Fa	39.69	39.67		
Wo	33.22	Wo	20.44	Tp	0.36	0.42		

wt.% - weight percentages; M - Mineral fragment; Ol - Olivine; Olivine formula cations/ 4 oxygen; Opx-Orthopyroxene, Cpx-Clinopyroxene, Orthopyroxene and Clinopyroxene formula cations/ 6 oxygen; Cr-rich Spl - Chromium-rich Spinel, formula cations/ 4 oxygen; Mg# - molar Mg/(Fe+Mg)*100

Table 33 Chemical compositions of mineral fragment in the matrix in NWA 15352.

	M 7						
wt.%	Pl		Cpx				Qtz
SiO2	43.92	SiO2	50.76	49		SiO2	97.82
TiO2	-	TiO2	1.02	2.35		TiO2	0.22
Al2O3	35.2	Al2O3	0.89	2.79		Al2O3	0.48
Cr2O3	-	Cr2O3	0.27	0.24		Cr2O3	-
FeO	0.27	FeO	14.65	14.31		FeO	0.34
MnO	-	MnO	-	0.3		MnO	-
MgO	-	MgO	11.28	10.46		MgO	0.28
CaO	19.22	CaO	19.49	19.24		CaO	0.18
Na2O	0.41	Na2O	-	-		Na2O	-
K2O	-	K2O	-	-		K2O	-
S	-	S	0.68	-		S	-
Total	99.02	Total	99.04	98.69		Total	99.32
Si	2.05	Si	1.97	1.89			
Al	1.94	Ti	0.03	0.07			
Ti	0.00	Al	0.04	0.13			
Fe++	0.01	Cr	0.01	0.01			
Mn	0.00	Fe++	0.47	0.46			
Mg	0.00	Mn	0.00	0.01			
Ca	0.96	Mg	0.65	0.60			
Na	0.04	Ca	0.81	0.80			
K	0.00	Na	0.00	0.00			
Total	5.00	Total	3.98	3.97			
Mg*	0.00	Mg*	68.63	65.15			
Or	0.00	En	33.67	30.87			
Ab	3.72	Fs	24.53	28.32			
An	96.28	Wo	41.81	40.81			

wt.% - weight percentages; M - mineral fragment; Pl - Plagioclase formula cations/8 oxygen
Cpx-Clinopyroxene, Clinopyroxene formula cations/ 6 oxygen; Qtz - quartz; Mg# - molar Mg/(Fe+Mg)*100

Table 34 Chemical compositions (wt.%) of mineral fragments in matrix NWA 15352.

	M 8								
wt.%	Pl		Ol		Cpx		Ch-rich Spl		Qtz
SiO2	43.78	SiO2	36.69	SiO2	51.85	SiO2	5.92	SiO2	99.40
TiO2	-	TiO2	-	TiO2	0.82	TiO2	17.15	TiO2	0.27
Al2O3	35.68	Al2O3	0.74	Al2O3	1.40	Al2O3	6.06	Al2O3	0.51
Cr2O3	-	Cr2O3	-	Cr2O3	0.44	Cr2O3	21.55	Cr2O3	-
FeO	0.30	FeO	33.13	FeO	15.69	FeO	41.82	FeO	0.31
MnO	-	MnO	0.30	MnO	0.25	MnO	-	MnO	-
MgO	-	MgO	27.00	MgO	17.08	MgO	6.61	MgO	-
CaO	19.63	CaO	0.36	CaO	11.07	CaO	0.90	CaO	-
Na2O	0.28	Na2O	-	Na2O	-	Na2O	-	Na2O	-
K2O	-	K2O	-	K2O	-	K2O	-	K2O	-
Total	99.67	Total	98.22	Total	98.60	Total	100.01	Total	100.49
Si	2.03	Si	1.03	Si	1.96	Si	0.20		
Al	1.95	Ti	0.00	Ti	0.02	Ti	0.43		
Ti	0.00	Al	0.02	Al	0.06	Al	0.24		
Fe++	0.01	Cr	0.00	Cr	0.01	Cr	0.57		
Mn	0.00	Fe++	0.78	Fe++	0.50	Fe++	1.17		
Mg	0.00	Mn	0.01	Mn	0.01	Mn	0.00		
Ca	0.98	Mg	1.13	Mg	0.96	Mg	0.33		
Na	0.03	Ni	0.00	Ca	0.45	Ca	0.03		
K	0.00	Ca	0.00	Na	0.00	Na	0.00		
Total	5.00	Total	2.97	Total	3.98	Total	2.97		
Mg*	0.00	Mg*	59.23	Mg*	65.99	Mg*	21.98		
Or	0.00	Fo	59.01	En	50.48				
Ab	2.52	Fa	40.61	Fs	26.01				
An	97.48	Tp	0.37	Wo	23.51				

wt.% - weight percentages; M - Mineral fragment; Pl-Plagiocalse, Plagioclase formula cations/8 oxygen; Ol -Olivine; Olivine formula cations/ 4 oxygen;
Cpx-Clinopyroxene, Clinopyroxene formula cations/ 6 oxygen; Cr-rich Spl-Chromium-rich Spinel, Spinel formua cations/6; Qtz-Quartz; Mg# - molar Mg/(Fe+Mg)*100

Table 35 Chemical compositions (wt.%) of mineral fragments in matrix NWA 15352.

	M 9							
wt.%	Pl		Ol			Opx		
SiO2	46.16	SiO2	37.07	36.25	SiO2	52.31	51.86
TiO2	-	TiO2	-	-	TiO2	0.66	0.71
Al2O3	33.64	Al2O3	0.26	-	Al2O3	1.33	1.25
Cr2O3	-	Cr2O3	-	-	Cr2O3	0.41	0.42
FeO	0.51	FeO	33.81	33.69	FeO	18.53	21.60
MnO	-	MnO	0.21	0.30	MnO	0.21	0.39
MgO	-	MgO	29.13	28.43	MgO	19.31	20.46
CaO	17.76	CaO	0.33	0.33	CaO	6.54	2.73
Na2O	1.01	Na2O	-	-	Na2O	-	-
K2O	-	K2O	-	-	K2O	-	-
Total	99.08	Total	100.81	99.00	Total	99.30	99.42
Si	2.14	Si	1.01	1.01	Si	1.96	1.95
Al	1.84	Ti	0.00	0.00	Ti	0.02	0.02
Ti	0.00	Al	0.01	0.00	Al	0.06	0.06
Fe++	0.02	Cr	0.00	0.00	Cr	0.01	0.01
Mn	0.00	Fe++	0.77	0.79	Fe++	0.58	0.68
Mg	0.00	Mn	0.00	0.01	Mn	0.01	0.01
Ca	0.88	Mg	1.19	1.18	Mg	1.08	1.15
Na	0.09	Ni	0.00	0.00	Ca	0.26	0.11
K	0.00	Ca	0.01	0.01	Na	0.00	0.00
Total	4.98	Total	2.99	3.00	Total	3.98	3.99
Mg*	0.00	Mg*	0.61	0.60	Mg*	0.65	0.63
Or	0.00	Fo	60.42	59.86	En	56.12	59.24
Ab	9.33	Fa	39.33	39.78	Fs	30.21	35.08
An	90.67	Tp	0.25	0.36	Wo	13.66	5.68

wt.% - weight percentages; M - Mineral fragment; Pl-Plagiocalse, Plagioclase formula cations/8 oxygen; Ol - Olivine; Olivine formula cations/ 4 oxygen; Opx-Orthopyroxene, Orthopyroxene formula cations/ 6 oxygen; Ilm-Ilmenite, formula cations/6 oxygen; Mg# - molar Mg/(Fe+Mg)*100

Table 36 Chemical compositions (wt.%) of mineral fragments in matrix NWA 15352.

	M 10													
wt.%	Pl				Cpx		Opx					Qtz		
SiO2	44.00	45.44	45.69	SiO2	51.85	SiO2	51.90	52.09	52.05	52.46	SiO2	98.29	98.60	97.53
TiO2	-	-	-	TiO2	1.05	TiO2	0.63	0.51	0.60	0.48	TiO2	-	-	-
Al2O3	35.00	33.97	33.32	Al2O3	1.18	Al2O3	0.99	1.09	1.26	0.82	Al2O3	0.42	0.46	0.92
Cr2O3	-	-	-	Cr2O3	0.47	Cr2O3	0.48	0.28	0.30	0.21	Cr2O3	-	-	-
FeO	0.41	0.45	0.61	FeO	13.34	FeO	19.91	19.76	19.06	20.26	FeO	0.31	-	0.35
MnO	-	-	-	MnO	0.34	MnO	0.43	0.24	0.48	0.35	MnO	-	-	-
MgO	-	-	-	MgO	16.18	MgO	19.96	19.03	18.49	19.39	MgO	0.25	-	-
CaO	18.83	17.97	17.49	CaO	14.32	CaO	4.50	6.60	7.31	5.22	CaO	0.16	-	-
Na2O	0.59	0.92	1.01	Na2O	-	Na2O	-	-	-	-	Na2O	0.24	0.23	-
K2O	-	-	0.20	K2O	-	K2O	-	-	0.14	0.10	K2O	0.15	-	0.19
Total	98.83	98.75	98.32	Total	98.73	Total	98.80	99.60	99.69	99.29	Total	99.82	99.29	98.99
Si	2.06	2.12	2.14	Si	1.96	Si	1.96	1.96	1.96	1.98				
Al	1.93	1.87	1.84	Ti	0.03	Ti	0.02	0.01	0.02	0.01				
Ti	0.00	0.00	0.00	Al	0.05	Al	0.04	0.05	0.06	0.04				
Cr	-	-	-	Cr	0.01	Cr	0.01	0.01	0.01	0.01				
Fe++	0.02	0.02	0.02	Fe++	0.42	Fe++	0.63	0.62	0.60	0.64				
Mn	0.00	0.00	0.00	Mn	0.01	Mn	0.01	0.01	0.02	0.01				
Mg	0.00	0.00	0.00	Mg	0.91	Mg	1.13	1.07	1.04	1.09				
Ca	0.94	0.90	0.88	Ca	0.58	Ca	0.18	0.27	0.29	0.21				
Na	0.05	0.08	0.09	Na	0.00	Na	0.00	0.00	0.00	0.00				
K	0.00	0.00	0.01	K	0.00	K	0.00	0.00	0.01	0.00				
Total	5.00	4.99	4.99	Total	3.98	Total	3.99	4.00	3.99	3.99				
Mg*	0.00	0.00	0.00	Mg*	68.38	Mg*	64.12	63.19	63.36	63.05				
Or	0.00	0.00	1.22	En	0.65	En	58.09	54.59	53.69	56.19				
Ab	5.37	8.48	9.35	Fs	1.16	Fs	32.50	31.80	31.05	32.94				
An	94.63	91.52	89.44	Wo	45.86	Wo	9.41	13.61	15.26	10.87				

wt.% - weight percentages; M - Mineral fragment; Pl-Plagiocalse, Plagioclase formula cations/8 oxygen; Opx-Orthopyroxene, Cpx-Clinopyroxene, Orthopyroxene and Clinopyroxene formula cations/ 6 oxygen; Qtz-Quartz; Mg# - molar Mg/(Fe+Mg)*100

Table 37 Chemical compositions (wt.%) of mineral fragments in matrix NWA 15352.

				M 11						
wt.%	Pl		Opx		Ilm				Troi	
SiO2	43.47	SiO2	49.15	SiO2	0.49	1.99	SiO2	0.27	0.65	0.36
TiO2	-	TiO2	0.54	TiO2	51.58	50.33	TiO2	-	-	-
Al2O3	34.79	Al2O3	2.56	Al2O3	0.45	1.47	Al2O3	0.16	0.75	0.14
Cr2O3	-	Cr2O3	0.42	Cr2O3	0.44	1.05	Cr2O3	-	-	-
FeO	1.06	FeO	21.15	FeO	41.28	39.51	FeO	60.46	58.56	58.8
MnO	-	MnO	0.26	MnO	0.39	0.48	MnO	-	-	-
MgO	-	MgO	18.89	MgO	3.63	3.65	MgO	-	-	-
CaO	18.45	CaO	3.86	CaO	0.35	0.97	CaO	0.24	0.63	0.32
Na2O	0.43	Na2O	-	Na2O	-	-	Na2O	-	-	-
K2O	-	K2O	-	K2O	-	-	K2O	-	-	-
S	0.26	S	-	S	-	-	S	37.14	38.22	37.82
V	-	V	-	V	0.41	0.43	V	-	-	-
P	-	P	-	P	0.23	0.00	P	-	-	-
Total	98.46	Total	96.83	Total	99.25	99.87	Total	98.27	98.81	97.44
Si	2.05	Si	1.91	Si	0.02	0.10				
Al	1.94	Ti	0.02	Ti	1.93	1.83				
Ti	0.00	Al	0.12	Al	0.03	0.06				
Fe++	0.04	Cr	0.01	Cr	0.02	0.06				
Mn	0.00	Fe++	0.69	Fe++	1.71	1.59				
Mg	0.00	Mn	0.01	Mn	0.02	0.02				
Ca	0.93	Mg	1.09	Mg	0.27	0.26	Ni	0.00	0.00	0.00
Na	0.04	Ca	0.16	Ca	0.02	0.05	Fe	7.48	7.04	7.14
K	0.00	Na	0.00	Na			S	8.00	8.00	8.00
Total	5.00	Total	4.01	Total	4.01	3.96	Total	15.48	15.04	15.14
Mg*	0.00	Mg*	61.42	Mg*	13.56	14.14				
Or	0.00	En	56.34							
Ab	4.05	Fs	35.39							
An	95.95	Wo	8.27							

wt.% - weight percentages; M - Mineral fragment; Pl-Plagiocalse, Plagioclase formula cations/8 oxygen; Opx-Orthopyroxene, Orthopyroxene formula cations/ 6 oxygen; Ilm-Ilmenite, formula cations/6 oxygen; Troi - Troilite, Troilite formula 8 sulfur; Mg# - molar Mg/(Fe+Mg)*100

Table 38 Chemical compositions (wt.%) of mineral fragments in matrix NWA 15352.

	M 12						
wt.%	Ol			Troi			Fe-Ni
SiO2	35.53	36.23	SiO2	0.28	0.14	SiO2	0.90
TiO2	-	-	TiO2	-	-	TiO2	-
Al2O3	0.40	0.29	Al2O3	0.17	0.18	Al2O3	0.90
Cr2O3	-	-	Cr2O3	0.10	0.00	Cr2O3	-
FeO	35.18	34.68	FeO	60.44	60.85	FeO	84.24
MnO	0.26	0.40	MnO	-	-	MnO	-
MgO	27.74	28.04	MgO	-	-	MgO	-
CaO	0.25	0.41	CaO	0.19	0.18	CaO	0.94
Na2O	-	-	Na2O	-	-	Na2O	-
K2O	-	-	K2O	-	-	K2O	-
S	-	-	S	37.91	37.70	S	-
Ni	-	-	Ni	-	-	Ni	9.51
F	-	-	F	-	-	F	1.11
Total	99.36	100.05	Total	99.09	99.05	Total	97.60
Si	0.99	1.00					
Ti	0.00	0.00					
Al	0.01	0.01					
Cr	0.00	0.00					
Fe++	0.82	0.80					
Mn	0.01	0.01					
Mg	1.16	1.16					
Ni	0.01	0.01					
Ca	0.01	0.01					
Total	3.01	3.00					
Mg*	58.43	59.04					
			Ni	0.00	0.00	Ni	0.10
Fo	58.25	58.76	Fe	7.32	7.41	Fe	0.90
Fa	41.44	40.76	S	8.00	8.00	S	0.00
Tp	0.31	0.48	Total	15.32	15.41	Total	1.00

wt.% - weight percentages; M - Mineral fragment; Ol - Olivine; Olivine formula cations/ 4 oxygen;
Troi - Troilite, Troilite formula 8 sulfur; Fe-Ni - iron-nickel metal, normalized to 1.0 cations ; Mg# - molar Mg/(Fe+Mg)*100

Table 39 Chemical compositions (wt.%) of mineral fragments in matrix NWA 15352.

							M 13									
wt.%	Pl		Ol		Opx		Ilm					Mg-rich Spl				Cr-rich Spl
SiO2	43.98	SiO2	36.59	SiO2	52.33	SiO2	0.36	0.36	2.10	0.49	SiO2	-	-	0.26	SiO2	0.47
TiO2	-	TiO2	0.23	TiO2	0.65	TiO2	53.17	51.64	49.48	53.20	TiO2	0.53	-	0.77	TiO2	3.38
Al2O3	35.65	Al2O3	-	Al2O3	1.08	Al2O3	0.00	0.27	1.43	0.33	Al2O3	62.28	61.79	60.64	Al2O3	38.19
Cr2O3	-	Cr2O3	-	Cr2O3	0.31	Cr2O3	0.58	1.10	0.51	0.45	Cr2O3	1.67	1.62	1.77	Cr2O3	19.06
FeO	0.30	FeO	34.57	FeO	20.80	FeO	39.47	41.17	41.79	39.12	FeO	22.27	21.23	22.37	FeO	26.84
MnO	-	MnO	0.33	MnO	0.28	MnO	0.51	0.29	0.39	0.51	MnO	-	0.22	-	MnO	-
MgO	-	MgO	28.84	MgO	20.56	MgO	5.13	3.72	3.23	5.11	MgO	14.09	14.13	13.55	MgO	9.25
CaO	19.58	CaO	0.22	CaO	4.04	CaO	0.33	0.63	1.14	0.57	CaO	-	-	-	CaO	2.45
Na2O	0.48	Na2O	-	Na2O	-	Na2O	-	-	-	-	Na2O	-	-	-	Na2O	-
K2O	-	K2O	-	K2O	-	K2O	-	-	-	-	K2O	-	-	-	K2O	-
ZrO2	-	ZrO2	-	ZrO2	-	ZrO2	-	-	-	0.48	ZrO2	-	-	-	ZrO2	-
Total	99.99	Total	100.78	Total	100.05	Total	0.00	0.00	0.00	100.26	Total	100.84	98.99	99.36	Total	99.64
Si	2.04	Si	1.00	Si	1.96	Si	0.02	0.02	0.10	0.02	Si	0.00	0.00	0.01	Si	0.01
Al	1.95	Ti	0.00	Ti	0.02	Ti	1.95	1.91	1.81	1.94	Ti	0.01	0.00	0.02	Ti	0.08
Ti	0.00	Al	0.00	Al	0.05	Al	0.00	0.02	0.08	0.02	Al	1.93	1.94	1.91	Al	1.33
Fe++	0.01	Cr	0.00	Cr	0.01	Cr	0.02	0.04	0.02	0.02	Cr	0.03	0.03	0.04	Cr	0.45
Mn	0.00	Fe++	0.79	Fe++	0.65	Fe++	1.61	1.70	1.70	1.59	Fe++	0.49	0.47	0.50	Fe++	0.67
Mg	0.00	Mn	0.01	Mn	0.01	Mn	0.02	0.01	0.02	0.02	Mn	0.00	0.00	0.00	Mn	0.00
Ca	0.97	Mg	1.18	Mg	1.15	Mg	0.37	0.27	0.23	0.37	Mg	0.55	0.56	0.54	Mg	0.41
Na	0.04	Ni	0.00	Ca	0.16	Ca	0.02	0.03	0.06	0.03	Ca	0.00	0.00	0.00	Ca	0.08
K	0.00	Ca	0.01	Na	0.00	Na	-	-	-	-	Na	0.00	0.00	0.00	Na	0.00
Total	5.01	Total	3.00	Total	4.00	Total	4.01	4.00	4.01	4.00	Total	3.01	3.01	3.01	Total	3.02
Mg*	0.00	Mg*	59.80	Mg*	63.79	Mg*	18.81	13.87	12.11	18.89	Mg*	53.01	54.27	51.92	Mg*	38.06
Or	0.00	Fo	59.57	En	58.52						Cr*	1.77	1.73	1.92		25.08
Ab	4.25	Fa	40.05	Fs	33.21											
An	95.75	Tp	0.39	Wo	8.26											

wt.% - weight percentages; M - Mineral fragment; Pl-Plagiocalse, Plagioclase formula cations/8 oxygen; Ol - Olivine; Olivine formula cations/ 4 oxygen; Opx-Orthopyroxene, Orthopyroxene formula cations/ 6 oxygen;
Ilm-Ilmenite, formula cations/6 oxygen; Spl-Spinel and Cr-rich Spl-Chromium-rich Spinel, Spinel formua cations/6; Mg# - molar Mg/(Fe+Mg)*100.

B. SEM BSE images

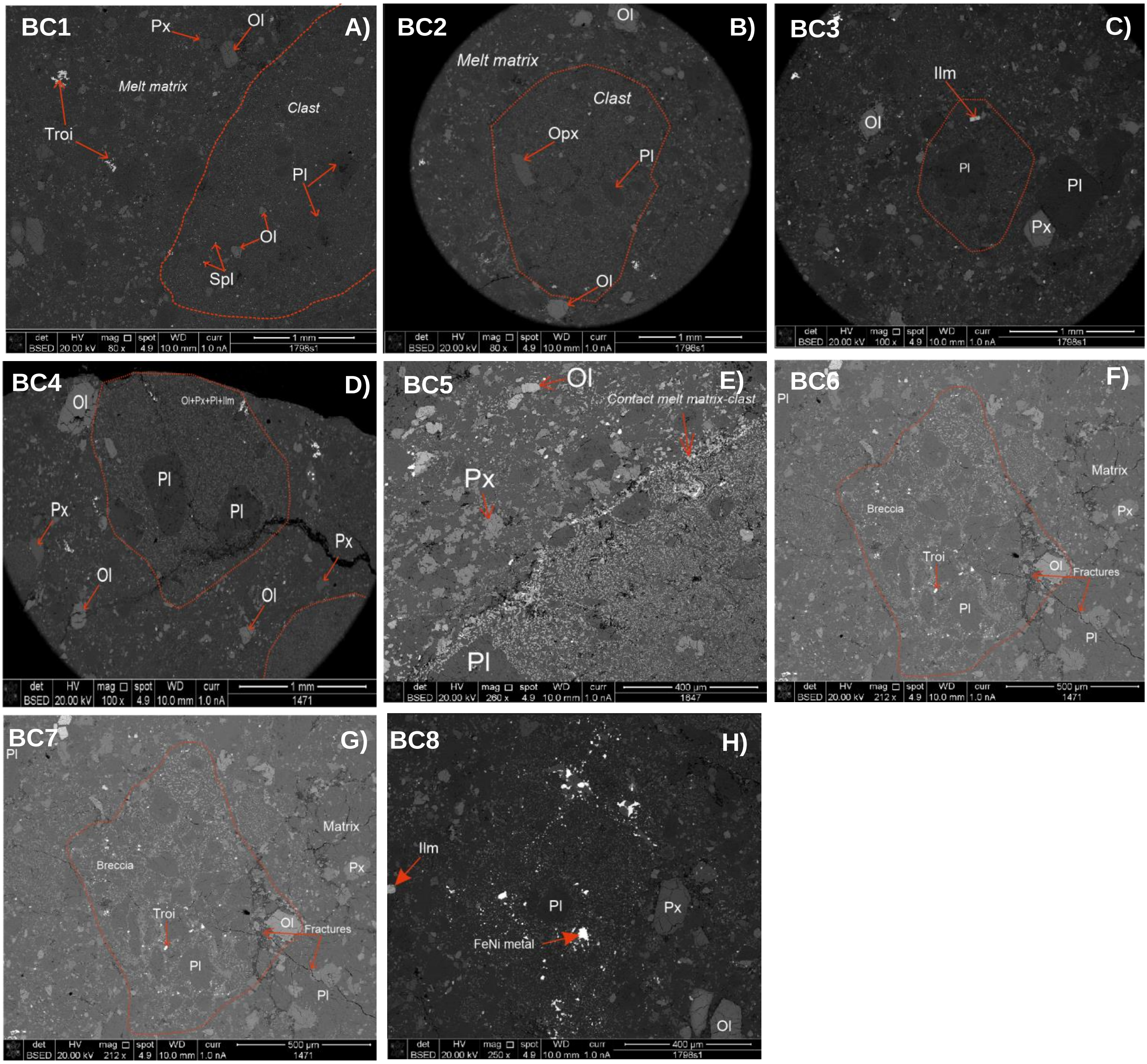

Fig. 20. BSE image of the breccia clasts. Pl – plagioclase, Px – pyroxene, Opx – orthopyroxene, Clpx – clinopyroxene, Ol – olivine, Troi – troilite, Spl – spinel, Ilm – ilmenite

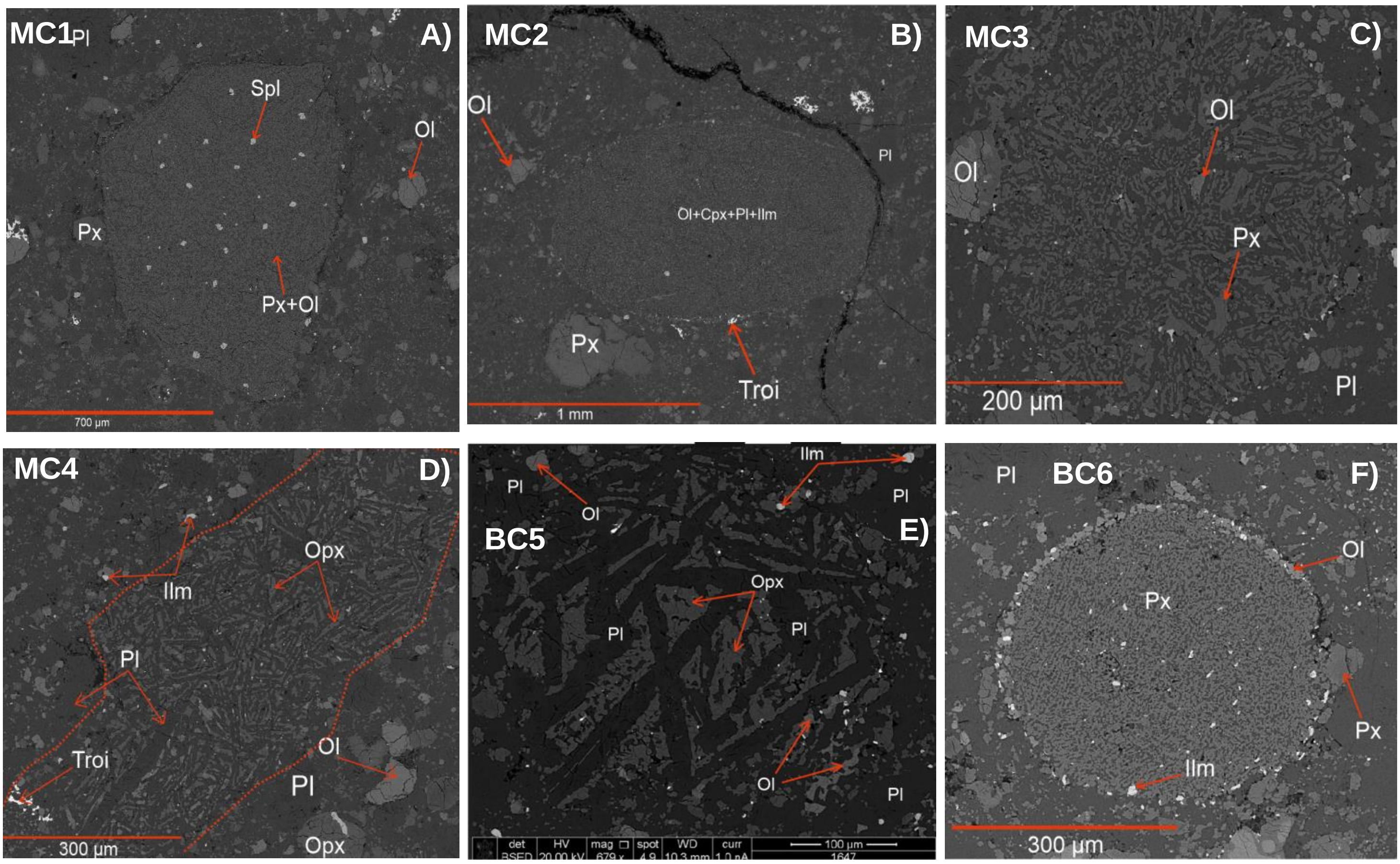

Fig. 21. BSE image of the melt clasts. Pl – plagioclase, Px – pyroxene, Opx – orthopyroxene, Clpx – clinopyroxene, Ol – olivine, Troi – troilite, Spl – spinel, Ilm – ilmenite

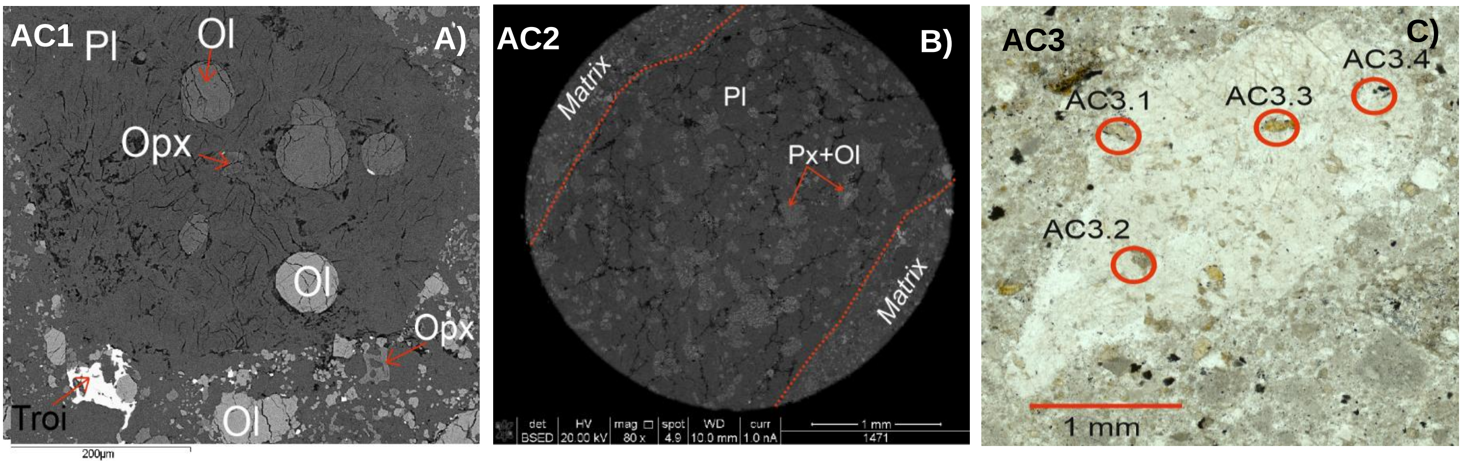

Fig. 22. BSE image of the anorthosite clasts. Pl – plagioclase, Px – pyroxene, Opx – orthopyroxene, Clpx – clinopyroxene, Ol – olivine, Troi – troilite, Spl – spinel, Ilm – ilmenite

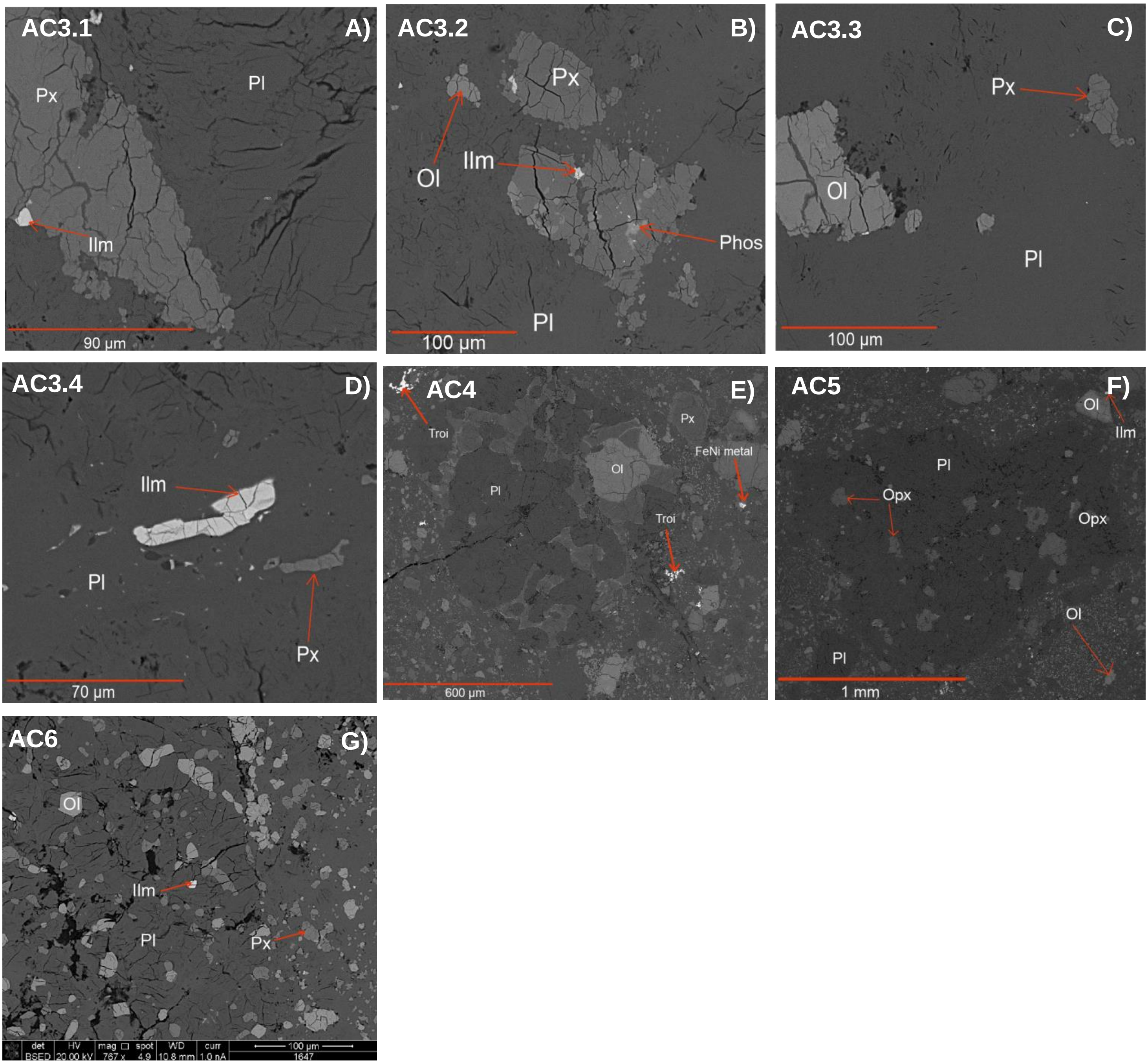

Fig. 23. BSE image of the anorthosite clasts. Pl – plagioclase, Px – pyroxene, Opx – orthopyroxene, Clpx – clinopyroxene, Ol – olivine, Troi – troilite, Spl – spinel, Ilm – ilmenite

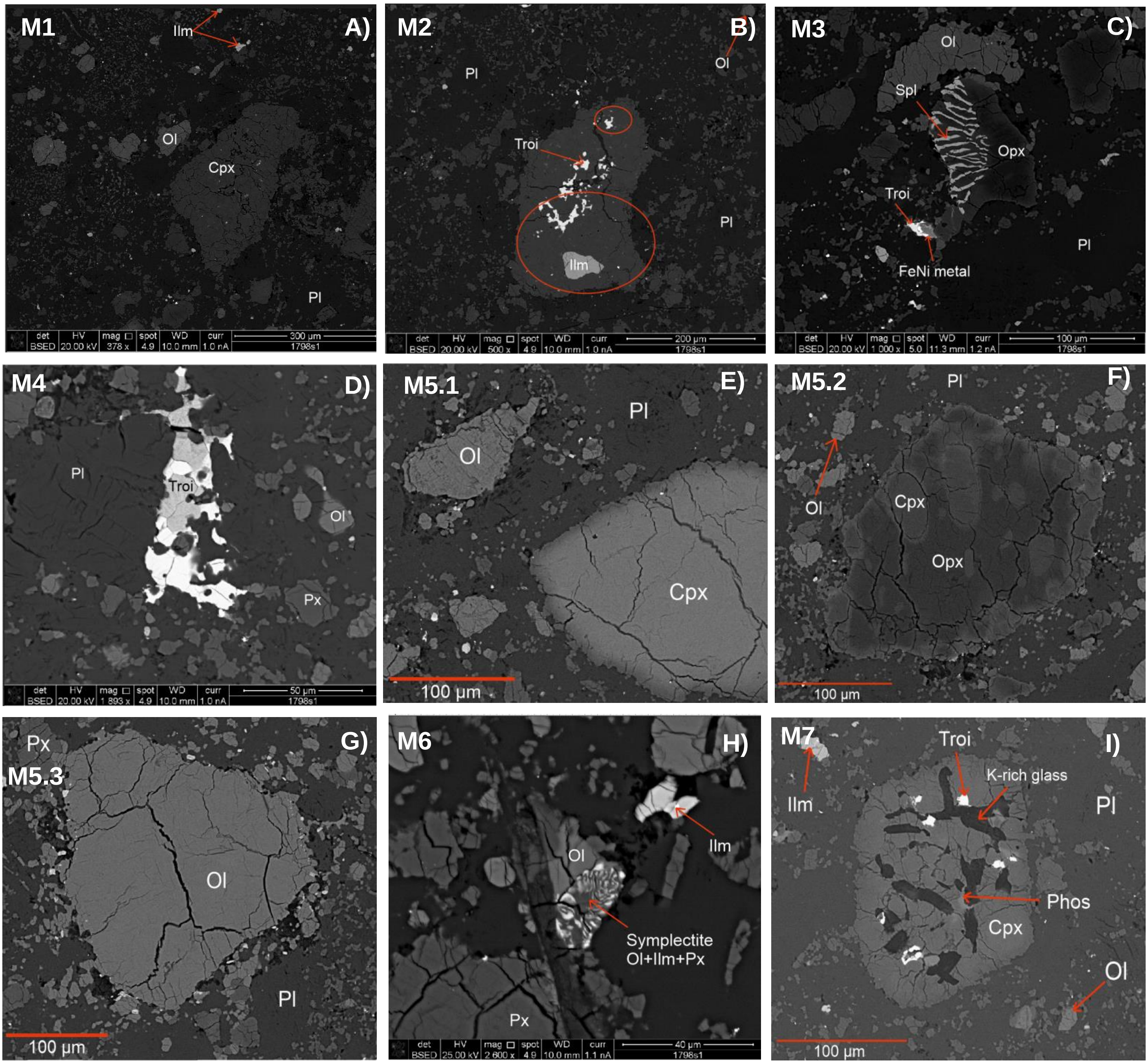

Fig. 24. BSE image of the anorthosite clasts. Pl – plagioclase, Px – pyroxene, Opx – orthopyroxene, Clpx – clinopyroxene, Ol – olivine, Troi – troilite, Spl – spinel, Ilm – ilmenite

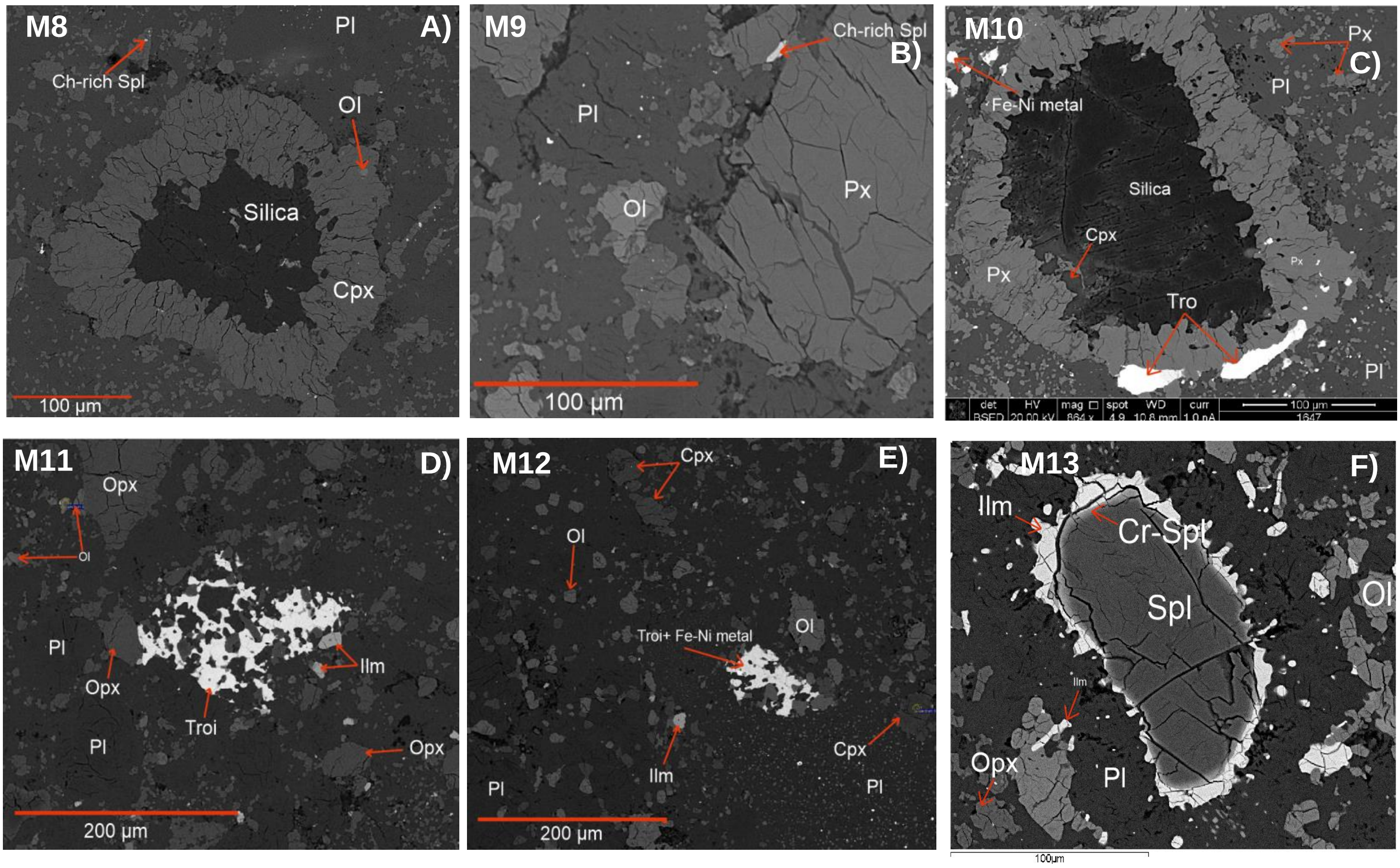

Fig. 25. BSE image of the mineral fragments. Pl – plagioclase, Px – pyroxene, Opx – orthopyroxene, Clpx – clinopyroxene, Ol – olivine, Troi – troilite, Spl – spinel, Ilm – ilmenite.

C. BSE images for the SIMS analysis.

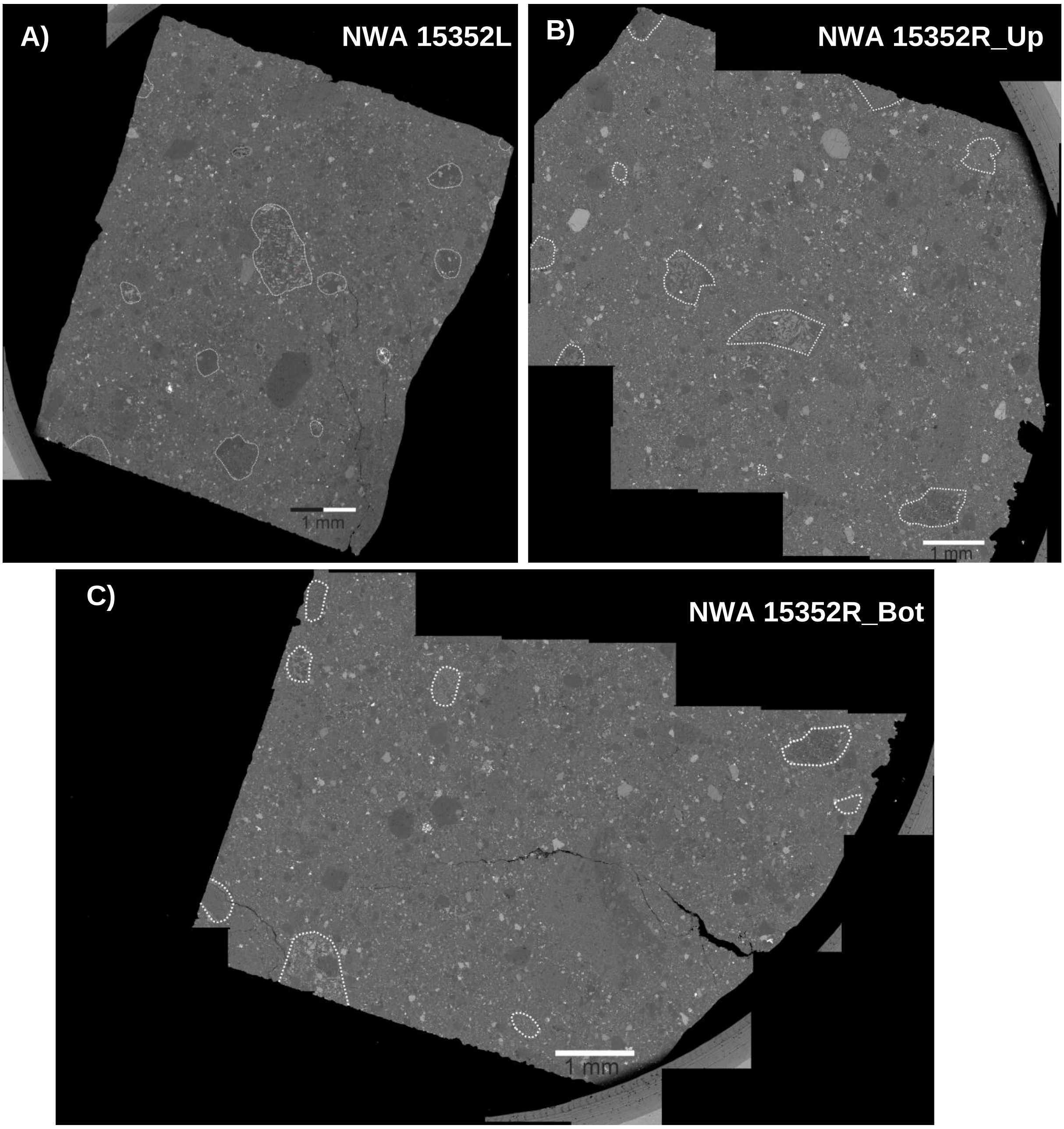

Fig. 26. BSE image of the NWA 15352L (left), NWA 15352R_Up (right up) and NWA 15352R_Bot (right bottom) thick sections with clasts.